

INFORMATION TO USERS

This material was produced from a microfilm copy of the original document. While the most advanced technological means to photograph and reproduce this document have been used, the quality is heavily dependent upon the quality of the original submitted.

The following explanation of techniques is provided to help you understand markings or patterns which may appear on this reproduction.

1. The sign or "target" for pages apparently lacking from the document photographed is "Missing Page(s)". If it was possible to obtain the missing page(s) or section, they are spliced into the film along with adjacent pages. This may have necessitated cutting thru an image and duplicating adjacent pages to insure you complete continuity.
2. When an image on the film is obliterated with a large round black mark, it is an indication that the photographer suspected that the copy may have moved during exposure and thus cause a blurred image. You will find a good image of the page in the adjacent frame.
3. When a map, drawing or chart, etc., was part of the material being photographed the photgrapher followed a definite method in "sectioning" the material. It is customary to begin photoing at the upper left hand corner of a large sheet and to continue photoing from left to right in equal sections with a small overlap. If necessary, sectioning is continued again — beginning below the first row and continuing on until complete.
4. The majority of users indicate that the textual content is of greatest value, however, a somewhat higher quality reproduction could be made from "photographs" if essential to the understanding of the dissertation. Silver prints of "photographs" may be ordered at additional charge by writing the Order Department, giving the catalog number, title, author and specific pages you wish reproduced.
5. PLEASE NOTE: Some pages may have indistinct print. Filmed as received.

Xerox University Microfilms

300 North Zeeb Road
Ann Arbor, Michigan 48106

7817887

AL-MARHOUN, MUHAMMAD ALI
OPTIMAL NUMERICAL PROCEDURE TO SOLVE
TWO-DIMENSIONAL THREE-PHASE PETROLEUM
RESERVOIR SIMULATOR.

THE UNIVERSITY OF OKLAHOMA, PH.D., 1978

University
Microfilms
International 300 N. ZEEB ROAD, ANN ARBOR, MI 48106

(C) 1978

MUHAMMAD ALI AL-MARHOUN

ALL RIGHTS RESERVED

THE UNIVERSITY OF OKLAHOMA
GRADUATE COLLEGE

OPTIMAL NUMERICAL PROCEDURE TO SOLVE TWO-DIMENSIONAL
THREE-PHASE PETROLEUM RESERVOIR SIMULATOR

A DISSERTATION
SUBMITTED TO THE GRADUATE FACULTY
in partial fulfillment of the requirements for the
degree of
DOCTOR OF PHILOSOPHY

By
MUHAMMAD ALI AL-MARHOUN
Norman, Oklahoma
1978

OPTIMAL NUMERICAL PROCEDURE TO SOLVE TWO-DIMENSIONAL
THREE-PHASE PETROLEUM RESERVOIR SIMULATOR
A DISSERTATION

APPROVED FOR THE DEPARTMENT OF PETROLEUM ENGINEERING

By

Ken Ciallo

James A. Payne
D E McKenzie

Adel A. Aly
A.W. McCray

ACKNOWLEDGEMENTS

The author wishes to express his appreciation to the Chairman of his Graduate Committee, Dr. H.B. Crichton, Director of the department of Petroleum and Geological Engineering, for his assistance in connection with this work.

Appreciation is also extended to Dr. D.E. Menzie, Dr. A.W. McCray of Petroleum Engineering Department, Dr. J.A. Payne of Computing Sciences Department, and Dr. A.A. Aly of Industrial Engineering Department for their revision of this dissertation and for serving as members of the author's Graduate Committee.

Particular thanks are due to the University of Petroleum and Minerals of Dhahran, Saudi Arabia, for their financial support.

The author also wishes to make a special recognition of his parents for their constant support and inspiration.

TABLE OF CONTENTS

	Page
ACKNOWLEDGEMENTS	iii
LIST OF TABLES	vi
LIST OF ILLUSTRATIONS	vii
Chapter	
I. INTRODUCTION	1
II. RESERVOIR MODEL.	9
III. FINITE DIFFERENCE SYSTEM	18
3.1 Implicit Solution of Pressure	18
3.2 Explicit Solution of Saturation.	25
3.3 Discretization of Flow Coefficient ($h\lambda$)	27
3.4 Boundary Conditions	32
IV. ITERATIVE METHODS.	33
4.1 Successive Overrelaxation	34
4.2 Alternating Direction Implicit.	38
4.3 Strongly Implicit	47
V. DIRECT METHODS	62
5.1 LU Factorization.	62
5.2 Ordering Schemes.	66
5.3 Generate-And-Solve Algorithms	77
5.4 Band Matrix Technique	77
VI. A NEW APPROACH TO THE APPLICATION OF DIRECT METHODS IN PETROLEUM RESERVOIR SIMULATION.	80
6.1 Restricted Alternating Diagonal Ordering.	80
6.2 LU Factorization Applied to RAD	84
6.3 Implementation of RAD Scheme into the Simulation Package.	92

Chapter	Page
VII. SIMULATION PACKAGE	94
7.1 Input Section	94
7.2 One-Time Calculation Section.	99
7.3 Time Control Section.	101
7.4 Coefficient Matrix Calculation Section.	103
7.5 Pressure Solution Section	104
7.6 Saturation Calculation Section.	104
7.7 Mass Balance Section.	104
7.8 Output Section.	106
7.9 Auxiluary Section	106
VIII. COMPARATIVE EVALUATION	110
8.1 Difficulties of Iterative Methods	110
8.2 Storage Requirements.	111
8.3 CPU Time Comparison	112
8.4 Mass Balance Errors	112
8.5 Average Reservoir Pressure.	125
IX. CONCLUSIONS.	128
NOMENCLATURE	130
REFERENCES	136
APPENDICES	
A. Units and Conversion Factors	140
B. Flow Chart Convention.	141
C. Constant Values Used in This Study	142
D. Geometry and Properties of the Reservoir Model .	144
E. Computer Listing of the Numerical Procedures .	158
F. A Sample of Computer Simulation Output	176

LIST OF TABLES

Table	Page
5.1 Work and Storage Requirements for ordering schemes.	74
8.1 Computer Storage Requirements	111
8.2 CPU Time for Homogeneous Case	113
8.3 CPU Time for Heterogeneous Case	115
8.4 Total Mass Balance Relative Error for Homogeneous Case. . .	117
8.5 Total Mass Balance Relative Error for Heterogeneous Case. .	118
8.6 Oil Mass Balance Relative Error for Homogeneous Case. . . .	119
8.7 Oil Mass Balance Relative Error for Heterogeneous Case. . .	120
8.8 Water Mass Balance Relative Error for Homogeneous Case. . .	121
8.9 Water Mass Balance Relative Error for Heterogeneous Case. .	122
8.10 Gas Mass Balance Relative Error for Homogeneous Case. . . .	123
8.11 Gas Mass Balance Relative Error for Heterogeneous Case. . .	124
8.12 Average Reservoir Pressure for Homogeneous Case	126
8.13 Average Reservoir Pressure for Heterogeneous Case	127

LIST OF ILLUSTRATIONS

Figure	Page
1.1 Stone's Comparative Study.	4
1.2 Breitenbach, et al.'s Comparative Study	5
1.3 Watts' Comparative Study	6
1.4 Weinstein, et al.'s Comparative Study	7
3.1 Discretized Reservoir System	19
3.2 Cell System Definition	20
3.3 Profile of Two Adjacent Cells.	28
3.4 Flow Chart for the Calculation of Interblock Relative Permeability	31
4.1 PSOR Flow Chart.	35
4.2 LSOR Flow Chart.	37
4.3 Typical Plot of Relaxation Parameter at Fixed Tolerance. .	39
4.4 Flow Chart for Close-Band Thomas Algorithm	42
4.5 Flow Chart for Wide-Band Thomas Algorithm.	45
4.6 ADI Flow Chart	46
4.7 Cell Arrangement	48
4.8 Matrix \mathbf{A} in SIP.	51
4.9 L and U Matrices for Odd-Numbered Iterations	52
4.10 B Matrix for Odd-Numbered Iterations	53
4.11 L and U Matrices for Even-Numbered Iterations.	56
4.12 B Matrix for Even-Numbered Iterations.	57
4.13 SIP Flow Chart	61

Figure	Page
5.1 $\mathbf{A} \mathbf{P} = \mathbf{d}$ System of Equations.	63
5.2 L U Factorization of \mathbf{A}	65
5.3 Standard Ordering.	68
5.4 Diagonal Ordering.	68
5.5 Matrix \mathbf{A} Corresponding to Standard Ordering.	69
5.6 Matrix \mathbf{A} Corresponding to Diagonal Ordering.	70
5.7 Alternating Point Ordering	71
5.8 Alternating Diagonal Ordering.	71
5.9 Matrix \mathbf{A} Corresponding to Alternating Point Ordering	72
5.10 Matrix \mathbf{A} Corresponding to Alternating Diagonal Ordering. . . .	73
5.11 Alternating Line Ordering.	75
5.12 Matrix \mathbf{A} Corresponding to Alternating Line Ordering.	76
6.1 RAD Ordering Along the Shortest Diagonal	81
6.2 RAD Ordering Along the Longest Diagonal.	81
6.3 Matrix \mathbf{A} Corresponding to RAD Along the Shortest Diagonal. . . .	82
6.4 Matrix \mathbf{A} Corresponding to RAD Along the Longest Diagonal . .	83
6.5 General Form of Matrix \mathbf{A} of RAD.	86
6.6 The Composite Matrix \mathbf{Q} of RAD.	87
6.7 The Lower Quarter of Matrix \mathbf{Q} of Semi Bandwidth m	89
6.8 RAD Ordering Enclosing Standard Ordering	93
7.1 Simulator Flow Chart	95
7.2 The Type of Well Identifier.	98
7.3 Simulation Numbering Scheme.	100
8.1 CPU Time vs. Real Time (Homogeneous Case-345 Cells).	114
8.2 CPU Time vs. Real Time (Heterogeneous Case-345 Cells).	116

Figure	Page
E.1 Discretized Reservoir System	148
E.2 Reservoir Thickness	149
E.3 Digitized Reservoir Thickness	150
E.4 Top of the Reservoir Depth	151
E.5 Digitized Middle of the Reservoir Depth	152
E.6 Digitized Reservoir Initial Pressure	153
E.7 Reservoir Heterogeneous Permeability	154
E.8 Digitized Reservoir Heterogeneous Permeability	155
E.9 Configuration of Wells	156
E.10 Production - Injection Flow Rates	157

CHAPTER I

INTRODUCTION

Mathematical models for petroleum reservoirs incorporate the reservoir physical properties and the interaction of natural and artificial forces to simulate reservoir behavior. Therefore, mathematical simulation helps in understanding reservoir behavior. Such information leads to the most economically desirable form of exploitation.

Reservoir simulators are used to design the most economical secondary recovery program and to lay out the complete reservoir management from discovery to depletion.

Natural reservoirs consist of one, two or three phases (oil, water, and gas) with various geometries. Therefore, various reservoir simulators were developed. They start with one-dimensional one-phase simple simulators and end up with complex three-dimensional three-phase ones. Although three-dimensional simulators are now available, the most popular simulator is the two-dimensional one because a well-organized two-dimensional simulator can be used to approximate three-dimensional one at a lower cost.

The efficiency of a simulator as a working and economical tool hinges upon the ability of its algorithms to solve the pressure equations efficiently.⁶ Most of the computer time is spent in performing pressure

solutions. For this reason, the best simulator is the one which requires the minimum work during the pressure solutions.

The pressure equations can be solved either by iterative or direct methods.

Iterative methods are by far the most common methods of solving the pressure equations used in simulation. This is because iterative methods are easy to program and require less storage and less computation compared to existing direct method algorithms. Hence during the early years of work in this discipline, the direct solution techniques were almost completely abandoned as a solution process. However, in recent years with the development of sparse matrix techniques, the direct solution process has become less costly, while producing as good a result. For this reason, direct solution techniques are once again being considered in reservoir simulation areas.

The existing numerical methods (direct or iterative) to solve the mathematical models of petroleum reservoirs are time consuming. Those methods consume different computer time when applied on reservoirs with different characteristics.

The computer time is expensive, therefore, a tool to choose the fastest, most efficient methods for a given reservoir is needed. A comparative study helps to show the features of each method. Such information leads to the choice of the most economically suitable method.

The comparative studies done in literature are limited to two or three methods and most of these comparative evaluations are done on a system of simultaneous equations not as part of a complete simulation. Also most of these comparative studies used idealized model of fixed rates and square reservoir with pre-determined flow coefficients.

Stone¹⁴ has presented a comparison among the following numerical procedures: alternating direction implicit (ADI), strongly implicit (SIP), point successive overrelaxation (PSOR), and point Jacobi. His study was in terms of computational work and residual. He used an idealized square reservoir with fixed flow rates and a combination of homogeneous regions. His results are presented in Figure 1.1. Stone concluded that both ADI and SIP possess convergence rates a great deal faster than those of the other two methods. For homogeneous case, ADI is slightly faster than SIP. However, SIP is significantly faster than ADI in case of heterogeneous reservoirs. Also he concluded that PSOR is more rapid than point Jacobi method.

Breitenbach, et al.³ gave a very brief comparison between Gauss elimination, PSOR, and ADI. For his model, he showed that PSOR and ADI are more efficient than Gauss elimination for more than 9x26 cell system. His results are shown in Figure 1.2.

Watts¹⁹ has presented a comparison among ADI, SIP, line successive overrelaxation (LSOR), and corrected LSOR in terms of accuracy. His results are shown in Figure 1.3. He concluded that for two-dimensional strongly anisotropic problems, the corrected LSOR is faster than other available techniques. However, in homogeneous isotropic square problem, the corrected LSOR is slower than ADI, SIP, and LSOR.

Weinstein, et al.²⁰ have compared SIP with ADI for a two-dimensional two-phase model. Their results are shown in Figure 1.4. They found that the computational work ratio, which is the ratio of ADI computer time to SIP computer time, generally increases with increasing transmissibility (ρ_{\max}). They also found that ADI fails to converge for higher transmissibility.

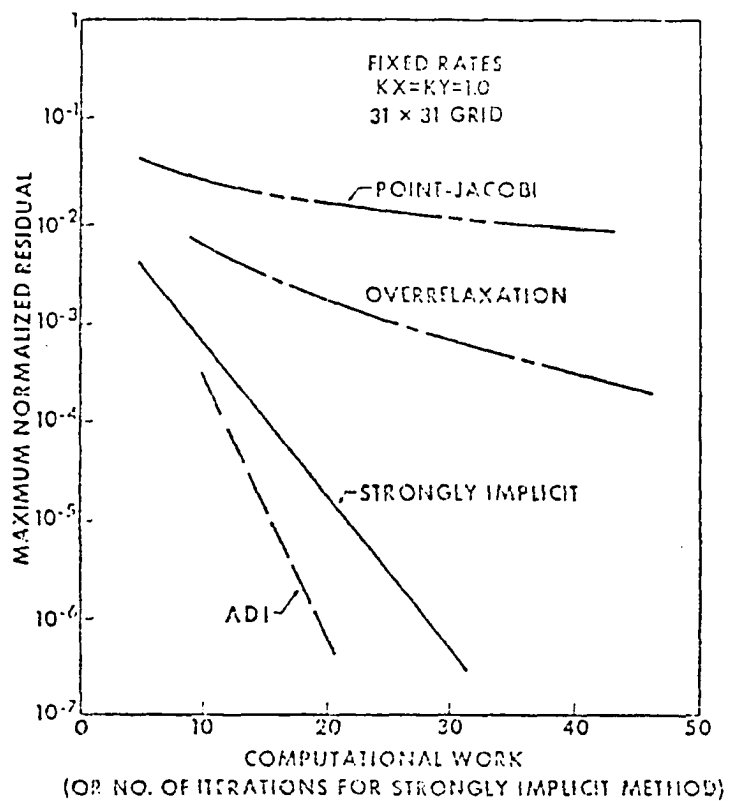
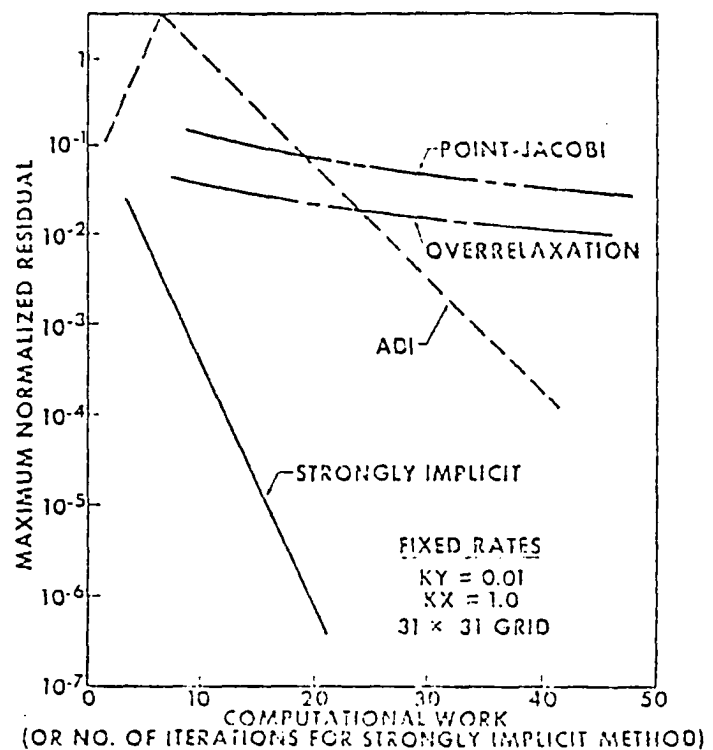


Figure 1.1 - Stone's Comparative Study

Grid	Method		
	Gauss	SOR	ADIPIT
3 x 5	2 ***	5	5
3 x 5 x 2	5	12 **	-
9 x 10	8	11	-
13 x 11	18	25	19
9 x 26 *	21	40 **	-
9 x 26	21	21	22
26 x 23	94	59	62
34 x 36	302	122	111
20 x 24 x 2	564	110	-

* Vertical cross section

** Line SOR

*** Time in second

Figure 1.2 - Breitenbach, et al.'s Comparative Study

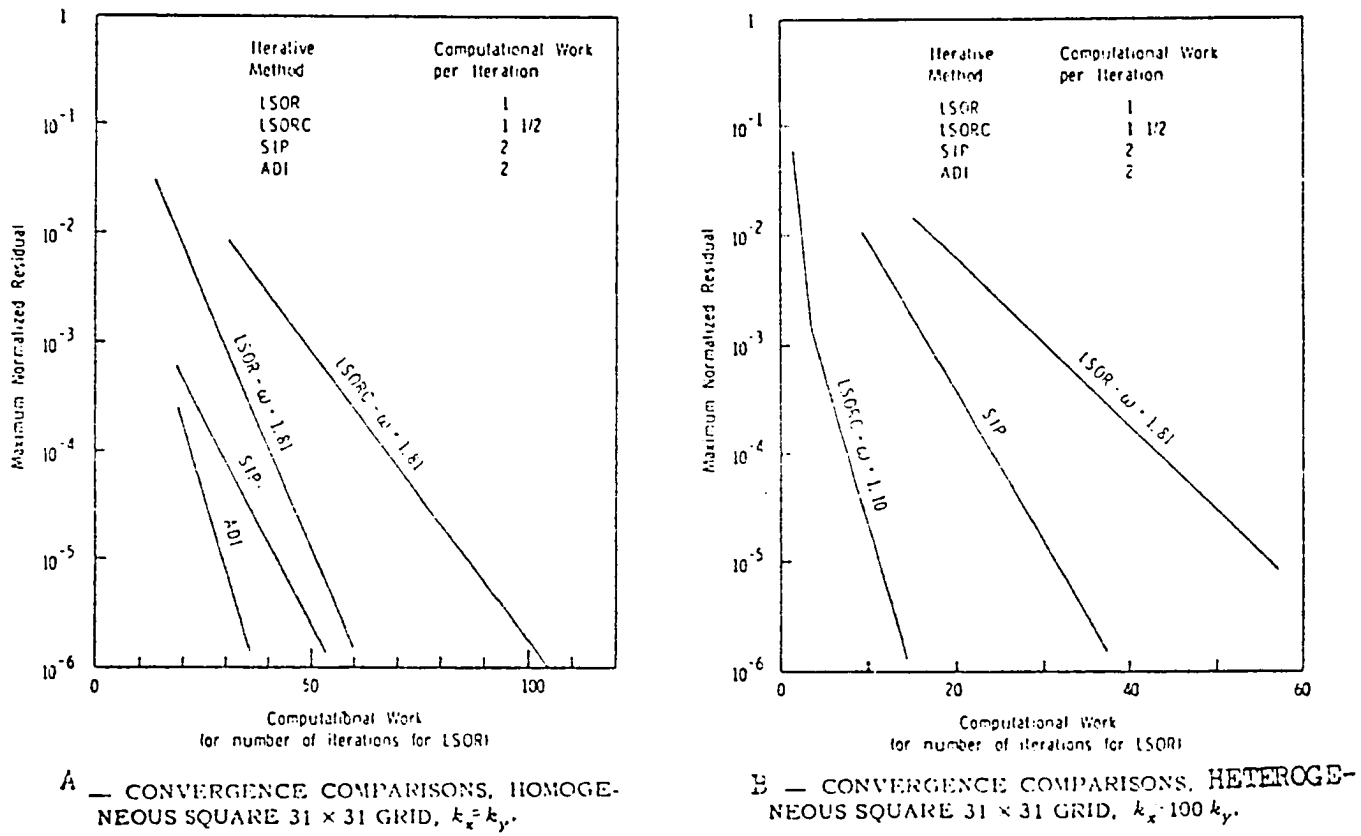


Figure 1.3 - Watts' Comparative Study

Problem	P_{\max}	Iteration Procedure	Parameter (Max SIP (Min ADIP))	Number of Time Steps	Number of Iterations	Average Iterations/ Time Step	Iteration Time (millisec/ Iterations/ Block)	Total Time (minutes)	Work Ratio
Dissolved Gas Drive Case I*	66	SIP	0.999942, 1	8	189	23.6	2.41	3.83	
		ADIP	$0.569 \times 10^{-4}, 0$	8	247	30.9	2.26	4.69	1.22
Dissolved Gas Drive Case II*	660	SIP	0.9999942, 1	8	193	24.2	2.40	3.89	
		ADIP	$0.231 \times 10^{-4}, 0$		∞				∞
Gas-Oil Incompressible	3,600	SIP	0.999998	25	77	3.1	1.97	0.993	
		ADIP	0.203×10^{-4}	25	389	15.6	1.48	3.75	3.78
Water-Oil Radial Coning	7.05×10^5	SIP	0.9995	9**	86	9.6	1.90	0.65	
		ADIP	0.001	9**	∞				∞

* All K_y of Case II are 10 times those of Case I.
 ** Simulation from 30.4 to 365 days. (The 0-30.4 day time step was not included, since both SIP and ADIP failed to converge.)

Figure 1.4-Weinstein, et al.'s Comparative Study

Price and Coats¹² have presented a comparison among four different ordering schemes outlined in chapter V. A direct solution method is used with these ordering-schemes to solve idealized reservoir problems. The Price and Coats study produces impressive results in terms of computational work reduction. However, these results in computational work reduction are limited to the computer time involved in elimination portion of non-zero elements of the equations system and do not include the additional work required to reorder the cell system from standard ordering to the appropriate ordering.

From the afore-mentioned survey, a development of a better direct method approach is needed. A more comprehensive comparative evaluation using a realistic petroleum reservoir is also needed. This study will address these two areas.

CHAPTER II

RESERVOIR MODEL

The introduction of Darcy's law into the two dimensional continuity equation for each of the three immiscible fluid phases in petroleum reservoirs leads to the following system of partial differential equations :

$$\frac{\partial}{\partial x} (h \rho_o \lambda_o \frac{\partial \Phi_o}{\partial x}) + \frac{\partial}{\partial y} (h \rho_o \lambda_o \frac{\partial \Phi_o}{\partial y}) + \frac{q_o \rho_o^*}{A} = h \frac{\partial}{\partial t} (\phi \rho_o S_o) \quad (2.1)^1$$

for the oil phase,

$$\frac{\partial}{\partial x} (h \rho_w \lambda_w \frac{\partial \Phi_w}{\partial x}) + \frac{\partial}{\partial y} (h \rho_w \lambda_w \frac{\partial \Phi_w}{\partial y}) + \frac{q_w \rho_w^*}{A} = h \frac{\partial}{\partial t} (\phi \rho_w S_w) \quad (2.2)^1$$

for the water phase, and

$$\begin{aligned} & \frac{\partial}{\partial x} (h \rho_g \lambda_g \frac{\partial \Phi_g}{\partial x} + R_{so} h \rho_o \lambda_o \frac{\partial \Phi_o}{\partial x} + R_{sw} h \rho_w \lambda_w \frac{\partial \Phi_w}{\partial x}) \\ & + \frac{\partial}{\partial y} (h \rho_g \lambda_g \frac{\partial \Phi_g}{\partial y} + R_{so} h \rho_o \lambda_o \frac{\partial \Phi_o}{\partial y} + R_{sw} h \rho_w \lambda_w \frac{\partial \Phi_w}{\partial y}) \\ & + \frac{q_g \rho_g^*}{A} = h \frac{\partial}{\partial t} (\phi \rho_g S_g + R_{so} \phi \rho_o S_o + R_{sw} \phi \rho_w S_w) \end{aligned} \quad (2.3)$$

for the gas phase.

where

$$\lambda_j = k \frac{k_{rj}}{\mu_j} , j = o, g, w \quad (2.4)$$

These equations have been derived making the following assumptions:

- 1) Darcy's law applies
- 2) Composition of each fluid phase is constant

The generalized multiphase flow equation for the unsteady-state flow of oil, gas, and water in a porous medium is developed by combining the three single-phase equations into one basic equation. In order to do this, we need to express the following auxiliary equations:

The potential terms are

$$\Phi_o = P_o + \rho_o g D \quad (2.5)$$

$$\Phi_g = P_g + \rho_g g D \quad (2.6)$$

$$\Phi_w = P_w + \rho_w g D \quad (2.7)$$

the capillary pressure terms are

$$P_{cw} = P_o - P_w \quad (2.8)$$

$$P_{cg} = P_g - P_o \quad (2.9)$$

and the saturation equation is

$$S_o + S_g + S_w = 1 \quad (2.10)$$

Thus:

$$\frac{\partial S_o}{\partial t} + \frac{\partial S_g}{\partial t} + \frac{\partial S_w}{\partial t} = 0 \quad (2.11)$$

The derivation of the generalized multiphase equation is as follows:

Divide the oil equation (2.1) by ρ_o and expand by differentiation:

$$\begin{aligned}
 & \frac{\partial}{\partial x} (h\lambda_o \frac{\partial P_o}{\partial x}) + \frac{\partial}{\partial x} \{ h\lambda_o \frac{\partial(\rho_o g D)}{\partial x} \} \\
 & + \frac{\partial}{\partial y} (h\lambda_o \frac{\partial P_o}{\partial y}) + \frac{\partial}{\partial y} \{ h\lambda_o \frac{\partial(\rho_o g D)}{\partial y} \} \\
 & = \frac{h}{\rho_o} (\phi \rho_o \frac{\partial S_o}{\partial t} + \phi S_o \frac{\partial \rho_o}{\partial P_o} \frac{\partial P_o}{\partial t} + \rho_o S_o \frac{\partial \phi}{\partial P_o} \frac{\partial P_o}{\partial t}) - \frac{q_o \rho_o^*}{A \rho_o} \\
 & - \{ \frac{(h\lambda_o)_x}{\rho_o} (\frac{\partial \Phi_o}{\partial x})^2 \frac{\partial \rho_o}{\partial \Phi_o} + \frac{(h\lambda_o)_y}{\rho_o} (\frac{\partial \Phi_o}{\partial y})^2 \frac{\partial \rho_o}{\partial \Phi_o} \} \tag{2.12}
 \end{aligned}$$

The water equation (2.2) is divided by ρ_w and expanded by differentiation:

$$\begin{aligned}
 & \frac{\partial}{\partial x} (h\lambda_w \frac{\partial P_o}{\partial x}) - \frac{\partial}{\partial x} (h\lambda_w \frac{\partial P_{cw}}{\partial x}) + \frac{\partial}{\partial x} \{ h\lambda_w \frac{\partial(\rho_w g D)}{\partial x} \} \\
 & + \frac{\partial}{\partial y} (h\lambda_w \frac{\partial P_o}{\partial y}) - \frac{\partial}{\partial y} (h\lambda_w \frac{\partial P_{cw}}{\partial y}) + \frac{\partial}{\partial y} \{ h\lambda_w \frac{\partial(\rho_w g D)}{\partial y} \} \\
 & = \frac{h}{\rho_w} (\phi \rho_w \frac{\partial S_w}{\partial t} + \phi S_w \frac{\partial \rho_w}{\partial P_o} \frac{\partial P_o}{\partial t} + \rho_w S_w \frac{\partial \phi}{\partial P_o} \frac{\partial P_o}{\partial t}) - \frac{q_w \rho_w^*}{A \rho_w} \\
 & - \{ \frac{(h\lambda_w)_x}{\rho_w} (\frac{\partial \Phi_w}{\partial x})^2 \frac{\partial \rho_w}{\partial \Phi_w} + \frac{(h\lambda_w)_y}{\rho_w} (\frac{\partial \Phi_w}{\partial y})^2 \frac{\partial \rho_w}{\partial \Phi_w} \} \tag{2.13}
 \end{aligned}$$

The gas equation (2.3) is divided by ρ_g and expanded by differentiation:

$$\frac{\partial}{\partial x} (h\lambda_g \frac{\partial P_o}{\partial x}) + \frac{\partial}{\partial x} \{ h\lambda_g \frac{\partial(\rho_g g D)}{\partial x} \} + \frac{\partial}{\partial x} (h\lambda_g \frac{\partial P_{cg}}{\partial x})$$

$$\begin{aligned}
& + \frac{\partial}{\partial y} (h\lambda_g \frac{\partial P_0}{\partial y}) + \frac{\partial}{\partial y} \{ h\lambda_g \frac{\partial(\rho_g g D)}{\partial y} \} + \frac{\partial}{\partial y} (h\lambda_g \frac{\partial P_{cg}}{\partial y}) \\
& = \frac{h}{\rho_g} (\phi \rho_g \frac{\partial S_g}{\partial t} + \phi S_g \frac{\partial \rho_g}{\partial P_0} \frac{\partial P_0}{\partial t} + \rho_g S_g \frac{\partial \phi}{\partial P_0} \frac{\partial P_0}{\partial t}) \\
& + \frac{h\phi}{\rho_g} (S_0 \rho_0 \frac{\partial R_{so}}{\partial P_0} + S_w \rho_w \frac{\partial R_{sw}}{\partial P_0}) \frac{\partial P_0}{\partial t} + s \\
& - \left\{ \frac{(h\lambda_g)_x}{\rho_g} \left(\frac{\partial \Phi_g}{\partial x} \right)^2 \frac{\partial \rho_g}{\partial \Phi_g} + \frac{(h\rho_0 \lambda_0)_x}{\rho_g} \left(\frac{\partial \Phi_0}{\partial x} \right)^2 \frac{\partial R_{so}}{\partial \Phi_0} + \frac{(h\rho_w \lambda_w)_x}{\rho_g} \left(\frac{\partial \Phi_w}{\partial x} \right)^2 \frac{\partial R_{sw}}{\partial \Phi_w} \right\} \\
& - \left\{ \frac{(h\lambda_g)_y}{\rho_g} \left(\frac{\partial \Phi_g}{\partial y} \right)^2 \frac{\partial \rho_g}{\partial \Phi_g} + \frac{(h\rho_0 \lambda_0)_y}{\rho_g} \left(\frac{\partial \Phi_0}{\partial y} \right)^2 \frac{\partial R_{so}}{\partial \Phi_0} + \frac{(h\rho_w \lambda_w)_y}{\rho_g} \left(\frac{\partial \Phi_w}{\partial y} \right)^2 \frac{\partial R_{sw}}{\partial \Phi_w} \right\} \quad (2.14)
\end{aligned}$$

where

$$\begin{aligned}
s &= - \frac{q_g \rho_g^*}{A \rho_g} + \frac{R_{so}}{\rho_g} \{ h \frac{\partial}{\partial t} (\phi \rho_0 S_0) - \frac{\partial}{\partial x} (h \rho_0 \lambda_0 \frac{\partial \Phi_0}{\partial x}) - \frac{\partial}{\partial y} (h \rho_0 \lambda_0 \frac{\partial \Phi_0}{\partial y}) \} \\
&+ \frac{R_{sw}}{\rho_g} \{ h \frac{\partial}{\partial t} (\phi \rho_w S_w) - \frac{\partial}{\partial x} (h \rho_w \lambda_w \frac{\partial \Phi_w}{\partial x}) - \frac{\partial}{\partial y} (h \rho_w \lambda_w \frac{\partial \Phi_w}{\partial y}) \} \quad (2.15)
\end{aligned}$$

Incorporating equations (2.1) and (2.2) into (2.15), we obtain

$$s = -(q_g \rho_g^* - R_{so} q_0 \rho_0^* - R_{sw} q_w \rho_w^*) / (\rho_g A) \quad (2.16)$$

Combining equations (2.10), (2.11), (2.12), (2.15) and (2.16), we obtain

$$\frac{\partial}{\partial x} (h\lambda_t \frac{\partial P_0}{\partial x}) + \frac{\partial}{\partial y} (h\lambda_t \frac{\partial P_0}{\partial y}) = B_1 \frac{\partial P_0}{\partial t} + B_2 + B_3 + B_4 + B_5 \quad (2.17)$$

Equation (2.17) has been derived using unified SI units, but if practical units (Appendix A) are used, equation (2.17) becomes

$$\frac{\partial}{\partial x} \left(h \lambda_t \frac{\partial P_0}{\partial x} \right) + \frac{\partial}{\partial y} \left(h \lambda_t \frac{\partial P_0}{\partial y} \right) = \\ 11.57407408 B_1 \frac{\partial P_0}{\partial t} + 11.57407408 B_2 + B_3 + 0.001 B_4 + B_5 \quad (2.18)$$

where the total mobility term is

$$\lambda_t = \lambda_o + \lambda_g + \lambda_w \quad (2.19)$$

the PVT term is

$$B_1 = h \phi (S_o C_o + S_w C_w + S_g C_g + C_r) \quad (2.20)$$

$$C_o = \frac{1}{\rho_o} \frac{\partial \rho_o}{\partial P_o} + \frac{\rho_o}{\rho_g} \frac{\partial R_{so}}{\partial P_o} \quad (2.21)$$

$$C_w = \frac{1}{\rho_w} \frac{\partial \rho_w}{\partial P_o} + \frac{\rho_w}{\rho_g} \frac{\partial R_{sw}}{\partial P_o} \quad (2.22)$$

$$C_g = \frac{1}{\rho_g} \frac{\partial \rho_g}{\partial P_o} \approx \frac{1}{P_o} \quad (2.23)$$

$$C_r = \frac{1}{\phi} \frac{\partial \phi}{\partial P_o} \quad (2.24)$$

the production term is

$$B_2 = \frac{-1}{A} \left\{ \frac{q_g \rho_g^*}{\rho_g} + q_o \rho_o^* \left(\frac{1}{\rho_o} - \frac{R_{so}}{\rho_g} \right) + q_w \rho_w^* \left(\frac{1}{\rho_w} - \frac{R_{sw}}{\rho_g} \right) \right\} \quad (2.25)$$

the capillary pressure term is

$$\begin{aligned} B_3 = & - \left\{ \frac{\partial}{\partial x} \left(h \lambda_g \frac{\partial P_{cg}}{\partial x} \right) + \frac{\partial}{\partial y} \left(h \lambda_g \frac{\partial P_{cg}}{\partial y} \right) \right\} \\ & + \left\{ \frac{\partial}{\partial x} \left(h \lambda_w \frac{\partial P_{cw}}{\partial x} \right) + \frac{\partial}{\partial y} \left(h \lambda_w \frac{\partial P_{cw}}{\partial y} \right) \right\} \end{aligned} \quad (2.26)$$

the gravity term is

$$B_4 = - \sum_j^{o,g,w} \left[\frac{\partial}{\partial x} \left\{ h \lambda_j \frac{\partial (\rho_j g D)}{\partial x} \right\} + \frac{\partial}{\partial y} \left\{ h \lambda_j \frac{\partial (\rho_j g D)}{\partial y} \right\} \right] \quad (2.27)$$

and the second degree derivative term is

$$\begin{aligned} B_5 = & - \sum_j^{o,g,w} \left\{ \frac{(h \lambda_j)_x}{\rho_j} \left(\frac{\partial \Phi_j}{\partial x} \right)^2 \frac{\partial \rho_j}{\partial \Phi_j} + \frac{(h \lambda_j)_y}{\rho_j} \left(\frac{\partial \Phi_j}{\partial y} \right)^2 \frac{\partial \rho_j}{\partial \Phi_j} \right\} \\ & - \sum_j^{o,w} \left\{ \frac{(h \rho_j \lambda_j)_x}{\rho_g} \left(\frac{\partial \Phi_j}{\partial x} \right)^2 \frac{\partial R_{sj}}{\partial \Phi_j} + \frac{(h \rho_j \lambda_j)_y}{\rho_g} \left(\frac{\partial \Phi_j}{\partial y} \right)^2 \frac{\partial R_{sj}}{\partial \Phi_j} \right\} \end{aligned} \quad (2.28)$$

Potential gradients are assumed to be small and the square of such terms are neglected, therefore

$$B_5 = 0 \quad (2.29)$$

The following auxiliary set of equations are necessary to define

equation (2.18):

Capillary pressure equations

$$P_g - P_o = P_{cg} = f_1(S_o, S_g, S_w) \quad (2.30)$$

$$P_o - P_w = P_{cw} = f_2(S_o, S_g, S_w) \quad (2.31)$$

Density equations

$$\rho_o = f_3(P_o) \quad (2.32)$$

$$\rho_g = f_4(P_g) \quad (2.33)$$

$$\rho_w = f_5(P_w) \quad (2.34)$$

Relative permeability equations

$$k_{ro} = f_6(S_o, S_g, S_w) \quad (2.35)$$

$$k_{rg} = f_7(S_o, S_g, S_w) \quad (2.36)$$

$$k_{rw} = f_8(S_o, S_g, S_w) \quad (2.37)$$

Reservoir geometry equations

$$D = f_9(x, y) \quad (2.38)$$

$$h = f_{10}(x, y) \quad (2.39)$$

Rock property equations

$$k = f_{11} (x, y) \quad (2.40)$$

$$\phi = f_{12} (P_o, \frac{1}{\phi} \frac{\partial \phi}{\partial P_o}) \quad (2.41)$$

Solubility equations

$$R_{so} = f_{13} (P_o) \quad (2.42)$$

$$R_{sw} = f_{14} (P_w) \quad (2.43)$$

Viscosity equations

$$\mu_o = f_{15} (P_o) \quad (2.44)$$

$$\mu_g = f_{16} (P_g) \quad (2.45)$$

$$\mu_w = f_{17} (P_w) \quad (2.46)$$

Initial condition equations

$$P_o(x, y, 0) = P_{o_i} (x, y) \quad (2.47)$$

$$S_o(x, y, 0) = S_{o_i} (x, y) \quad (2.48)$$

$$S_w(x,y,0) = S_{w_i}(x,y) \quad (2.49)$$

Boundary condition equations (Newmann type)

$$\frac{\partial P_0}{\partial x} = 0 \quad (2.50)$$

$$\frac{\partial P_0}{\partial y} = 0 \quad (2.51)$$

Equation (2.18) with the auxilury equations constitute a complete mathematical formulation of the two-dimensional three-phase simulation problem using implicit pressure explicit saturation (IMPES) technique.

The mathematical derivation is similar to that given by Peaceman and Rachford¹¹ and Crichlow⁶ except for the SI units incorporated in this derivation.

CHAPTER III

FINITE DIFFERENCE SYSTEM

Equation (2.18) is far too complicated to be amenable to analytical solution. This nonlinear partial differential equation is approximated by finite differences where a variety of numerical techniques are adequate to solve it.

This chapter develops the finite difference system necessary to solve equation (2.18). In applying difference techniques, the continuum of space and time is divided into discrete intervals. Figure 3.1 shows the spatial discretized reservoir system. Thus, the difference system is defined only at the points (i,n) where i is the location of the cell and n is the time level. Figure 3.2 shows the definition of the cell system.

In this study, the implicit pressure - explicit saturation (IMPES) method will be used. The IMPES method solves equation (2.18) implicitly for pressure distribution. The saturation distribution is then explicitly calculated for each point.

3.1 Implicit Solution of Pressure

The finite difference formulation of equation (2.18) can be carried out by substituting for each term of the differential equation the appropriate finite difference approximation. Here, the noniterative

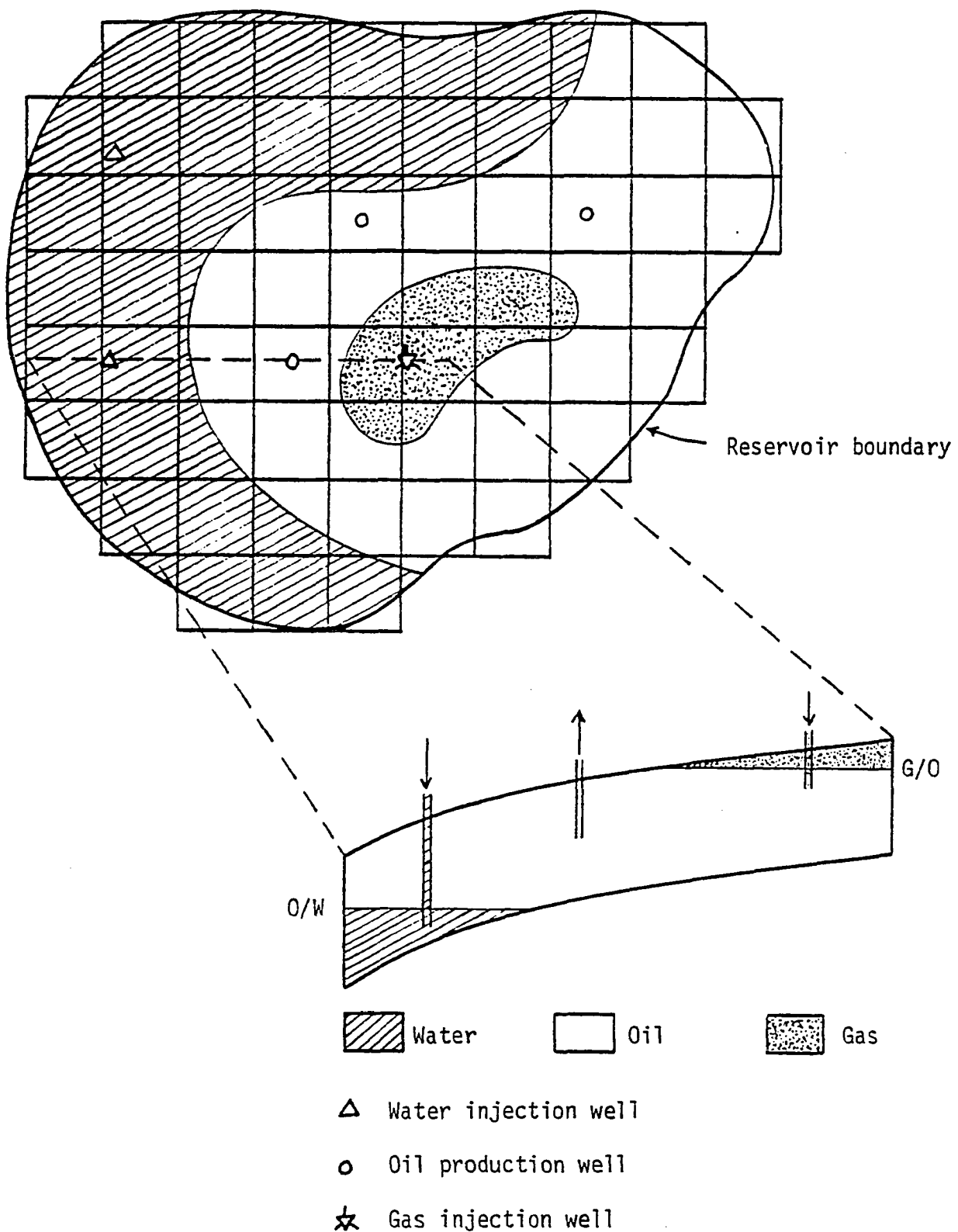
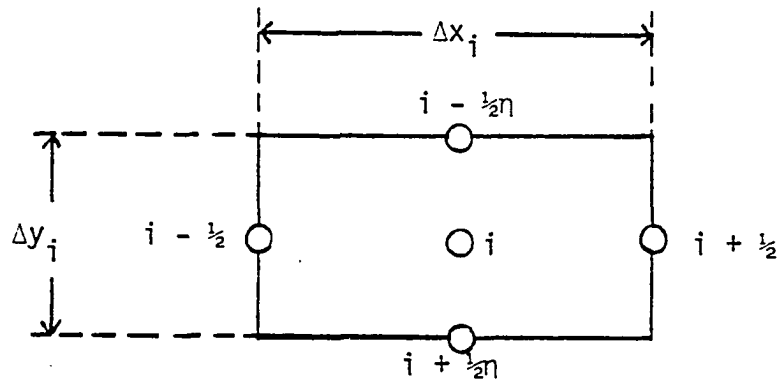
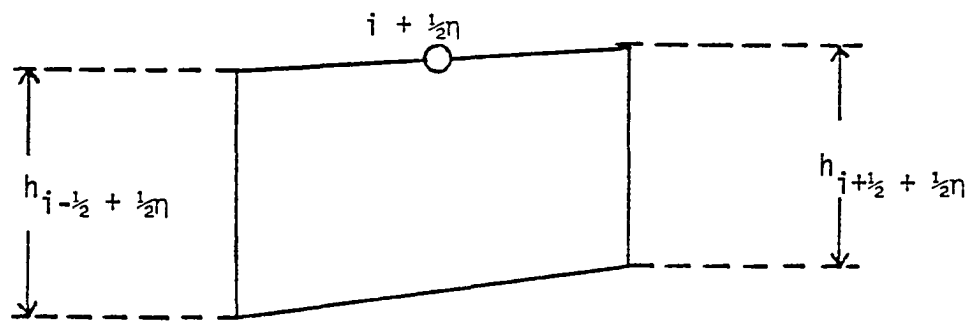


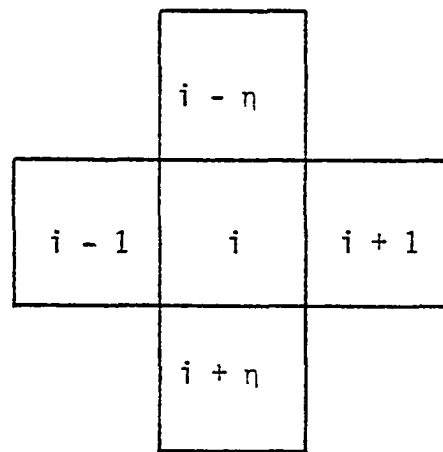
Figure 3.1 - Discretized Reservoir System



Typical cell - Top view



Typical cell - Side view



Typical cell - Arrangement

Figure 3.2 - Cell System Definition

IMPES approach will be used. Thus, the mobility, capillary and gravity terms will be evaluated at the previous time level. Hence equation (2.18) becomes

$$\frac{\partial}{\partial x} (h\lambda_t \frac{\partial P^{n+1}}{\partial x}) + \frac{\partial}{\partial y} (h\lambda_t \frac{\partial P^{n+1}}{\partial y}) = 11.57407408 B_1^n \frac{\partial P^{n+1}}{\partial t} + OT \quad (3.1)$$

for simplicity the subscript "0" is dropped from P.

Each term of equation (3.1) can be differenced separately. The finite difference form of the first term on the left of equation (3.1) is:

$$\begin{aligned} \frac{\partial}{\partial x} (h\lambda_t \frac{\partial P^{n+1}}{\partial x})_i &= \frac{\theta}{\Delta x_i} \left\{ (h\lambda_t)_{x_{i+\frac{1}{2}}} \frac{P_{i+1}^{n+1} - P_i^{n+1}}{\Delta x_{i+\frac{1}{2}}} - (h\lambda_t)_{x_{i-\frac{1}{2}}} \frac{P_i^{n+1} - P_{i-1}^{n+1}}{\Delta x_{i-\frac{1}{2}}} \right\} \\ &+ \frac{(1-\theta)}{\Delta x_i} \left\{ (h\lambda_t)_{x_{i+\frac{1}{2}}} \frac{P_{i+1}^n - P_i^n}{\Delta x_{i+\frac{1}{2}}} - (h\lambda_t)_{x_{i-\frac{1}{2}}} \frac{P_i^n - P_{i-1}^n}{\Delta x_{i-\frac{1}{2}}} \right\} \end{aligned} \quad (3.2)$$

where the variables subscripted as $i-\frac{1}{2}$ or $i+\frac{1}{2}$ are the values of those variables evaluated at the boundary between the i'th and i-1, or i'th and i+1 cells, respectively. The parameter θ is a weighted factor such that if

$\theta = 0$, then the scheme is explicit

$\theta = \frac{1}{2}$, then the scheme is Crank-Nicholson

$\theta = 1$, then the scheme is fully implicit

Similarly the finite difference form of the second term on the left of equation (3.1) is

$$\begin{aligned} \frac{\partial}{\partial y} (h\lambda_t \frac{\partial P^{n+1}}{\partial y})_i &= \frac{\theta}{\Delta y_i} \left\{ (h\lambda_t)_{y_{i+\frac{1}{2}\eta}} \frac{P_{i+\eta}^{n+1} - P_i^{n+1}}{\Delta y_{i+\frac{1}{2}\eta}} - (h\lambda_t)_{y_{i-\frac{1}{2}\eta}} \frac{P_i^{n+1} - P_{i-\eta}^{n+1}}{\Delta y_{i-\frac{1}{2}\eta}} \right\} \\ &+ \frac{(1-\theta)}{\Delta y_i} \left\{ (h\lambda_t)_{y_{i+\frac{1}{2}\eta}} \frac{P_{i+\eta}^n - P_i^n}{\Delta y_{i+\frac{1}{2}\eta}} - (h\lambda_t)_{y_{i-\frac{1}{2}\eta}} \frac{P_i^n - P_{i-\eta}^n}{\Delta y_{i-\frac{1}{2}\eta}} \right\} \end{aligned} \quad (3.3)$$

where the variables subscripted as $i-\frac{1}{2}\eta$ or $i+\frac{1}{2}\eta$ are the values of those variables evaluated at the boundary between the $i^{\text{'}}\text{th}$ and $i-\eta$, or $i^{\text{'}}\text{th}$ and $i+\eta$ cells, respectively.

The time derivative of pressure is differenced as follows:

$$\left(\frac{\partial p}{\partial t}\right)_i = \frac{p_i^{n+1} - p_i^n}{\Delta t} \quad (3.4)$$

where

$$\Delta t = t^{n+1} - t^n \quad (3.5)$$

After the development of the finite difference equations for each term of equation (3.1), the linearized finite difference system can be written in the following rearranged form

$$e_i p_{i-\eta}^{n+1} + a_i p_{i-1}^{n+1} + b_i p_i^{n+1} + c_i p_{i+1}^{n+1} + f_i p_{i+\eta}^{n+1} = d_i \quad (3.6)$$

where the coefficients are

$$e_i = \frac{\theta(h\lambda_t) y_{i-\frac{1}{2}\eta}}{\Delta y_i \Delta y_{i-\frac{1}{2}\eta}} \quad (3.7)$$

$$a_i = \frac{\theta(h\lambda_t) x_{i-\frac{1}{2}}}{\Delta x_i \Delta x_{i-\frac{1}{2}}} \quad (3.8)$$

$$c_i = \frac{\theta(h\lambda_t) x_{i+\frac{1}{2}}}{\Delta x_i \Delta x_{i+\frac{1}{2}}} \quad (3.9)$$

$$f_i = \frac{\theta(h\lambda_t) y_{i+\frac{1}{2}\eta}}{\Delta y_i \Delta y_{i+\frac{1}{2}\eta}} \quad (3.10)$$

$$b_i = -e_i - a_i - c_i - f_i - 11.57407408 B_{1i}/\Delta t \quad (3.11)$$

the right hand side is

$$d_i = -11.57407408 B_{1i} P_i^n / \Delta t + OT_i \quad (3.12)$$

where the variable OT_i consists of all of the values based on the last time step and is defined by

$$OT_i = 11.57407408 B_{2i} + B_{3i} + 0.001 B_{4i} + CN_i \quad (3.13)$$

the Crank-Nicholson term is:

$$CN_i = \frac{1-\theta}{\theta} \{ -e_i P_{i-\eta}^n - a_i P_{i-1}^n + (e_i + a_i + c_i + f_i) P_i^n - c_i P_{i+1}^n - f_i P_{i+\eta}^n \} \quad (3.14)$$

the weighted dimensions of the cells are

$$\Delta y_{i-\frac{1}{2}\eta} = \frac{1}{2} (\Delta y_i + \Delta y_{i-\eta}) \quad (3.15)$$

$$\Delta x_{i-\frac{1}{2}} = \frac{1}{2} (\Delta x_i + \Delta x_{i-1}) \quad (3.16)$$

$$\Delta x_{i+\frac{1}{2}} = \frac{1}{2} (\Delta x_{i+1} + \Delta x_i) \quad (3.17)$$

$$\Delta y_{i+\frac{1}{2}\eta} = \frac{1}{2} (\Delta y_{i+\eta} + \Delta y_i) \quad (3.18)$$

the PVT term is

$$B_{1i} = h_i \phi_i (S_o C_o + S_w C_w + S_g C_g + C_r)_i \quad (3.19)$$

The production term is

$$B_{2i} = -\frac{1}{\Delta x_i \Delta y_i} \left\{ \frac{q_g \rho_g^*}{\rho_g} + q_o \rho_o^* \left(\frac{1}{\rho_o} - \frac{R_{so}}{\rho_g} \right) + q_w \rho_w^* \left(\frac{1}{\rho_w} - \frac{R_{sw}}{\rho_g} \right) \right\}_i \quad (3.20)$$

the capillary pressure term is

$$B_{3i} = B_{3wi} - B_{3gi} \quad (3.21)$$

$$\begin{aligned} B_{3ji} &= (h\lambda_j)_{x_{i+\frac{1}{2}}} \frac{(p_{cj})_{i+1} - (p_{cj})_i}{\Delta x_i \Delta x_{i+\frac{1}{2}}} \\ &- (h\lambda_j)_{x_{i-\frac{1}{2}}} \frac{(p_{cj})_i - (p_{cj})_{i-1}}{\Delta x_i \Delta x_{i-\frac{1}{2}}} \\ &+ (h\lambda_j)_{y_{i+\frac{1}{2}\eta}} \frac{(p_{cj})_{i+\eta} - (p_{cj})_i}{\Delta y_i \Delta y_{i+\frac{1}{2}\eta}} \\ &- (h\lambda_j)_{y_{i-\frac{1}{2}\eta}} \frac{(p_{cj})_i - (p_{cj})_{i-\eta}}{\Delta y_i \Delta y_{i-\frac{1}{2}\eta}} \end{aligned} \quad (3.22)$$

and the gravity term is

$$\begin{aligned} B_{4i} &= - \sum_j^{o,g,w} \{ (h\lambda_j)_{x_{i+\frac{1}{2}}} \frac{(\rho_j g D)_{i+1} - (\rho_j g D)_i}{\Delta x_i \Delta x_{i+\frac{1}{2}}} \\ &- (h\lambda_j)_{x_{i-\frac{1}{2}}} \frac{(\rho_j g D)_i - (\rho_j g D)_{i-1}}{\Delta x_i \Delta x_{i-\frac{1}{2}}} \\ &+ (h\lambda_j)_{y_{i+\frac{1}{2}\eta}} \frac{(\rho_j g D)_{i+\eta} - (\rho_j g D)_i}{\Delta y_i \Delta y_{i+\frac{1}{2}\eta}} \\ &- (h\lambda_j)_{y_{i-\frac{1}{2}\eta}} \frac{(\rho_j g D)_i - (\rho_j g D)_{i-\eta}}{\Delta y_i \Delta y_{i-\frac{1}{2}\eta}} \} \end{aligned} \quad (3.23)$$

If the finite difference approximation, equation (3.6), developed for cell i is written for all cells in the $x-y$ rectangular mesh, a set of linear equations is obtained. Those equations can be written in the following matrix form:

$$\underline{A} \underline{P} = \underline{d} \quad (3.24)$$

The form of matrix A depends upon the ordering scheme by which the cells of the x-y mesh are linearly indexed. This system of equations can be solved either by iterative methods or by direct methods. These methods will be discussed in chapter IV, V, and VI.

3.2 Explicit Solution of Saturations

The new oil saturation can be developed from the oil phase equation. Neglecting the second degree derivative term in equation (2.12), the saturation time derivative would be:

$$\begin{aligned} \frac{\partial S_o}{\partial t} = & \frac{1}{h\phi} \left[\frac{\partial}{\partial x} (h\lambda_o \frac{\partial P}{\partial x}) + \frac{\partial}{\partial x} \{ h\lambda_o \frac{\partial (\rho_o g D)}{\partial x} \} \right. \\ & \left. + \frac{\partial}{\partial y} (h\lambda_o \frac{\partial P}{\partial y}) + \frac{\partial}{\partial y} \{ h\lambda_o \frac{\partial (\rho_o g D)}{\partial y} \} \right] \\ & - \frac{S_o}{\rho_o} \frac{\partial \rho_o}{\partial t} - \frac{S_o}{\phi} \frac{\partial \phi}{\partial t} + \frac{q_o \rho_o^*}{h\phi A \rho_o} \end{aligned} \quad (3.25)$$

Similarly, the new water saturation can be developed from the water phase equation. Neglecting the second degree derivative term in equation (2.13), the saturation time derivative would be:

$$\begin{aligned} \frac{\partial S_w}{\partial t} = & \frac{1}{h\phi} \left[\frac{\partial}{\partial x} (h\lambda_w \frac{\partial P}{\partial x}) + \frac{\partial}{\partial x} \{ h\lambda_w \frac{\partial (\rho_w g D)}{\partial x} \} - \frac{\partial}{\partial x} (h\lambda_w \frac{\partial P_{cw}}{\partial x}) \right. \\ & \left. + \frac{\partial}{\partial y} (h\lambda_w \frac{\partial P}{\partial y}) + \frac{\partial}{\partial y} \{ h\lambda_w \frac{\partial (\rho_w g D)}{\partial y} \} - \frac{\partial}{\partial y} (h\lambda_w \frac{\partial P_{cw}}{\partial y}) \right] \\ & - \frac{S_w}{\rho_w} \frac{\partial \rho_w}{\partial t} - \frac{S_w}{\phi} \frac{\partial \phi}{\partial t} + \frac{q_w \rho_w^*}{h\phi A \rho_w} \end{aligned} \quad (3.26)$$

The finite difference approximation of the oil and water saturation equations is

$$\begin{aligned}
 S_{ji}^{n+1} = & \left[S_{ji}^n + \frac{0.0864\Delta t}{h_i \phi_i^{n+1}} \{ (h\lambda_j)_{x_{i+\frac{1}{2}}} \frac{p_{i+1}^{n+1} - p_i^{n+1}}{\Delta x_i \Delta x_{i+\frac{1}{2}}} \right. \\
 & - (h\lambda_j)_{x_{i-\frac{1}{2}}} \frac{p_i^{n+1} - p_{i-1}^{n+1}}{\Delta x_i \Delta x_{i-\frac{1}{2}}} + (h\lambda_j)_{y_{i+\frac{1}{2}\eta}} \frac{p_{i+\eta}^{n+1} - p_i^{n+1}}{\Delta y_i \Delta y_{i+\frac{1}{2}\eta}} \\
 & \left. - (h\lambda_j)_{y_{i-\frac{1}{2}\eta}} \frac{p_i^{n+1} - p_{i-\eta}^{n+1}}{\Delta y_i \Delta y_{i-\frac{1}{2}\eta}} \} + B_{ji}^n \right] / (3 - \frac{\phi_i^n}{\phi_i^{n+1}} - \frac{\rho_{ji}^n}{\rho_{ji}^{n+1}}) \quad (3.27)
 \end{aligned}$$

where

$$B_{oi} = \frac{\Delta t}{h_i \phi_i^{n+1} \Delta x_i \Delta y_i} \left(\frac{q_{oi} \rho_o^*}{\rho_{oi}^{n+1}} \right) + \frac{0.0864\Delta t}{h_i \phi_i^{n+1}} B_{4oi} \quad (3.28)$$

$$B_{wi} = \frac{\Delta t}{h_i \phi_i^{n+1} \Delta x_i \Delta y_i} \left(\frac{q_{wi} \rho_w^*}{\rho_{wi}^{n+1}} \right) + \frac{0.0864\Delta t}{h_i \phi_i^{n+1}} (-B_{3wi} + B_{4wi}) \quad (3.29)$$

$$\begin{aligned}
 B_{3wi} = & (h\lambda_w)_{x_{i+\frac{1}{2}}} \frac{(P_{cw})_{i+1} - (P_{cw})_i}{\Delta x_i \Delta x_{i+\frac{1}{2}}} - (h\lambda_w)_{x_{i-\frac{1}{2}}} \frac{(P_{cw})_i - (P_{cw})_{i-1}}{\Delta x_i \Delta x_{i-\frac{1}{2}}} \\
 & + (h\lambda_w)_{y_{i+\frac{1}{2}\eta}} \frac{(P_{cw})_{i+\eta} - (P_{cw})_i}{\Delta y_i \Delta y_{i+\frac{1}{2}\eta}} - (h\lambda_w)_{y_{i-\frac{1}{2}\eta}} \frac{(P_{cw})_i - (P_{cw})_{i-\eta}}{\Delta y_i \Delta y_{i-\frac{1}{2}\eta}}
 \end{aligned} \quad (3.30)$$

$$\begin{aligned}
 B_{4ji} = & 0.001 g \{ (h\lambda_j)_{x_{i+\frac{1}{2}}} \frac{(\rho_j^D)_{i+1} - (\rho_j^D)_i}{\Delta x_i \Delta x_{i+\frac{1}{2}}} - (h\lambda_j)_{x_{i-\frac{1}{2}}} \frac{(\rho_j^D)_i - (\rho_j^D)_{i-1}}{\Delta x_i \Delta x_{i-\frac{1}{2}}} \\
 & + (h\lambda_j)_{y_{i+\frac{1}{2}\eta}} \frac{(\rho_j^D)_{i+\eta} - (\rho_j^D)_i}{\Delta y_i \Delta y_{i+\frac{1}{2}\eta}} - (h\lambda_j)_{y_{i-\frac{1}{2}\eta}} \frac{(\rho_j^D)_i - (\rho_j^D)_{i-\eta}}{\Delta y_i \Delta y_{i-\frac{1}{2}\eta}} \}
 \end{aligned} \quad (3.31)$$

The gas saturation is determined from equation (2.10)

$$S_{g_i} = 1 - S_{o_i} - S_{w_i} \quad (3.32)$$

3.3 Discretization of the Flow Coefficient ($h\lambda$)

The flow coefficient is broken into three different units as follows:

$$(h\lambda_j)_{x_{i-\frac{1}{2}}} = (k_x h)_{i-\frac{1}{2}} (k_{rj})_{i-\frac{1}{2}} / (\mu_j)_i \quad (3.33)$$

$$(h\lambda_j)_{y_{i-\frac{1}{2}\eta}} = (k_y h)_{i-\frac{1}{2}\eta} (k_{rj})_{i-\frac{1}{2}\eta} / (\mu_j)_i \quad (3.34)$$

where $j = o, g, w$

The coefficient $(k_x h)_{i-\frac{1}{2}}$ is evaluated by averaging k_x and h at cells i and $i-1$. The average k_x for series flow in linear bed is⁴

$$k_{x_{i-\frac{1}{2}}} = \frac{\frac{\Delta x_i + \Delta x_{i-1}}{2}}{\frac{k_{x_i}}{\Delta x_i} + \frac{k_{x_{i-1}}}{\Delta x_{i-1}}} \quad (3.35)$$

The value of $h_{i-\frac{1}{2}}$ is evaluated by considering a profile of two adjacent cells as shown in Figure 3.3. The shaded area in Figure 3.3 is equal to

$$\frac{h_{i-1} + h_i}{2} \left(\frac{\Delta x_i}{2} + \frac{\Delta x_{i-1}}{2} \right) \quad (3.36)$$

but, this area is also equal to

$$\frac{h_i + h_{i-\frac{1}{2}}}{2} \left(\frac{\Delta x_{i-1}}{2} \right) + \frac{h_{i-\frac{1}{2}} + h_i}{2} \left(\frac{\Delta x_i}{2} \right) \quad (3.37)$$

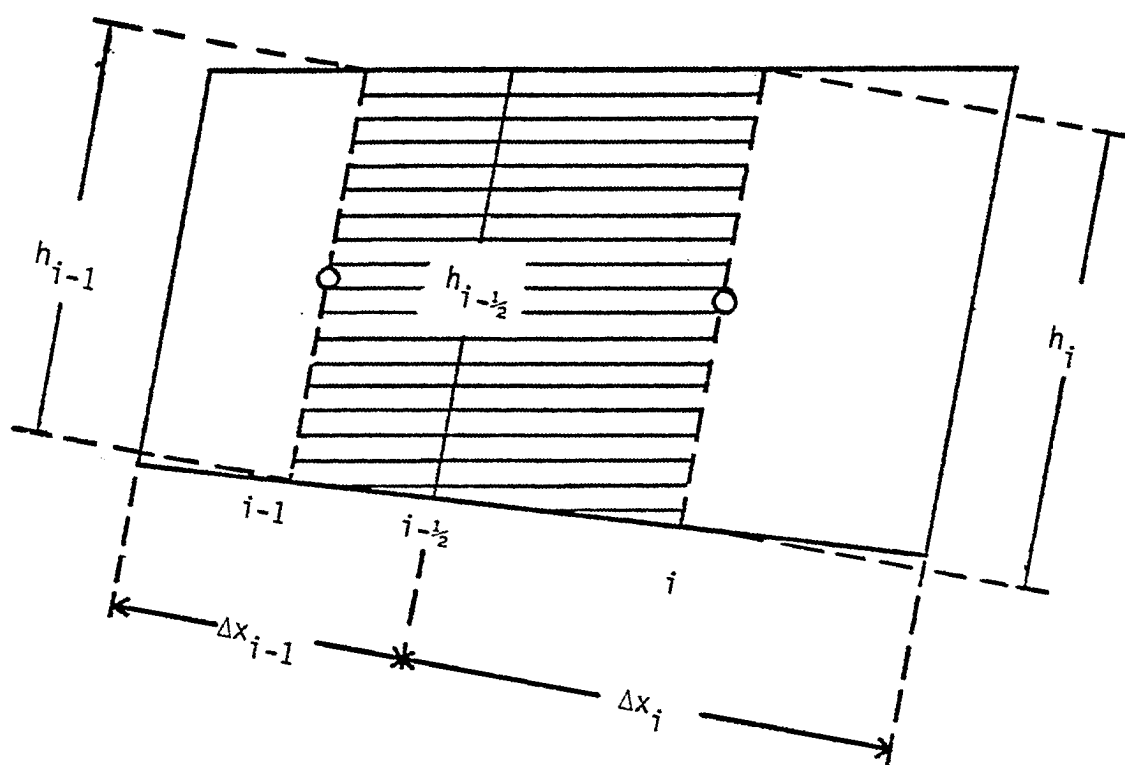


Figure 3.3 - Profile of Two Adjacent Cells

Equating equations (3.36) and (3.37) and solving for $h_{i-\frac{1}{2}}$, we obtain

$$h_{i-\frac{1}{2}} = \frac{h_{i-1}\Delta x_i + h_i\Delta x_{i-1}}{\Delta x_{i-1} + \Delta x_i} \quad (3.38)$$

Combining equations (3.35) and (3.38), we get

$$(k_x h)_{i-\frac{1}{2}} = \frac{\Delta x_i h_{i-1} + \Delta x_{i-1} h_i}{\Delta x_i/k_{x_i} + \Delta x_{i-1}/k_{x_{i-1}}} \quad (3.39)$$

At the left boundary where $i-1$ is outside the reservoir

$$(k_x h)_{i-\frac{1}{2}} = (k_x h)_i \quad (3.40)$$

and at the right boundary where i is outside the reservoir

$$(k_x h)_{i-\frac{1}{2}} = (k_x h)_{i-1} \quad (3.41)$$

with similar equations for $(k_y h)_{i-\frac{1}{2}}$.

The extrapolated relative permeability method developed by Todd, et al.¹⁶ is used to evaluate $(k_r)_{x_{i-\frac{1}{2}}}$ and $(k_r)_{y_{i-\frac{1}{2}}}$ for oil, water and gas phases. For flow in the plus x-direction (ascending values of i)

$$(k_r)_{x_{i-\frac{1}{2}}} = k_{r_{i-1}} + \frac{\Delta x_{i-1}}{\Delta x_{i-1} + \Delta x_{i-2}} (k_{r_{i-1}} - k_{r_{i-2}}) \quad (3.42)$$

For flow in the minus x-direction (decreasing values of i)

$$(k_r)_{x_{i-\frac{1}{2}}} = k_{r_i} - \frac{\Delta x_i}{\Delta x_i + \Delta x_{i+1}} (k_{r_{i+1}} - k_{r_i}) \quad (3.43)$$

The above two equations are subjected to the following constraints:

$$(k_r)_{x_{i-\frac{1}{2}}} \geq 0 \quad (3.44)$$

and

$$(k_r)_{x_{i-\frac{1}{2}}} \leq \max \{(k_r)_{x_i}, (k_r)_{x_{i-1}}\} \quad (3.45)$$

with similar equations and constraints for $(k_r)_{y_{i-\frac{1}{2n}}}$.

It is obvious from equation (3.42) and (3.43) that the method of Todd, et al.¹⁶ is based on the extrapolation of relative permeability value at the interblock location based on the two upstream values. At the points where application of equation (3.42) and (3.43) would result in error, the single point upstream relative permeability is used instead. This happens at the boundary and near sink or source cells. The upstream equation for flow in the plus x-direction is

$$(k_r)_{x_{i-\frac{1}{2}}} = k_{r_{i-1}} \quad (3.46)$$

and for flow in the minus x-direction is

$$(k_r)_{x_{i-\frac{1}{2}}} = k_{r_i} \quad (3.47)$$

with similar equations for $(k_r)_{y_{i-\frac{1}{2n}}}$. The flow chart for the calculation of interblock relative permeability is given in Figure 3.4.

The viscosity terms are evaluated at the cell i because the viscosity is a weak function of pressure.

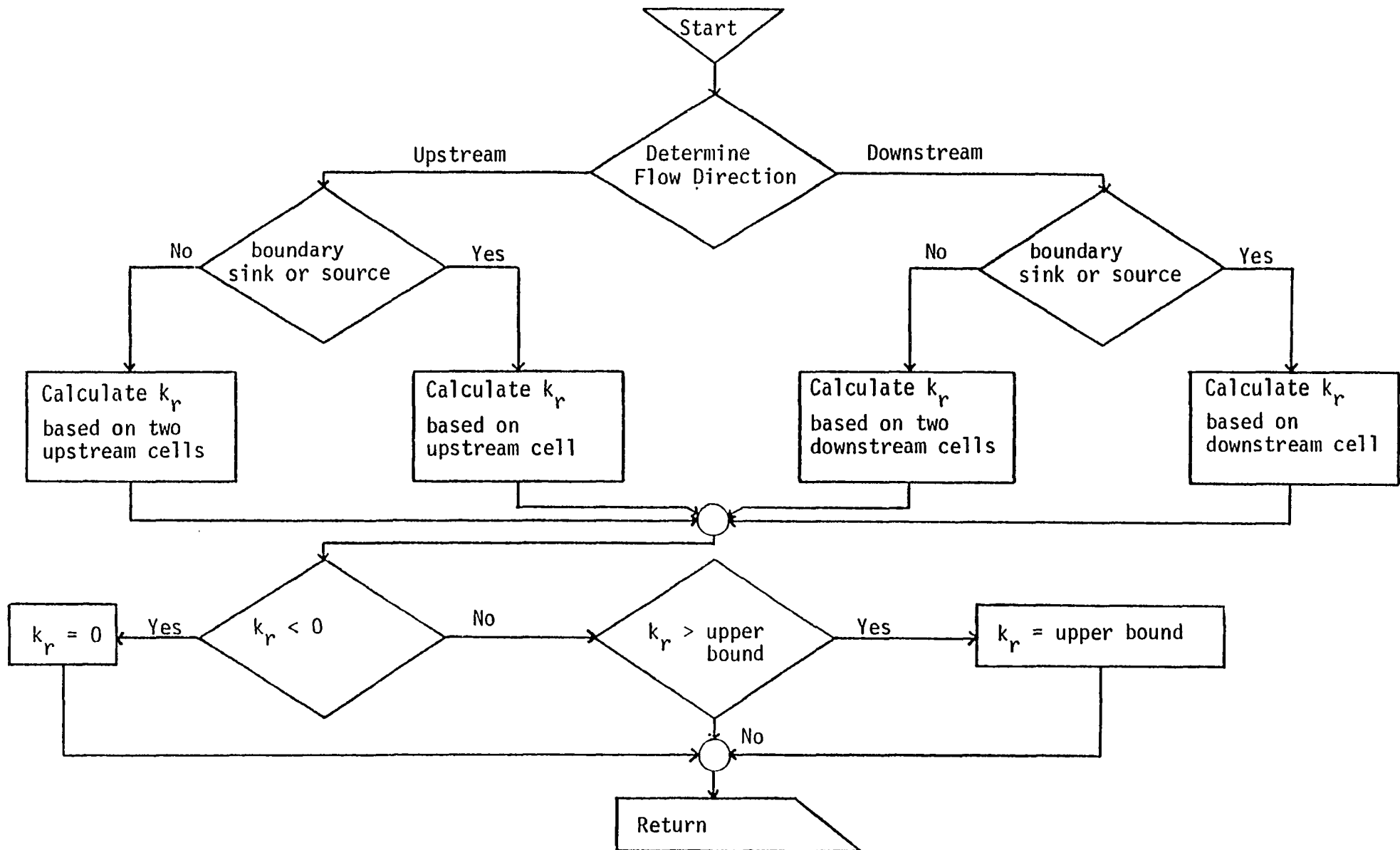


Figure 3.4 - Flow chart for the calculation of interblock relative permeability

3.4 Boundary Conditions

Equations (2.50) and (2.51) are satisfied by the use of reflection principle.

$$P_i - P_{i-\eta} = 0 \quad \forall i \ni h_{i-\eta} = 0 \quad (3.48)$$

$$P_i - P_{i-1} = 0 \quad \forall i \ni h_{i-1} = 0 \quad (3.49)$$

$$P_{i+1} - P_i = 0 \quad \forall i \ni h_{i+1} = 0 \quad (3.50)$$

$$P_{i+\eta} - P_i = 0 \quad \forall i \ni h_{i+\eta} = 0 \quad (3.51)$$

It is noticeable that these terms are associated with certain flow coefficients all the time. Equations (3.48) through (3.51) can be replaced by

$$(h\lambda_j)_{i-\frac{1}{2}\eta} = 0 \quad \forall i \ni h_{i-\eta} = 0 \quad (3.52)$$

$$(h\lambda_j)_{i-\frac{1}{2}} = 0 \quad \forall i \ni h_{i-1} = 0 \quad (3.53)$$

$$(h\lambda_j)_{i+\frac{1}{2}} = 0 \quad \forall i \ni h_{i+1} = 0 \quad (3.54)$$

$$(h\lambda_j)_{i+\frac{1}{2}\eta} = 0 \quad \forall i \ni h_{i+\eta} = 0 \quad (3.55)$$

where $j = o, w, g$.

CHAPTER IV

ITERATIVE METHODS

The iterative methods are based on solving the system of equations by successive approximations until the procedure converges to a pre-defined tolerance or an action due to the failure of convergence is taken.

The most popular and effective iterative methods used in petroleum reservoir simulation are

1. Successive Overrelaxation
2. Alternating Direction Implicit
3. Strongly Implicit

These iterative methods will be used to solve the system of linearized equations whose general form is

$$e_i p_{i-\eta} + a_i p_{i-1} + b_i p_i + c_i p_{i+1} + f_i p_{i+\eta} = d_i \quad (4.1)$$

In this study, the maximum absolute relative error of successive iterations is used as the convergence criterion. The maximum absolute relative error r_{\max} must be within the pre-defined tolerance ε as follows:

$$r_{\max} \leq \varepsilon \quad (4.2)$$

where

$$r_{\max} = \max |r_i| \quad \forall i \ni h_i \neq 0 \quad (4.3)$$

and

$$r_i = \frac{p_i^k - p_i^{k-1}}{p_i^k} \quad (4.4)$$

4.1 Successive Overrelaxation

The most popular versions of successive overrelaxation methods used in two dimensional petroleum reservoir simulation are the point and line relaxation.

Point Successive Overrelaxation (PSOR)

The PSOR method is an iterative technique in which improved estimate is computed by applying the following formula at each cell:

$$\tilde{p}_i^{k+1} = \frac{1}{b_i} (d_i - e_i p_{i-n}^{k+1} - a_i p_{i-1}^{k+1} - c_i p_{i+1}^k - f_i p_{i+n}^k) \quad (4.5)$$

After each point, the value of \tilde{p}_i^{k+1} is relaxed

$$p_i^{k+1} = p_i^k + \omega (\tilde{p}_i^{k+1} - p_i^k) \quad (4.6)$$

The factor ω is called the relaxation parameter, and its presence accelerates the convergence process. The PSOR flow chart is given in Figure 4.1.

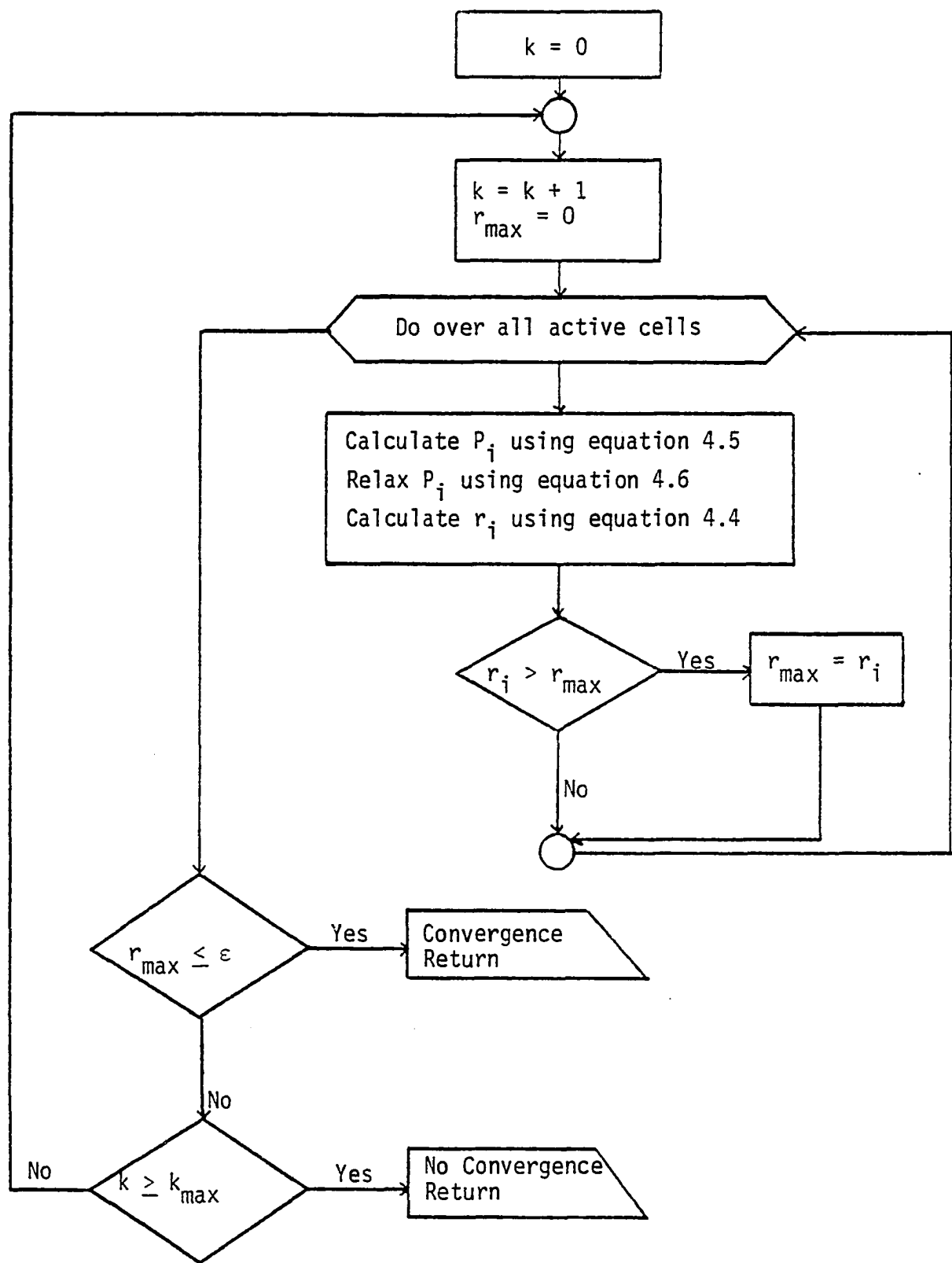


Figure 4.1 - PSOR flow chart

Line Successive Overrelaxation (LSOR)

This technique resolves the two-dimensional problem to a succession of temporary one-dimensional problems which can be solved rather efficiently. Equation (4.1) is written for a general row as

$$a_i \tilde{p}_{i-1}^{k+1} + b_i \tilde{p}_i^{k+1} + c_i \tilde{p}_{i+1}^{k+1} = d'_i \quad (4.7)$$

where

$$d'_i = d_i - e_i p_{i-n}^{k+1} - f_i p_{i+n}^k \quad (4.8)$$

This equation forms a close-band tridiagonal matrix which can be solved by the close-band Thomas algorithm outlined in the next section. The values of P_i obtained for each row at a time are relaxed

$$p_i^{k+1} = p_i^k + \omega (\tilde{p}_i^{k+1} - p_i^k) \quad (4.9)$$

where i is for all the elements in that given row. The LSOR flow chart is given in Figure 4.2.

Relaxation Parameter

An optimum relaxation parameter ω is necessary for maximum efficiency of overrelaxation methods. The selection of this optimum value requires the development of the relationship between the number of iterations required for convergence against a constant tolerance and the relaxation parameter. Several abbreviated simulation runs are usually made with various relaxation parameters. This data is plotted

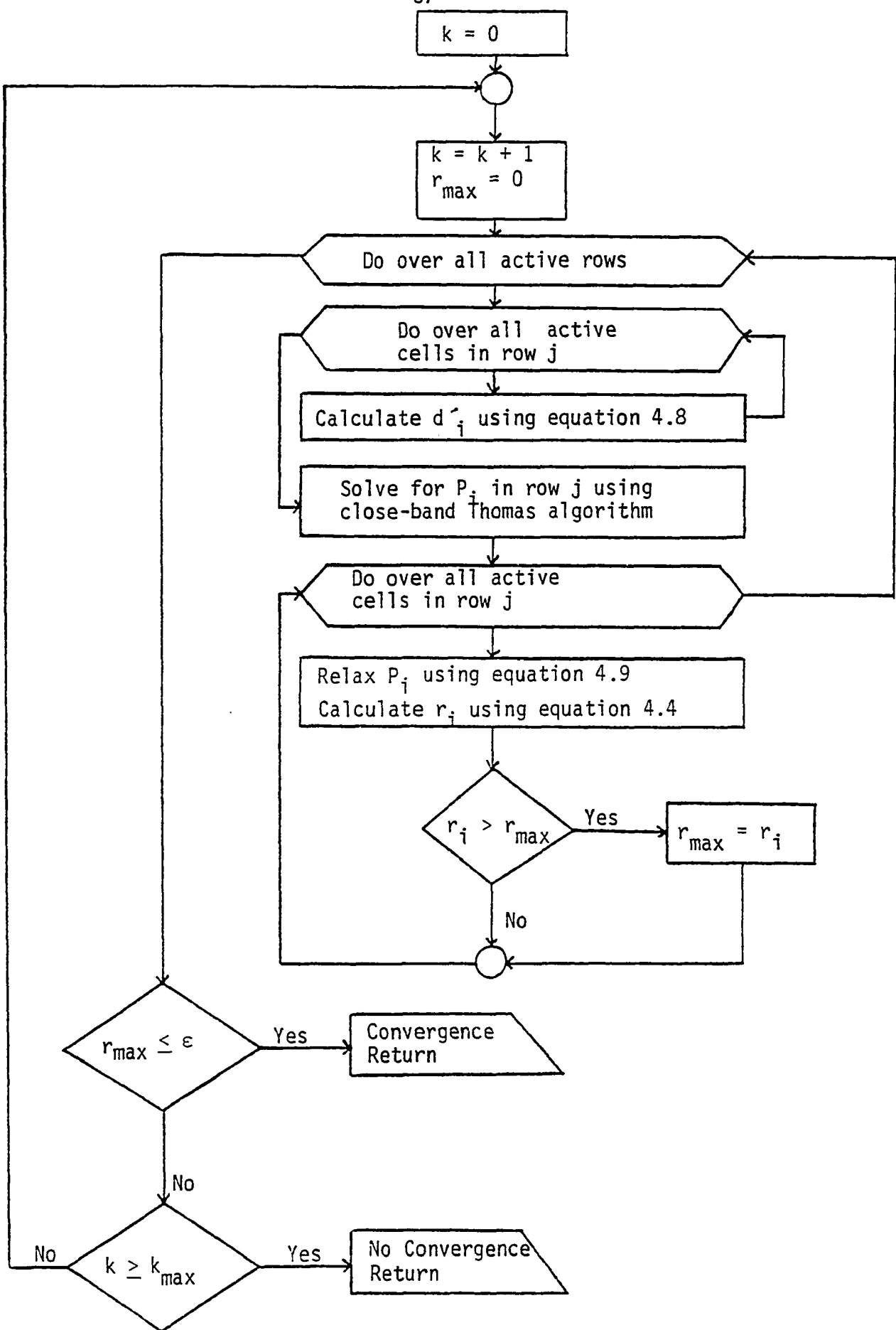


Figure 4.2 - LSOR flow chart

graphically as shown in Figure 4.3. The curve has a characteristic shape, and the best value of ω is the lowest point on the curve. Generally, the more homogeneous the system is, the closer the value of ω to 1.0, while the value of ω approaches 2.0 as the degree of anisotropy of the system increases.

The slope of ω curve is close to linear beyond the optimum ω . This implies that it is generally better to overestimate ω than to underestimate it.

4.2 Alternating Direction Implicit (ADI)

In the ADI¹¹ method, each iteration step is divided into two equal substeps. "During the first substep the cells are swept in the x-direction one row at a time solving for the unknown pressures. In the second substep the system is swept in the y-direction one column at a time solving for the unknown pressures."⁶ The ADI flow chart is given in Figure 4.6.

X-Direction Sweep

Here only those terms contributed by $\frac{\partial}{\partial x} (h\lambda_t \frac{\partial P}{\partial x})$ and $\frac{\partial P}{\partial t}$ will be assumed unknowns. Hence at the k'th iteration, the general equation for the x-direction sweep is

$$a_i p_{i-1}^{k+\frac{1}{2}} + b x_i p_i^{k+\frac{1}{2}} + c_i p_{i+1}^{k+\frac{1}{2}} = d x_i \quad (4.10)$$

where

$$b x_i = -(a_i + c_i + 11.57407408 B_{1i}/\Delta t + \gamma_i \beta)$$

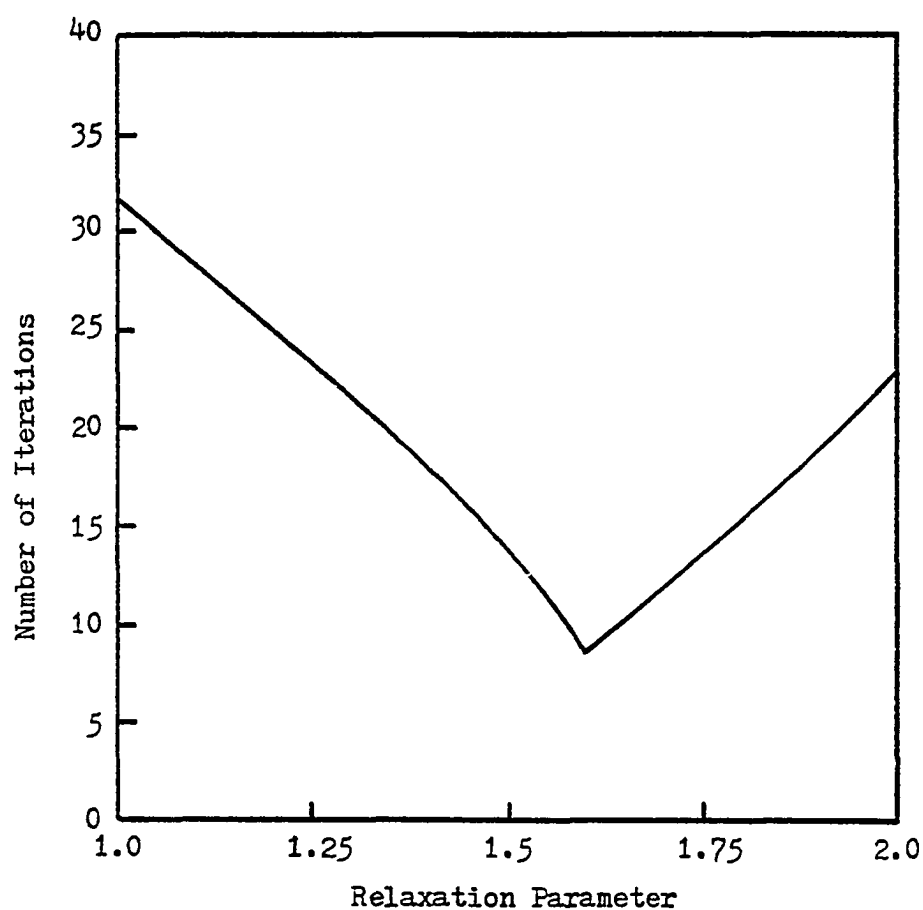


Figure 4.3 - Typical Plot of Relaxation Parameter at Fixed Tolerance

or

$$bx_i = b_i + e_i + f_i - \gamma_i \beta \quad (4.11)$$

$$dx_i = d_i - e_i p_{i-n}^k + (e_i + f_i - \gamma_i \beta) p_i^k - f_i p_{i+n}^k \quad (4.12)$$

and β is an acceleration parameter added to speed up convergence, γ_i is the normalizing factor to account for possible differences in areal size of the cell and for reservoir heterogeneity. The normalizing factor is defined in this study as

$$\gamma_i = \frac{(hk)_{avg}}{\Delta x_i \Delta y_i} \quad (4.13)$$

where

$$(hk)_{avg} = \frac{1}{N} \sum_{i=1}^N h_i \sqrt{k_x i k_y i} \quad (4.14)$$

Equation (4.10) forms a close-band tridiagonal matrix which can be solved by close-band Thomas algorithm.

Close-Band Thomas Algorithm

The equations are

$$a_i p_{i-1} + b_i p_i + c_i p_{i+1} = d_i$$

$$\text{for } 1 \leq i \leq N \quad \text{with } a_1 = a_N = 0 \quad (4.15)$$

The algorithm is as follows:

First, for $1 \leq i \leq N$, compute

$$\zeta_i = b_i - \frac{a_i c_{i-1}}{\zeta_{i-1}} \quad \text{with } \zeta_1 = b_1 \quad (4.16)$$

and

$$\xi_i = \frac{d_i - a_i \zeta_{i-1}}{\zeta_i} \quad \text{with } \xi_1 = \frac{d_1}{b_1} \quad (4.17)$$

The values of the unknowns (P 's) are then computed from

$$P_N = \xi_N \quad \text{and} \quad P_i = \xi_i - \frac{c_i P_{i+1}}{\zeta_i}$$

for $i = N-1, N-2, \dots, 1$ (4.18)

the flow chart for close-band Thomas algorithm is given in Figure 4.4.

y-Direction Sweep

Here only those terms contributed by $\frac{\partial}{\partial y} (h\lambda_t \frac{\partial P}{\partial y})$ and $\frac{\partial P}{\partial t}$ will be assumed unknowns. Hence at the k 'th iteration, the general equation for the y -direction sweep is

$$e_i p_{i-\eta}^{k+1} + b y_i p_i^{k+1} + f_i p_{i+\eta}^{k+1} = d y_i \quad (4.19)$$

where

$$b y_i = -(e_i + f_i + 11.57407408 B_{1i}/\Delta t + \gamma_i \beta)$$

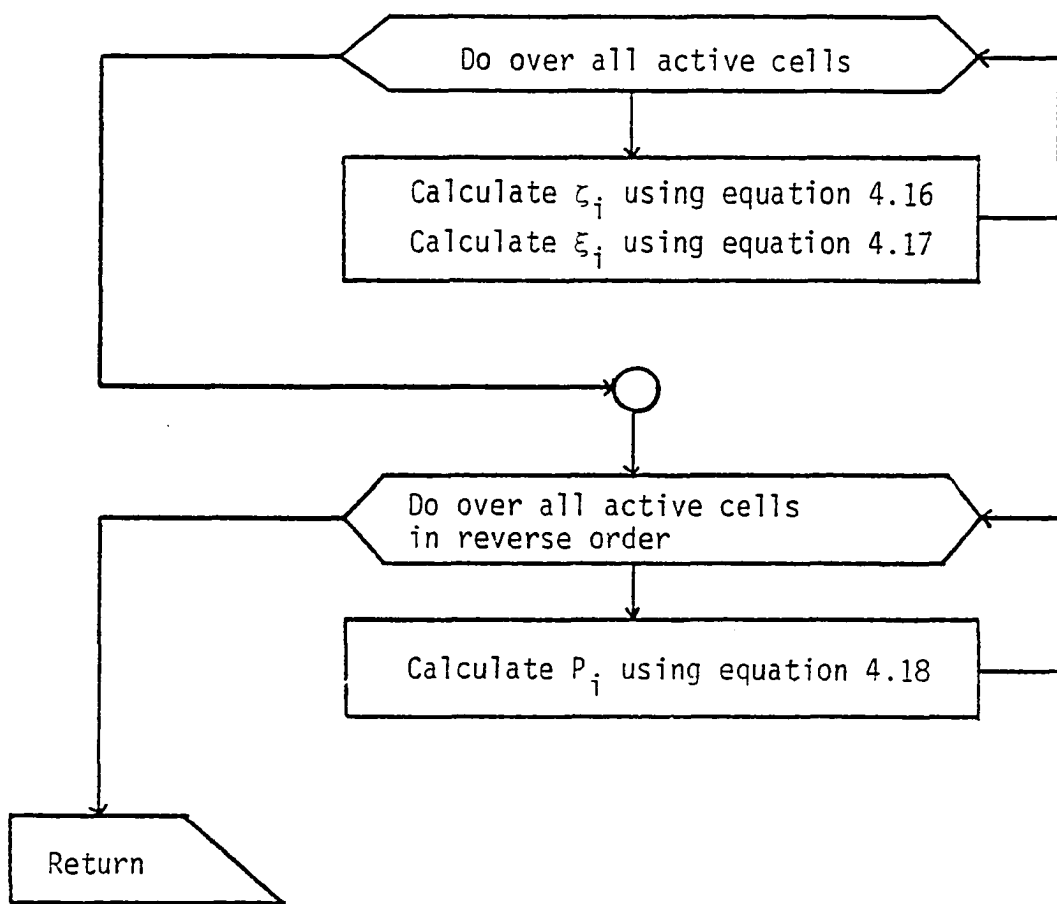


Figure 4.4 - Flow Chart for Close - Band Thomas Algorithm

or

$$by_i = b_i + a_i + c_i - \gamma_i \beta \quad (4.20)$$

$$dy_i = d_i - a_i p_{i-1}^{k+\frac{1}{2}} + (a_i + c_i - \gamma_i \beta) p_i^{k+\frac{1}{2}} - c_i p_{i+1}^{k+\frac{1}{2}} \quad (4.21)$$

Equation (4.19) forms a wide-band tridiagonal matrix which can be solved by wide-band Thomas Algorithm.

Wide-Band Thomas Algorithm

The equations are

$$e_i p_{i-\eta} + b_i p_i + f_i p_{i+\eta} = d_i$$

$$\text{for } 1 \leq i \leq N \quad \text{with } e_i = f_{N-i} = 0 \quad \text{for } 1 \leq i \leq \eta \quad (4.22)$$

The algorithm is as follows:

First for $1 \leq i \leq N$, compute

$$\zeta_i = b_i - \frac{e_i f_{i-\eta}}{\zeta_{i-\eta}} \quad \text{with } \zeta_i = b_i \quad \text{for } 1 \leq i \leq \eta \quad (4.23)$$

and

$$\xi_i = \frac{d_i - e_i \zeta_{i-\eta}}{\zeta_i} \quad \text{with } \xi_i = \frac{d_i}{b_i} \quad \text{for } 1 \leq i \leq \eta \quad (4.24)$$

The values of the unknowns are then computed from

$$p_i = \xi_i \quad \text{for } i=N, N-1, \dots, N-\eta + 1$$

and

$$P_i = \xi_i - \frac{f_i P_{i+n}}{\xi_i} \quad \text{for } i=N-n, N-n-1, \dots, 1 \quad (4.25)$$

The flow chart for wide-band Thomas algorithm is given in Figure 4.5.

ADI Acceleration Parameters

To achieve a faster rate of convergence a series of parameters used in sequence is employed. Crichlow⁶ outlined the procedure of Peaceman and Rachford¹¹ to determine the upper and lower limits of the parameter range from the reservoir data.

Four parameters are defined as functions of the x- and y-direction interblock transmissibilities (T_x and T_y) and the number of cells in the x- and y-direction (N_x and N_y) in the following manner

$$M_1 = \frac{2T_x}{T_x + T_y} - \frac{\pi^2}{4N_x^2} \quad (4.26)$$

$$M_2 = \frac{2T_x}{T_x + T_y} \quad (4.27)$$

$$M_3 = \frac{2T_y}{T_x + T_y} - \frac{\pi^2}{4N_y^2} \quad (4.28)$$

$$M_4 = \frac{2T_y}{T_x + T_y} \quad (4.29)$$

where

$$T_x = \frac{\sum_{i=1}^N k_{x_i} \Delta y_i / \Delta x_i}{N} \quad (4.30)$$

$$T_y = \frac{\sum_{i=1}^N k_{y_i} \Delta x_i / \Delta y_i}{N} \quad (4.31)$$

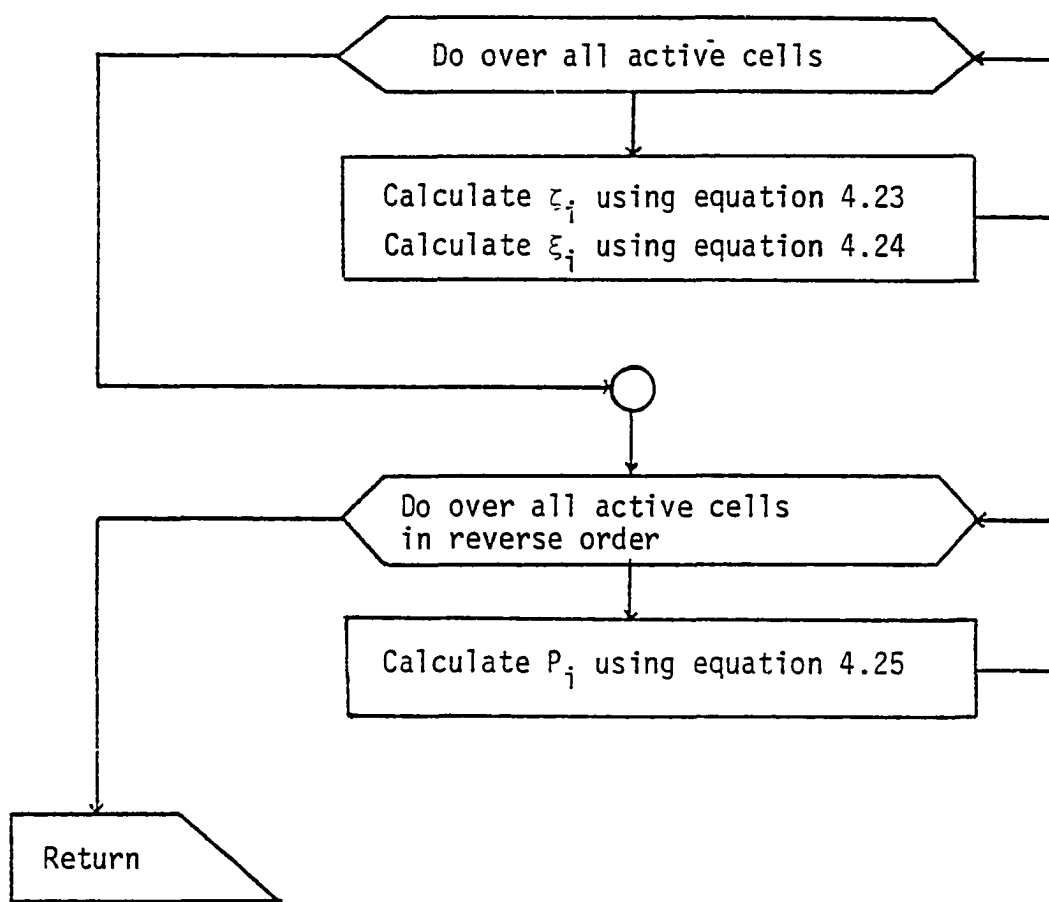


Figure 4.5 - Flow Chart for Wide-Band Thomas Algorithm

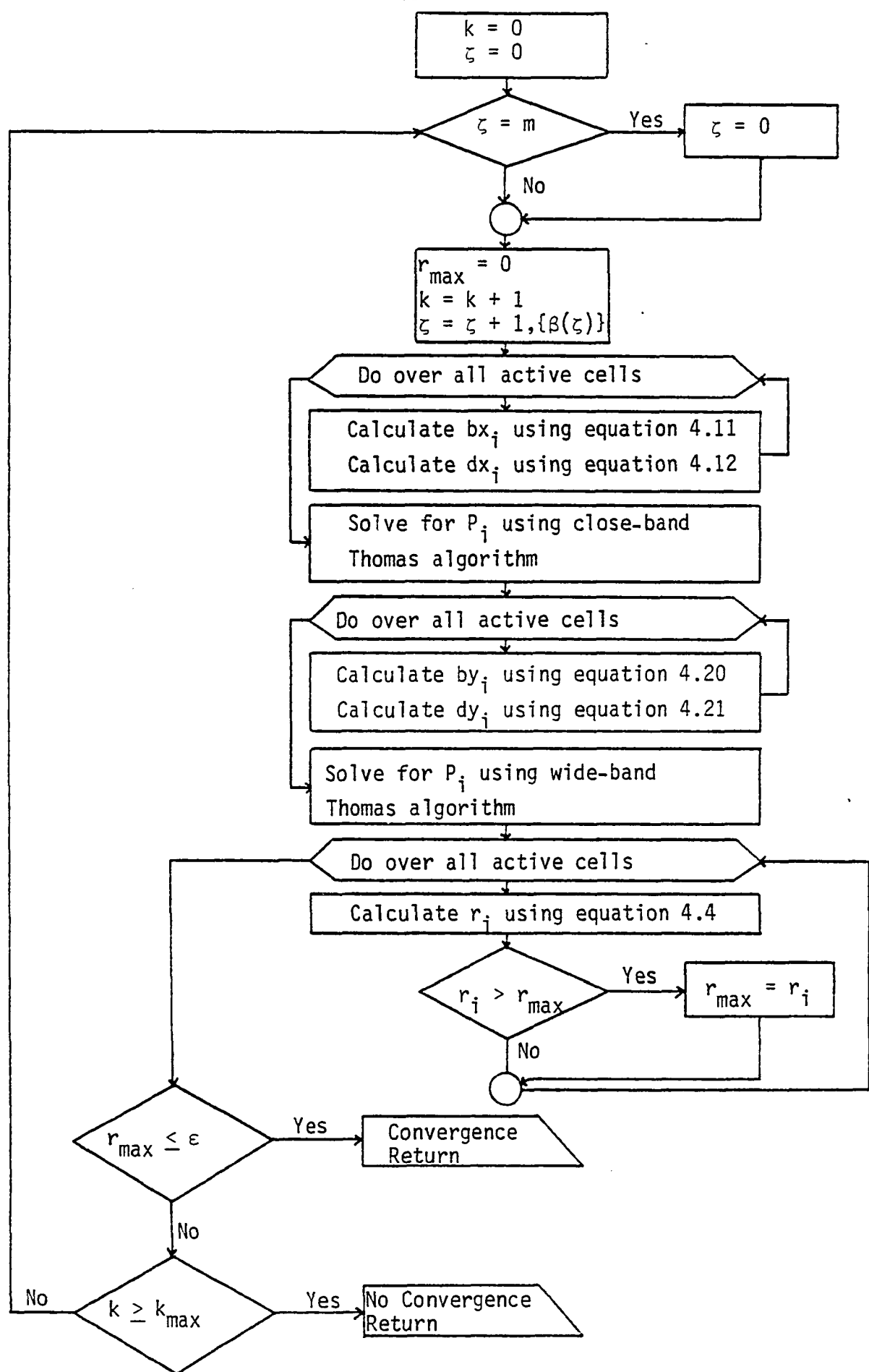


Figure 4.6 - ADI flow chart

The lower limit of the acceleration parameter is calculated from

$$\beta_{\min} = \min(M_1, M_3) \quad (4.32)$$

and the upper limit is calculated from

$$\beta_{\max} = \max(M_2, M_4) \quad (4.33)$$

Several authors^{16,17} have pointed out that the acceleration parameters should be in a geometric series such that

$$\beta_{k+1} = r\beta_k \quad (4.34)$$

where r is the constant multiplier defined by

$$r = (\beta_{\max}/\beta_{\min})^{\frac{1}{m-1}} \quad (4.35)$$

where m is the number of acceleration parameters in the system.

These equations are only a guide and the user must experiment in order to obtain an adequate lower value for β . Since the convergence is very sensitive to β_{\min} .

4.3 Strongly Implicit Procedure (SIP)

The strongly implicit procedure is an iterative technique developed by Stone¹⁴. SIP involves the solution of the system of simultaneous linear equations by an elimination process working on a modified version of the original matrix system. The original pentadiagonal matrix A is

transformed to a heptadiagonal matrix B which is more easily factorable into an LU product. The L and U matrices have only three nonzero elements in each row in contrary to the factorization of matrix A . All SIP associated matrices are shown in Figure 4.8 through 4.12. The SIP flow chart is given in Figure 4.13.

The elements of L and U cannot be selected in such a way that the original A matrix is identical with matrix B . Two matrices are equal if their corresponding elements are equal. This would lead to the following set of relations for each cell point i :

$$e'_i = e_i \quad (4.36)$$

$$g'_i = 0 \quad (4.37)$$

$$a'_i = a_i \quad (4.38)$$

$$b'_i = b_i \quad (4.39)$$

$$c'_i = c_i \quad (4.40)$$

$$h'_i = 0 \quad (4.41)$$

$$f'_i = f_i \quad (4.42)$$

The elements of B are defined in Figure (4.10) and (4.12). The above seven relationships (equation 4.36 through 4.42) cannot all be satisfied. Hence, the transformation of A to B involves the addition of two new elements in equation (4.1). These two elements are associated with the cells $(i-\eta+1)$ and $(i+\eta-1)$ whose coefficients we shall call g_i and h_i respectively. These associated cells are shown in Figure 4.7.

	$i-\eta$	$i-\eta+1$
$i-1$	i	$i+1$
$i+\eta-1$	$i+\eta$	

Figure 4.7 - Cell Arrangement

The new coefficients are multiplied by ε_1 and ε_2 , which are obtained by Taylor's series expansions.

$$\varepsilon_1 = p_{i-\eta+1} - \alpha(-p_i + p_{i-\eta} + p_{i+1}) \quad (4.43)$$

$$\varepsilon_2 = p_{i+\eta-1} - \alpha(-p_i + p_{i-1} + p_{i+\eta}) \quad (4.44)$$

where α is the iteration parameter which accelerates the convergence process. The influence of the new coefficients is minimal since ε_1 and ε_2 are very small.

The addition of the new elements to equation (4.1) results in

$$\begin{aligned} & e_i p_{i-\eta} + a_i p_{i-1} + b_i p_i + c_i p_{i+1} + f_i p_{i+\eta} \\ & + g_i \{ p_{i-\eta+1} - \alpha(-p_i + p_{i-\eta} + p_{i+1}) \} \\ & + h_i \{ p_{i+\eta-1} - \alpha(-p_i + p_{i-1} + p_{i+\eta}) \} = d_i \end{aligned} \quad (4.45)$$

or

$$\begin{aligned} & (e_i - \alpha g_i) p_{i-\eta} + g_i p_{i-\eta+1} + (a_i - \alpha h_i) p_{i-1} \\ & + (b_i + \alpha g_i + \alpha h_i) p_i + (c_i - \alpha g_i) p_{i+1} \\ & + h_i p_{i+\eta-1} + (f_i - \alpha h_i) p_{i+\eta} = d_i \end{aligned} \quad (4.46)$$

The modified coefficient matrix \bar{A} is shown in Figure 4.8.

The strongly implicit procedure consists of an algorithm for odd-numbered iterations and another for even-numbered iterations. Suarez and Farouq Ali¹⁵ have presented a comparison among the three versions of SIP method. They concluded that the two equations of SIP (odd and even) when used give the best results. Hence, a combination of odd and even algorithms will be used in this study.

Odd-Numbered Iteration Algorithm

In odd-numbered iterations, the L and U matrices are chosen as shown in Figure 4.9. With this choice, the coefficients of matrix B(=LU) would be as shown in Figure 4.10. Furthermore, the modified heptadiagonal \bar{A} matrix is identical to B. This is done by the following relations for each cell i:

$$E_i = e_i - \alpha g_i \quad (4.47)$$

$$E_i C_{i-\eta} = g_i \quad (4.48)$$

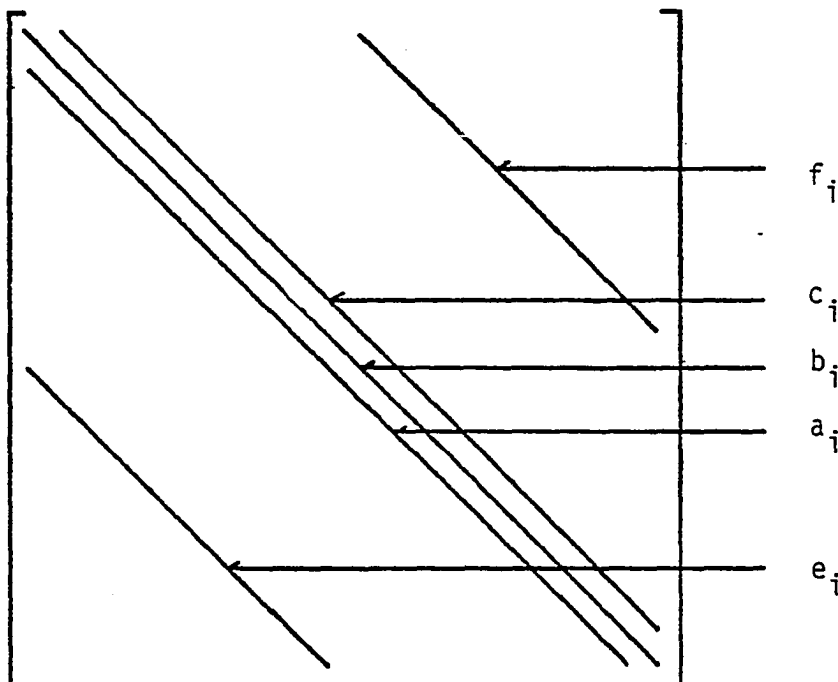
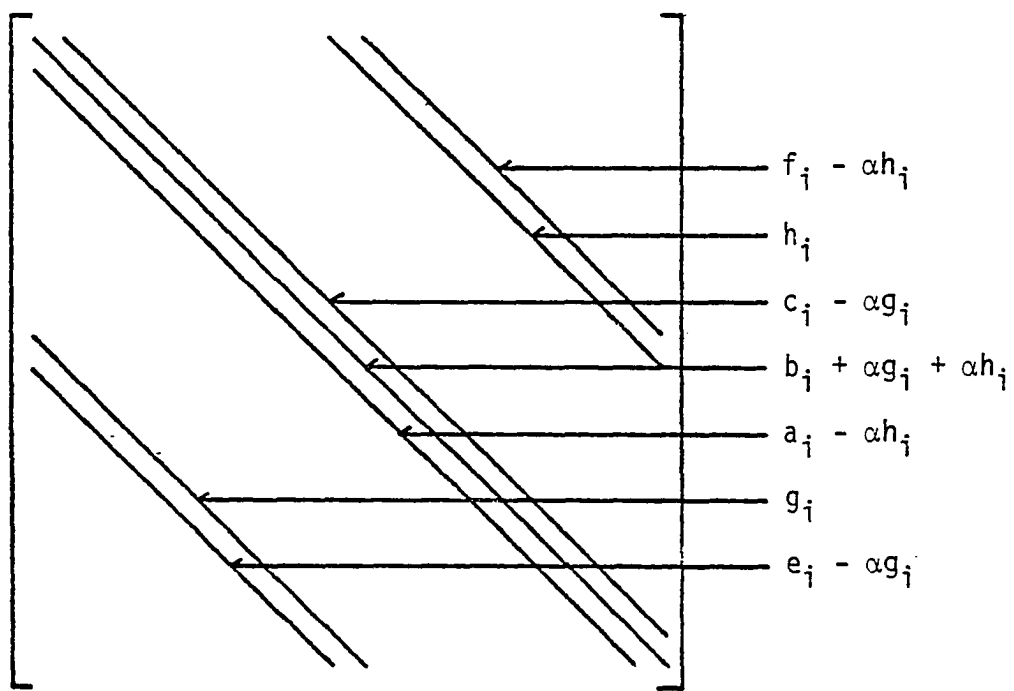
$$A_i = a_i - \alpha h_i \quad (4.49)$$

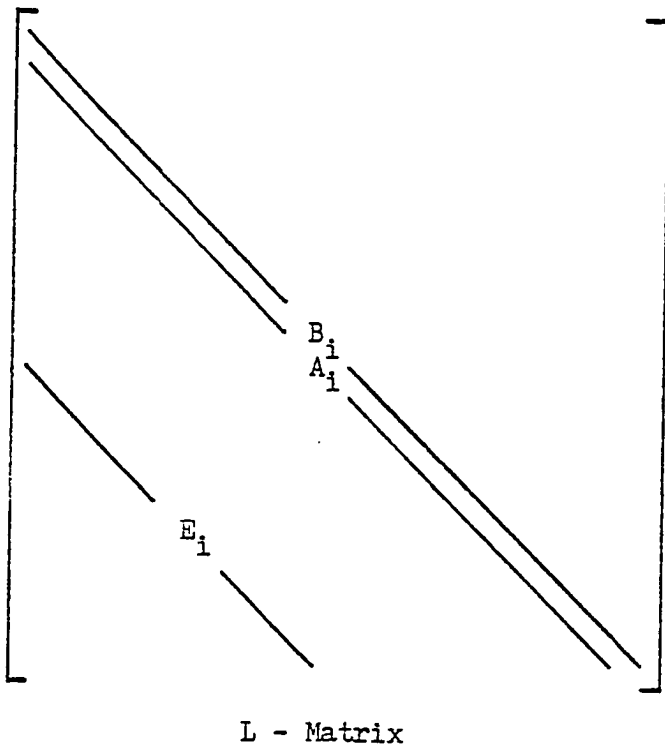
$$B_i + E_i F_{i-\eta} + A_i C_{i-1} = b_i + \alpha g_i + \alpha h_i \quad (4.50)$$

$$B_i C_i = c_i - \alpha g_i \quad (4.51)$$

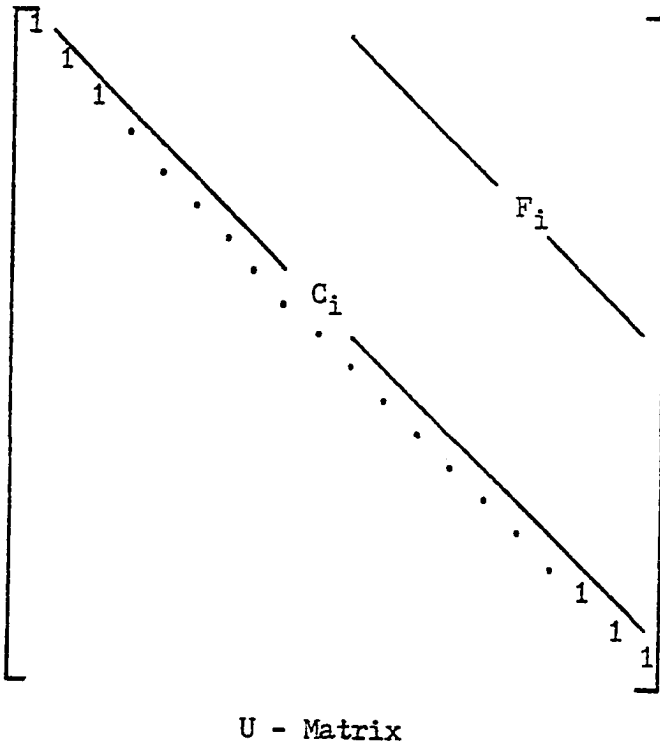
$$A_i F_{i-1} = h_i \quad (4.52)$$

$$B_i F_i = f_i - \alpha h_i \quad (4.53)$$

Original \mathbf{A} matrixModified \mathbf{A} matrixFigure 4.8 - Matrix \mathbf{A} in SIP

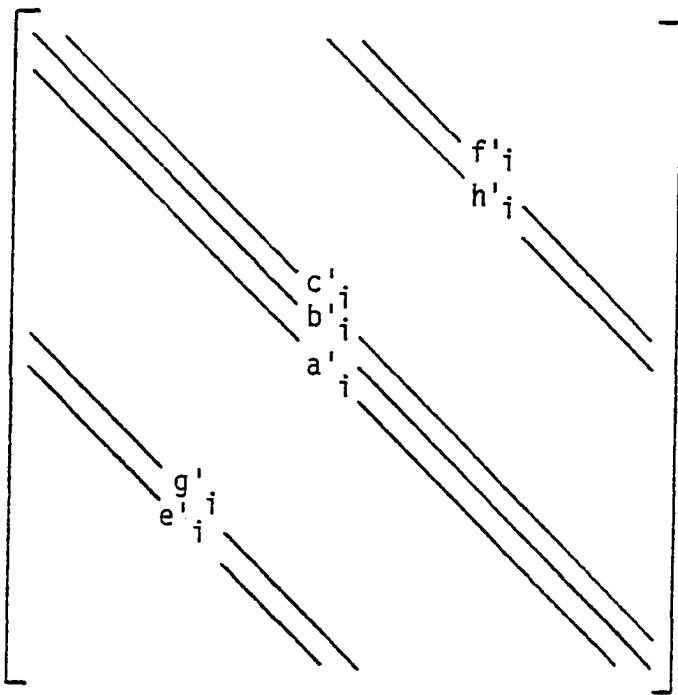


L - Matrix



U - Matrix

Figure 4.9 - L and U matrices for odd-numbered iterations



$$e'_i = E_i$$

$$g'_i = E_i C_{i-\eta}$$

$$a'_i = A_i$$

$$b'_i = B_i + E_i F_{i-\eta} + A_i C_{i-1}$$

$$c'_i = B_i C_i$$

$$h'_i = A_i F_{i-1}$$

$$f'_i = B_i F_i$$

Figure 4.10 - B matrix for odd-numbered iterations
(Coefficients in terms of L and U elements)

The algorithm of the odd-numbered iterations is as follows:

Given

$$\underline{B}\underline{P} = \underline{D} \quad (4.54)$$

where

$$\underline{B} = \underline{L}\underline{U} \quad (4.55)$$

Therefore

$$\underline{L}\underline{U}\underline{P} = \underline{D} \quad (4.56)$$

Letting

$$\underline{U}\underline{P} = \underline{y} \quad (4.57)$$

Then

$$\underline{L}\underline{y} = \underline{D} \quad (4.58)$$

Solving equations (4.58) and (4.57) successively for \underline{y} and \underline{P} respectively:

$$\underline{y} = \underline{L}^{-1}\underline{D} \quad (4.59)$$

and

$$\underline{P} = \underline{U}^{-1}\underline{y} \quad (4.60)$$

Equations (4.47) through (4.53) can be used to compute the elements of L and U matrices recursively for $i=1,2,\dots,N$ as follows:

$$g_i = \frac{e_i c_{i-n}}{\alpha c_{i-n} + 1} \quad (4.61)$$

$$h_i = \frac{a_i f_{i-1}}{\alpha f_{i-1} + 1} \quad (4.62)$$

$$E_i = e_i - \alpha g_i \quad (4.63)$$

$$A_i = a_i - \alpha h_i \quad (4.64)$$

$$B_i = b_i + \alpha g_i + \alpha h_i - E_i F_{i-\eta} - A_i C_{i-1} \quad (4.65)$$

$$C_i = (c_i - \alpha g_i) / B_i \quad (4.66)$$

$$F_i = (f_i - \alpha h_i) / B_i \quad (4.67)$$

The intermediate vector y is computed by forward substitution.

$$y_i = (d_i - E_i y_{i-\eta} - A_i y_{i-1}) / B_i \quad , i = 1, 2, \dots, N \quad (4.68)$$

The pressure vector is calculated by backward substitution.

$$P_i = y_i - C_i P_{i+1} - F_i P_{i+\eta} \quad , i = N, N-1, \dots, 1 \quad (4.69)$$

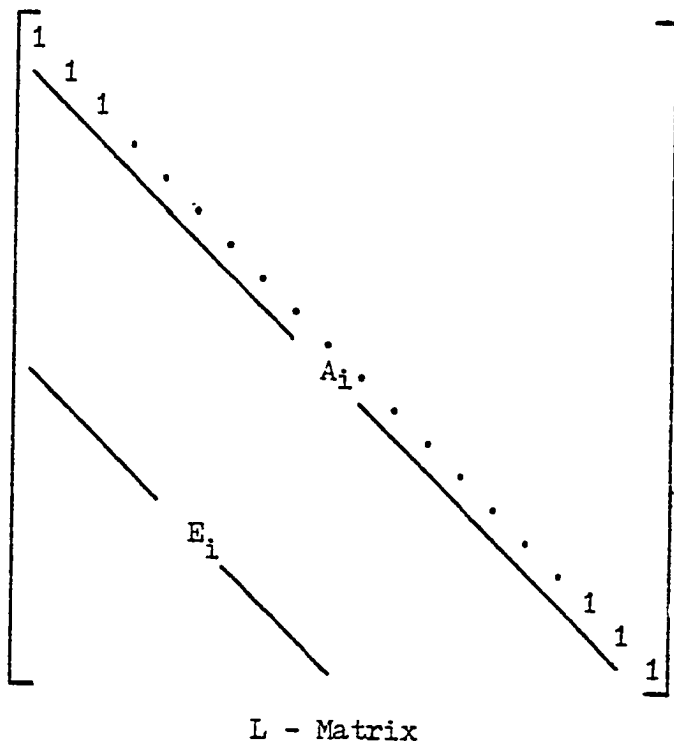
Even-Numbered Iteration Algorithm

In even-numbered iterations, the L and U matrices are chosen as shown in Figure 4.11. With this choice, the coefficients of matrix $B (=UL)$ would be as shown in Figure 4.12. Furthermore, the modified A matrix is identical to B . This is done by the following relations for each cell i :

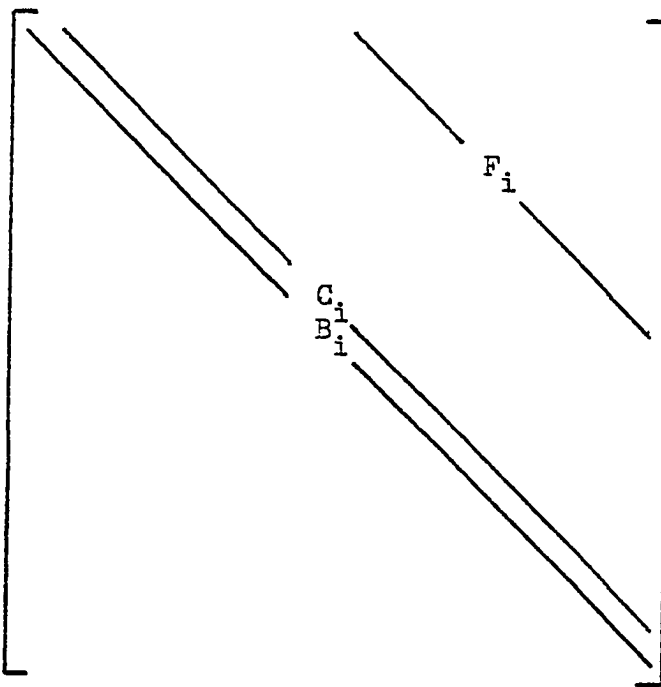
$$E_i B_i = e_i - \alpha g_i \quad (4.70)$$

$$C_i E_{i+1} = g_i \quad (4.71)$$

$$A_i B_i = a_i - \alpha h_i \quad (4.72)$$



L - Matrix



U - Matrix

Figure 4.11 - L and U matrices for even-numbered iterations

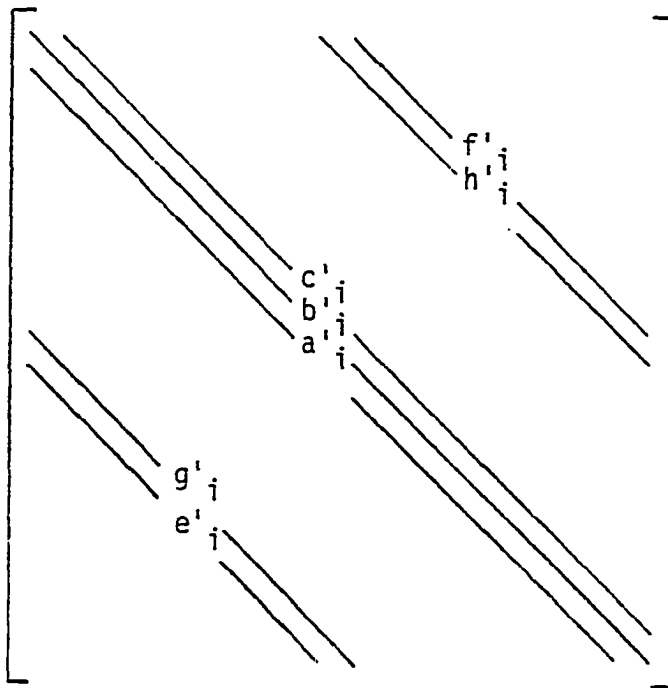


Figure 4.12 - B matrix for even-numbered iterations
(Coefficients in terms of L and U elements)

$$B_i + C_i A_{i+1} + F_i E_{i+\eta} = b_i + \alpha g_i + \alpha h_i \quad (4.73)$$

$$C_i = c_i - \alpha g_i \quad (4.74)$$

$$F_i A_{i+\eta} = h_i \quad (4.75)$$

$$F_i = f_i - \alpha h_i \quad (4.76)$$

The algorithm of the even-numbered iterations is as follows:

Given

$$\underline{BP} = \underline{D} \quad (4.77)$$

Where

$$B = UL \quad (4.78)$$

Therefore

$$\underline{ULP} = \underline{D} \quad (4.79)$$

Letting

$$\underline{LP} = \underline{y} \quad (4.80)$$

Then

$$\underline{Uy} = \underline{D} \quad (4.81)$$

Solving equations (4.81) and (4.80) successively for \underline{y} and \underline{P} respectively:

$$\underline{y} = \underline{U}^{-1} \underline{D} \quad (4.82)$$

and

$$\underline{P} = \underline{L}^{-1} \underline{y} \quad (4.83)$$

Equations (4.70) through (4.76) can be used to compute the elements of L and U matrices recursively for $i=N, N-1, \dots, 1$ as follows:

$$g_i = \frac{c_i E_{i+1}}{\alpha E_{i+1} + 1} \quad (4.84)$$

$$h_i = \frac{f_i A_{i+\eta}}{\alpha A_{i+\eta} + 1} \quad (4.85)$$

$$F_i = f_i - \alpha h_i \quad (4.86)$$

$$C_i = c_i - \alpha g_i \quad (4.87)$$

$$B_i = b_i + \alpha g_i + \alpha h_i - C_i A_{i+1} - F_i E_{i+\eta} \quad (4.88)$$

$$A_i = (a_i - \alpha h_i)/B_i \quad (4.89)$$

$$E_i = (e_i - \alpha g_i)/B_i \quad (4.90)$$

The intermediate vector y is computed by backward substitution.

$$y_i = (d_i - C_i y_{i+1} - F_i y_{i+\eta})/B_i \quad , \quad i=N, N-1, \dots, 1 \quad (4.91)$$

The pressure vector is calculated by forward substitution.

$$P_i = y_i - E_i P_{i-\eta} - A_i P_{i-1} \quad , \quad i=1, 2, \dots, N \quad (4.92)$$

Iteration Parameter α

The minimum parameter used is zero and the maximum (α_{\max}) is determined by²⁰

$$\alpha_{\max} = 1 - \frac{1}{N} \sum_{i=1}^N \min \left[\frac{\pi^2}{2N_x^2 (1 + \zeta)} , \frac{\pi^2}{2N_y^2 (1 + 1/\zeta)} \right] \quad (4.93)$$

where

$$\zeta = \frac{k_y \Delta x^2}{k_x \Delta y^2}$$

Stone¹⁴ concluded that a minimum of four parameters is desirable and each parameter is to be used twice in succession for odd and even numbered iterations respectively. Also, the individual parameters should be geometrically spaced as follows:

$$\alpha_i = 1 - (1 - \alpha_{\max})^{\frac{i-1}{m-1}}, \quad i = 1, 2, \dots, m \quad (4.94)$$

where m is the number of parameters in the system.

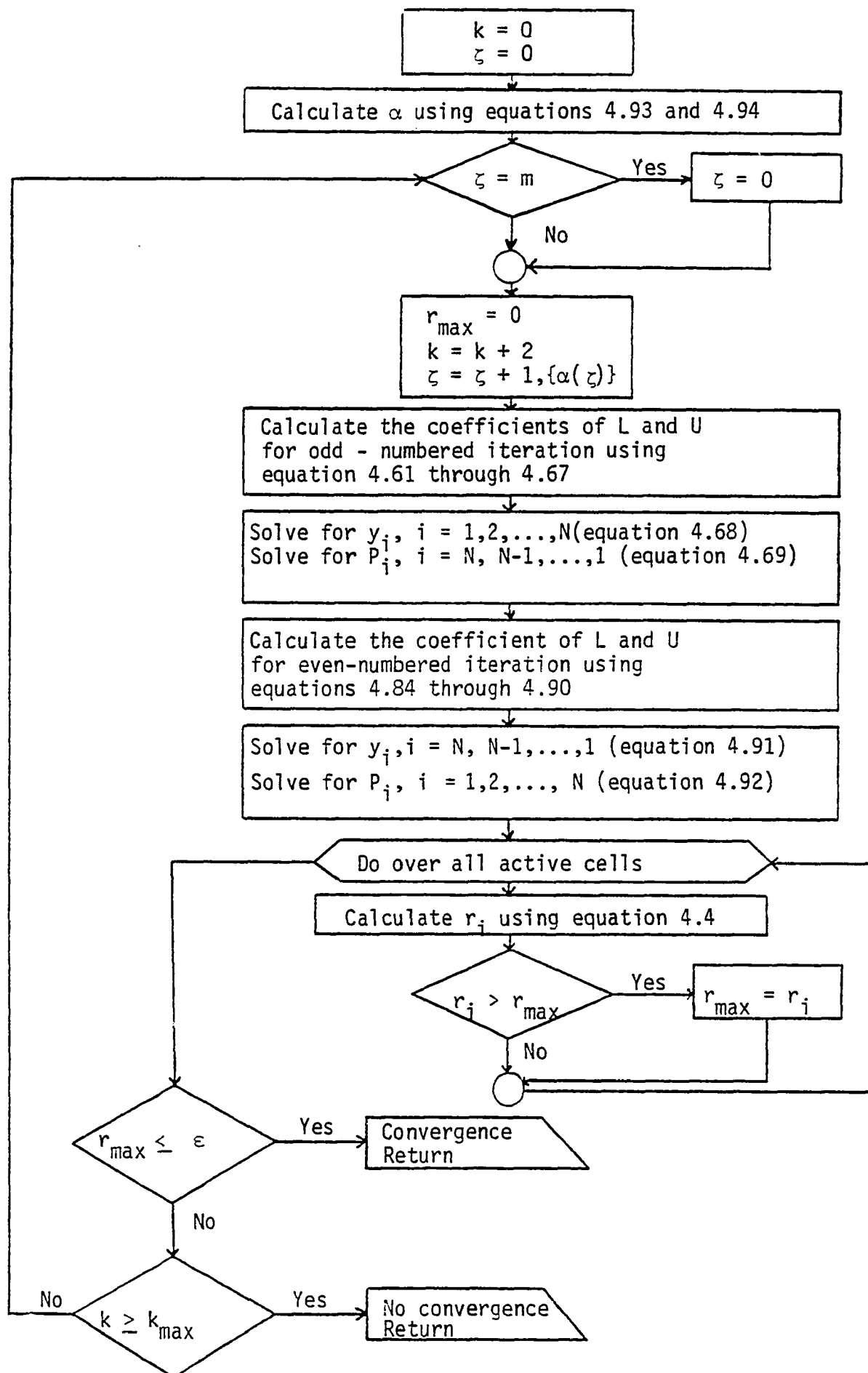


Figure 4.13 - SIP flow chart

CHAPTER V

DIRECT METHODS

Direct methods are those in which the solution to the system of equations is obtained upon the completion of a finite number of arithmetic operations. All direct methods require the same number of arithmetic operations²¹, but the most popular direct method used in reservoir simulation is the LU factorization. The LU factorization method will be outlined to solve the following system of equations (see Figure 5.1):

$$\underline{A} \underline{P} = \underline{d} \quad (5.1)$$

Thereafter, the band and sparsity matrix techniques will be reviewed.

5.1 LU Factorization

This algorithm has been developed by Crout⁷ and it involves the decomposition of the coefficient matrix into a lower triangular matrix and an upper triangular matrix. This decomposition is followed by two consecutive substitution steps to compute the answer. The scheme of this technique is as follows:

Given

$$\underline{A} \underline{P} = \underline{d}$$

then

$$\underline{A} = \underline{L} \underline{U} \quad (5.2)$$

$$\begin{bmatrix} a_{11} & a_{12} & a_{13} & \cdot & \cdot & \cdot & \cdot & \cdot & \cdot & a_{1N} \\ a_{21} & a_{22} & a_{23} & \cdot & \cdot & \cdot & \cdot & \cdot & \cdot & a_{2N} \\ \cdot & \cdot \\ \cdot & \cdot \\ \cdot & \cdot \\ \cdot & \cdot \\ \cdot & \cdot \\ \cdot & \cdot \\ \cdot & \cdot \\ a_{N1} & \cdot & a_{NN} \end{bmatrix} = \begin{bmatrix} p_1 \\ p_2 \\ \cdot \\ p_N \end{bmatrix} = \begin{bmatrix} d_1 \\ d_2 \\ \cdot \\ d_N \end{bmatrix}$$

Figure 5.1 - $\underline{A} \underline{P} = \underline{d}$ System of Equations

The L and U matrices are given in Figure 5.2.

Therefore

$$LUP = \underline{d} \quad (5.3)$$

Letting

$$UP = \underline{y} \quad (5.4)$$

Then

$$Ly = \underline{d} \quad (5.5)$$

Solving equations (5.5) and (5.4) successively for \underline{y} and \underline{P} respectively:

$$\underline{y} = L^{-1}\underline{d} \quad (5.6)$$

and

$$\underline{P} = U^{-1}\underline{y} \quad (5.7)$$

Hence, the LU factorization technique consists of two major steps, the computation of L and U and the back substitution.

Computation of L and U

$$l_{ij} = 0 \quad \text{if} \quad i < j \quad (5.8)$$

$$u_{ij} = 0 \quad \text{if} \quad i = j \quad (5.9)$$

$$u_{ij} = 0 \quad \text{if} \quad i > j \quad (5.10)$$

for $i = 1, 2, \dots, N$ and $j = 1, 2, \dots, N$

$$l_{i1} = a_{i1}, \quad i = 1, 2, \dots, N \quad (5.11)$$

$$u_{1j} = a_{1j}/l_{11}, \quad j = 2, 3, \dots, N \quad (5.12)$$

$$\begin{bmatrix} l_{11} & & & & & & & & \\ l_{21} & l_{22} & & & & & & & \\ l_{31} & l_{32} & l_{33} & & & & & & \\ \cdot & \cdot & \cdot & \cdot & & & & & \\ \cdot & \cdot & \cdot & \cdot & \cdot & & & & \\ \cdot & \cdot & \cdot & & \cdot & \cdot & & & \\ \cdot & \cdot & \cdot & & & \cdot & \cdot & & \\ \cdot & \cdot & \cdot & & & & \cdot & \cdot & \\ l_{N1} & l_{N2} & l_{N3} & \cdot & \cdot & \cdot & \cdot & \cdot & l_{NN} \end{bmatrix}$$

L - Matrix

$$\begin{bmatrix} 1 & u_{12} & u_{13} & \cdot & \cdot & \cdot & \cdot & \cdot & u_{1N} \\ & 1 & u_{23} & \cdot & \cdot & \cdot & \cdot & \cdot & u_{2N} \\ & & 1 & \cdot & \cdot & \cdot & \cdot & \cdot & u_{3N} \\ & & & \cdot & & & & & \cdot \\ & & & & \cdot & & & & \cdot \\ & & & & & \cdot & & & \cdot \\ & & & & & & \cdot & & \cdot \\ & & & & & & & \cdot & \cdot \\ & & & & & & & & 1 \end{bmatrix}$$

U - Matrix

Figure 5.2 - L U Factorization of \bar{A}

The rest of the elements are calculated for $m = 2, 3, \dots, N$ as follows:

$$l_{im} = a_{im} - \sum_{k=1}^{m-1} l_{ik} u_{km} , \quad i = m, m+1, \dots, N \quad (5.13)$$

Then compute successively

$$u_{mj} = \frac{1}{l_{mm}} (a_{mj} - \sum_{k=1}^{m-1} l_{mk} u_{kj}) , \quad j = m+1, m+2, \dots, N \quad (5.14)$$

The matrices L and U can be designated by a composite matrix G such that $G = L \setminus U$ meaning

$$G_{ij} = l_{ij}, \quad i \geq j ; \quad G_{ij} = u_{ij}, \quad i < j \quad (5.15)$$

Back Substitution

$$y_1 = d_1 / l_{11} \quad (5.16)$$

$$y_i = \frac{1}{l_{ii}} (d_i - \sum_{k=1}^{i-1} l_{ik} y_k) , \quad i = 2, 3, \dots, N \quad (5.17)$$

$$p_N = y_N \quad (5.18)$$

$$p_i = y_i - \sum_{k=i+1}^N u_{ik} p_k , \quad i = N-1, N-2, \dots, 1 \quad (5.19)$$

5.2 Ordering Schemes

In reservoir simulators using implicit pressure explicit saturation technique, the coefficient matrix (matrix A in equation 3.24) is a sparse matrix. The order of the unknowns of such a sparse system of linear algebraic equations drastically affects the amount of computation and storage requirements.

Price and Coats¹² presented four different ordering schemes based on optimal ordering. The work and storage involved are given as functions of the size of coefficient matrix. These ordering

schemes are standard, diagonal, alternating point, and alternating diagonal. McDonald and Trimble⁹ presented a fifth ordering scheme that we will call alternating line. The work requirement for this scheme is also presented.

1. Standard Ordering: In this scheme, the cells are numbered consecutively along the rows or columns starting with the shortest direction to reduce the numerical computation. Figure 5.3 depicts such an ordering scheme in two dimensions.

The resulting coefficient matrix corresponding to standard ordering is of a pentadiagonal form as shown in Figure 5.5.

2. Diagonal Ordering: In this ordering, the cells are numbered consecutively along the diagonals starting with the shortest direction. This ordering scheme is shown in Figure 5.4.

The resulting coefficient matrix corresponding to diagonal ordering is shown in Figure 5.6.

3. Alternating Point Ordering: In this ordering, the cells are numbered such that each point is separated from its adjacent number by at least one other point.

The resulting coefficient matrix corresponding to alternating point ordering scheme of Figure 5.7 is shown in Figure 5.9.

4. Alternating Diagonal Ordering: In this scheme, the cells are numbered consecutively along alternating diagonals. This ordering scheme is shown in Figure 5.8.

Figure 5.10 shows the resulting coefficient matrix corresponding to alternating diagonal ordering scheme.

	1	2	3	4	5	6	= I
1	1	6	11	16	21	26	
2	2	7	12	17	22	27	
3	3	8	13	18	23	28	
4	4	9	14	19	24	29	
J = 5	5	10	15	20	25	30	

Figure 5.3 - Standard Ordering

	1	2	3	4	5	6	= I
1	1	3	6	10	15	20	
2	2	5	9	14	19	24	
3	4	8	13	18	23	27	
4	7	12	17	22	26	29	
J = 5	11	16	21	25	28	30	

Figure 5.4 - Diagonal Ordering

b	c	f
a	b	c
a	b	c
a	b	c
a	b	f
e	b	c
e	a	b
e	a	b
e	a	b
e	a	b
e	b	c
e	a	b
e	a	b
e	a	b
e	b	c
e	a	b
e	a	b
e	b	c
e	a	b
e	a	b
e	b	c
e	a	b
e	a	b
e	b	c
e	a	b
e	a	b
e	b	c
e	a	b
e	a	b
e	b	c
e	a	b
e	a	b
e	b	c
e	a	b
e	a	b

Figure 5.5-Matrix \mathbf{A} Corresponding to Standard Ordering

b c f
b c f
e b c f
a b c f
e a b c f
e b c f
a b c f
e a b c f
e b c f
a b f
e a b c f
e a b c f
e a b c f
e a b c f
e a b c f
e a b c f
e a b f
e a b c f
e a b c f
e a b c f
e a b c
e a b f
e a b c f
e a b c f
e a b c
e a b f
e a b f
e a b

Figure 5.6-Matrix A Corresponding to Diagonal Ordering

	1	2	3	4	5	6	= I
1	1	16	2	17	3	18	
2	19	4	20	5	21	6	
3	7	22	8	23	9	24	
4	25	10	26	11	27	12	
J = 5	13	28	14	29	15	30	

Figure 5.7 - Alternating Point Ordering

	1	2	3	4	5	6	= I
1	1	17	4	21	9	26	
2	16	3	20	8	25	13	
3	2	19	7	24	12	29	
4	18	6	23	11	28	15	
J = 5	5	22	10	27	14	30	

Figure 5.8 - Alternating Diagonal Ordering

b		c f	
b		a c f	
b		a c f	
b		e a c f	
b		e a c f	
b		e a f	
b		e c f	
b		e a c f	
b		e a c f	
b		e a c f	
b		e a f	
b		e c	
b		e a c	
a c f		b	
a c f		b	
a f		b	
e c f		b	
e a c f		b	
e a c f		b	
e a c f		b	
e a c f		b	
e a f		b	
e c f		b	
e a c f		b	
e a c f		b	
e a c		b	
e a c		b	
e a		b	

Figure 5.9-Matrix \mathbf{A} Corresponding to Alternating Point Ordering

b	c f
b	a c f
b	e a c f
b	e c f
b	a f
b	e a c f
b	e a c f
b	e a c f
b	e a c f
b	e a c f
b	e a f
b	e a c
a c f	b
e c f	b
a c f	b
e a c f	b
e a c f	b
e a c f	b
e a f	b
e a c f	b
e a c f	b
e a c f	b
e a c	b
e a f	b
e a c f	b
e a c	b
e a	b

Figure 5.10-Matrix A Corresponding to Alternating Diagonal Ordering

5. Alternating Line Ordering: In this ordering, the cells are numbered consecutively along the shortest rows or columns, in an alternating pattern. Figure 5.11 depicts such an ordering scheme.

Figure 5.12 shows the resulting coefficient matrix corresponding to alternating line ordering scheme.

Here a summary of the work and storage requirements of an $I \times J$ two-dimensional mesh is presented with large I and J such that $J \leq I$. The work is defined as the number of multiplications and divisions necessary to solve for the unknowns without operating on zero elements. The storage is required only for nonzero elements.

Ordering Scheme	Work	Storage
Standard	IJ^3	IJ^2
Diagonal	$IJ^3 - \frac{J^4}{2}$	$IJ^2 - \frac{J^3}{3}$
Alternating Point	$\frac{IJ^3}{2}$	$\frac{IJ^2}{2}$
Alternating Line	$\frac{IJ^3}{2}$	
Alternating Diagonal	$\frac{IJ^3}{2} - \frac{J^4}{4}$	$\frac{IJ^2}{2} - \frac{J^3}{6}$

Table 5.1 - Work and Storage Requirements for Ordering Schemes

	1	2	3	4	5	6	= I
1	1	16	6	21	11	26	
2	2	17	7	22	12	27	
3	3	18	8	23	13	28	
4	4	19	9	24	14	29	
J = 5	5	20	10	25	15	30	

Figure 5.11 - Alternating Line Ordering

b c		f	
a b c		f	
a b c		f	-
a b c		f	-
a b		f	-
b c	e	f	-
a b c	e	f	-
a b c	e	f	-
a b c	e	f	-
a b	e	f	-
b c	e	f	-
a b c	e	f	-
a b c	e	f	-
a b c	e	f	-
a b	e	f	-
e f	b c		
e f	a b c		
e f	a b c		
e f	a b c		
e f	a b		
e f	b c		
e f	a b c		
e f	a b c		
e f	a b		
e	b c		
e	a b c		
e	a b c		
e	a b c		
e	a b		

Figure 5.12-Matrix \mathbf{A} Corresponding to Alternating Line Ordering

5.3 Generate - and - Solve Algorithms

The optimal ordering technique can be improved by the use of processes which are geared specifically to the direct solution. One method is the generate - and - solve algorithms used by Woo, et al²¹ in reservoir simulation. Their method makes use of the computer architecture in developing the algorithm. The basis of the method is summarized by Crichlow⁶ as follows:

1. In a given matrix there is a fixed number of nontrivial operations required to solve the system by some given direct scheme.
2. The solution process produces some nonzero elements which will always be present at a given (i,j) location in the matrix.
3. If the location of all nonzero quantities is fixed a priori both in the matrix and in its solution, then a straightforward, nonbranching, nonlooping computer code can be developed to solve this system very efficiently.

The major drawback of this technique is the fact that it requires large storage and overhead work to store and generate the nonlooping computer code.

5.4 Band Matrix Technique

Direct processes, although they are conceptually easy, are rarely used without extensive modification to solve the pressure system in simulation because these processes usually require large computer storage space and long computation times, unless special techniques such as band matrix or sparsity are employed.

The treatment of zeros within the bands as non-zeros is called band matrix technique. The band matrix algorithm will be applied on standard ordering which we will call STBAND.

STBAND

For band matrix technique applied on standard ordering, all elements between F-vector and E-vector in Figure 5.5 are assumed to be nonzero.

By letting

$$G_{\eta,j} = e_j \quad (5.20)$$

$$G_{1,j} = a_j \quad (5.21)$$

$$H_{1,j} = c_j \quad (5.22)$$

$$H_{\eta,j} = f_j \quad (5.23)$$

the general equation of STBAND would be

$$\begin{aligned} & G_{1,j} p_{j-\eta} + G_{2,j} p_{j-\eta+1} + \dots + G_{\eta,j} p_{j-1} + b_j p_j \\ & + H_{\eta,j} p_{j+1} + H_{\eta-1,j} p_{j+2} + \dots + H_{1,j} p_{j+\eta} = d_j \\ & 1 \leq j \leq N, N \geq \eta \end{aligned} \quad (5.24)$$

The algorithm used is as follows¹⁸:

$$\alpha_{i,j} = G_{i,j} = 0 \quad \text{for } i \geq j \quad (5.25)$$

$$H_{i,j} = 0 \quad \text{for } i \geq N + 1 - j \quad (5.26)$$

Forward Solution ($j = 1, 2, \dots, N$)

$$\alpha_{i,j} = g_{i,j} - \sum_{k=i+1}^{k=n} \alpha_{k,j} y_{k-i,j-k} , \quad i = n, n-1, \dots, 1 \quad (5.27)$$

$$\beta_j = b_j - \sum_{k=1}^{k=n} \alpha_{k,j} y_{k,j-k} \quad (5.28)$$

$$y_{i,j} = \frac{1}{\beta_j} \{ h_{i,j} - \sum_{k=i+1}^{k=n} \alpha_{k-i,j} y_{k,j-k+i} \} , \quad i = 1, 2, \dots, n \quad (5.29)$$

$$\gamma_j = \frac{1}{\beta_j} \{ d_j - \sum_{k=1}^{k=n} \alpha_{k,j} \gamma_{j-k} \} \quad (5.30)$$

Backward Solution ($j = N, N-1, \dots, 1$)

$$p_j = \gamma_j - \sum_{k=1}^{k=n} y_{k,j} p_{j+k} \quad (5.31)$$

CHAPTER VI

A NEW APPROACH TO THE APPLICATION OF DIRECT METHODS IN PETROLEUM RESERVOIR SIMULATION

The yet known systematic optimal ordering in petroleum reservoir simulation is alternating diagonal as shown in Table 5.1. However, there is a major drawback to this ordering scheme. In alternating diagonal scheme, the elements in the upper right and lower left corners of matrix \mathbf{A} do not form a perfect secondary diagonals as shown in Figure 5.10. This problem forced us to use band algorithm which treats the zeros within the band as nonzeros. The band algorithm was discussed in the preceding chapter. The treatment of the zeros as nonzeros makes the band matrix technique require a larger storage space and more computational labor.

6.1 Restricted Alternating Diagonal Ordering

Here a modification to the alternating diagonal ordering that produces perfect secondary diagonals in the orginal \mathbf{A} matrix is proposed. This ordering will be called restricted alternating diagonal (RAD). Figures 6.1 and 6.2 depict the RAD ordering. Figures 6.3 and 6.4 show the resulting coefficient matrix corresponding to RAD ordering scheme.

The numbering of this scheme must go along the shortest diagonal to reduce the band width of the new nonzero elements that will be

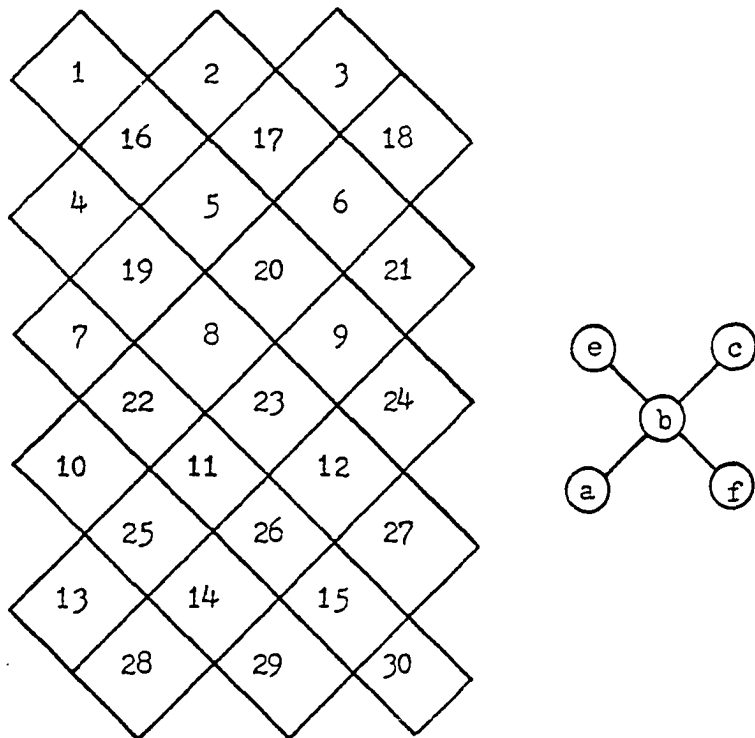


Figure 6.1 - RAD Ordering Along the Shortest Diagonal

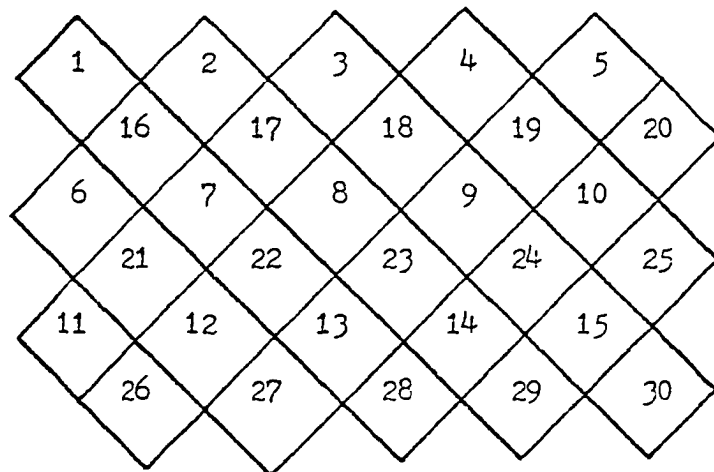


Figure 6.2 - RAD Ordering Along the Longest Diagonal

b		f
b		a f
b		a f
b		c f
b		e c a f
b		e c a f
b		c f
b		e c a f
b		e c a f
b		c f
b		e c a f
b		e c a f
e c a f		b o o o o
e c a f		o b o o o o
e a		o o b o o o o
e c a f		o o o b o o o o
e c a f		o o o o b o o o o
e a		o o o o b o o o o
e c a f		o o o o b o o o o
e c a f		o o o o b o o o o
e a		o o o o b o o o o
e c a f		o o o o b o o o o
e c a f		o o o o b o o o o
e c		o o o o b o o o
e c		o o o o b o o
e		o o o o b o
		o o o o b

Figure 6.3-Matrix \mathbf{A} Corresponding to RAD Along the Shortest Diagonal

b		f	
b		a f	
b		a f	
b		a f	
b		a f	
b	c	f	
b	e c	a f	
b	e c	a f	
b	e c	a f	
b	c	f	
b	e c	a f	
b	e c	a f	
b	e c	a f	
e c	a f	b o	o o o
e c	a f	o b o	o o o o
e c	a f	o b o o	o o o o o
e c	a f	o b o o o	o o o o o o
e	a	o o o o b	o o o o o o o
e c	a f	o o o o o b	o o o o o o o
e c	a f	o o o o o o b	o o o o o o o
e c	a f	o o o o o o o b	o o o o o o o o
e	a	o o o o o o b	o o o o o o o o
e c		o o o o o o b	o o o o o o o o
e c		o o o o o o b	o o o o o o o o
e c		o o o o o o b	o o o o o o o o
e c		o o o o o o b	o o o o o o o o
e		o o o o o o b	o o o o o o o o

Figure 6.4 - Matrix \bar{A} Corresponding to RAD Along the Longest Diagonal

generated later in the process of factorization. This will be obvious when we compare Figures 6.3 and 6.4.

6.2 LU Factorization Applied to RAD

In the process of LU factorization, no new elements will be generated except for the elements in the lower right corner of the matrix as shown in Figures 6.3 and 6.4 where the new elements are entered as small circles. The new elements form a band of width equals $(2m-1)$, where m is the semi-bandwidth of matrix \bar{A} .

The semi-bandwidth m for RAD scheme is defined as follows:

$$m = L_d + 2 \quad (6.1)$$

where L_d is the length of the diagonal along which numbering is applied.

The upper section of matrix \bar{A} and G has a length of N_u , while the length of the lower section of \bar{A} and G is N_l . These terms are defined as follows:

$$\begin{aligned} N_u &= N/2 && , \text{ if } N_d \text{ is even} \\ &&& \} \\ N_u &= (N-m)/2 + m && , \text{ if } N_d \text{ is odd} \end{aligned} \quad (6.2)$$

and

$$N_l = N - N_u \quad (6.3)$$

where N_d is the number of diagonals in the system.

The work requirement, when LU factorization is applied to RAD to solve the pressure equations is

$$W \approx 2N + 5N_u + (16 + m^2)N_l \quad (6.4)$$

and the storage requirement is

$$S < 5N + (2m-2)N_l \quad (6.5)$$

The application of LU factorization to the RAD of Figure 6.5 results in the composite matrix G of Figure 6.6. The RAD scheme consists of the computation of G and the back substitution. These two steps are outlined next.

Computation of the Composite Matrix G (= $L\backslash U$)

The elements in the left half of matrix G are the same as those of matrix A .

In the process of factorization, there are no new elements introduced in the upper right corner of matrix G , but the existing elements are modified for $j = 1, 2, \dots, N_u$ as follows:

$$a'_j = a_j/b_j \quad (6.6)$$

$$c'_j = c_j/b_j \quad (6.7)$$

$$e'_j = e_j/b_j \quad (6.8)$$

$$f'_j = f_j/b_j \quad (6.9)$$

There are $2m-2$ new vectors introduced in the lower right quarter of matrix G in the process of factorization as shown in Figure 6.6. These vectors and the principal diagonal vector are calculated into two steps. The first step is the computation of the contribution of the mutual product of vectors A, C, E and F . There are 8 vectors out of the $2m-2$ vectors which receive such contribution. This contribution is computed for $j = 1, 2, \dots, N_l$ by the following equations:

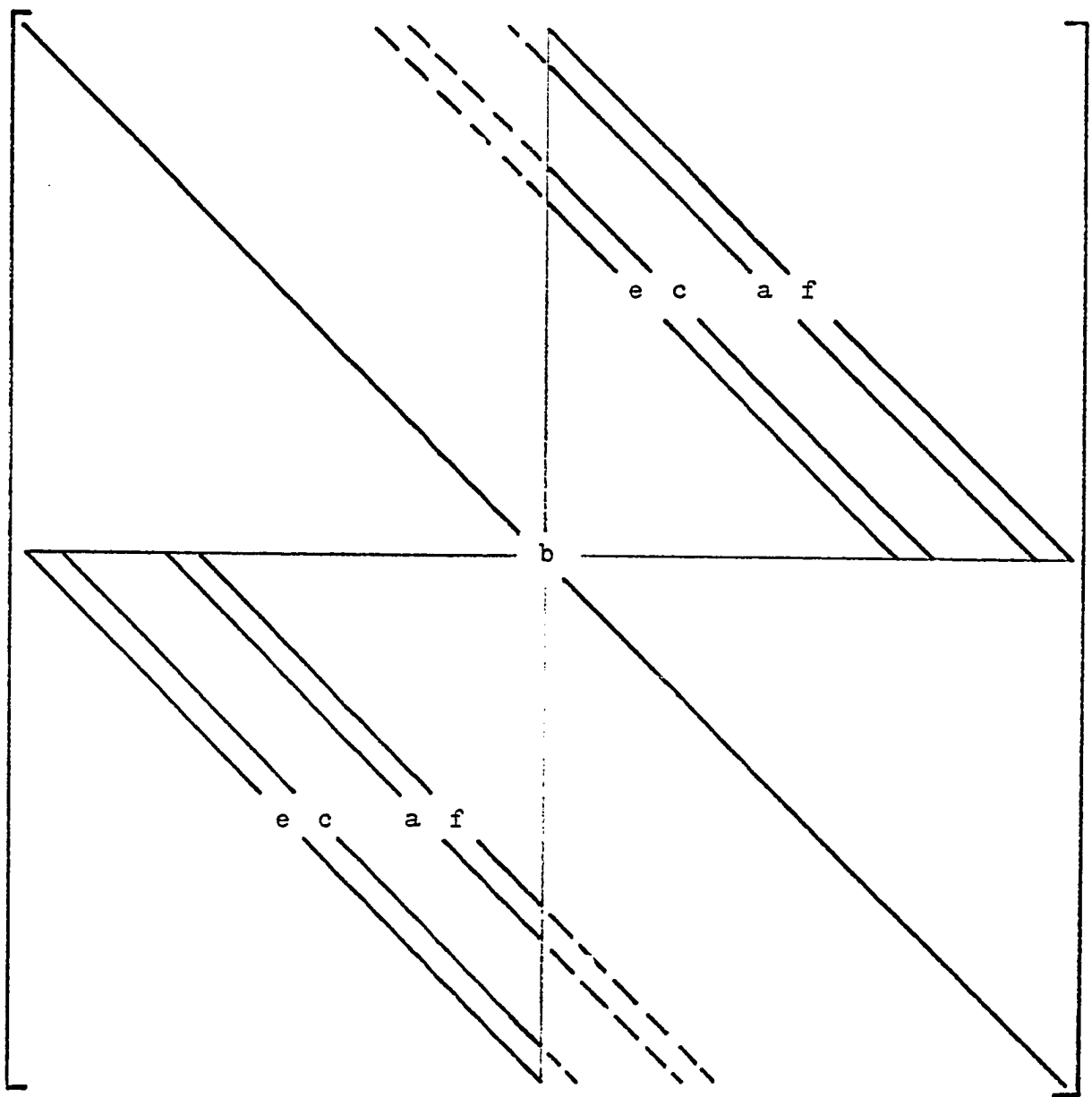


Figure 6.5 - General form of Matrix \bar{A} of RAD

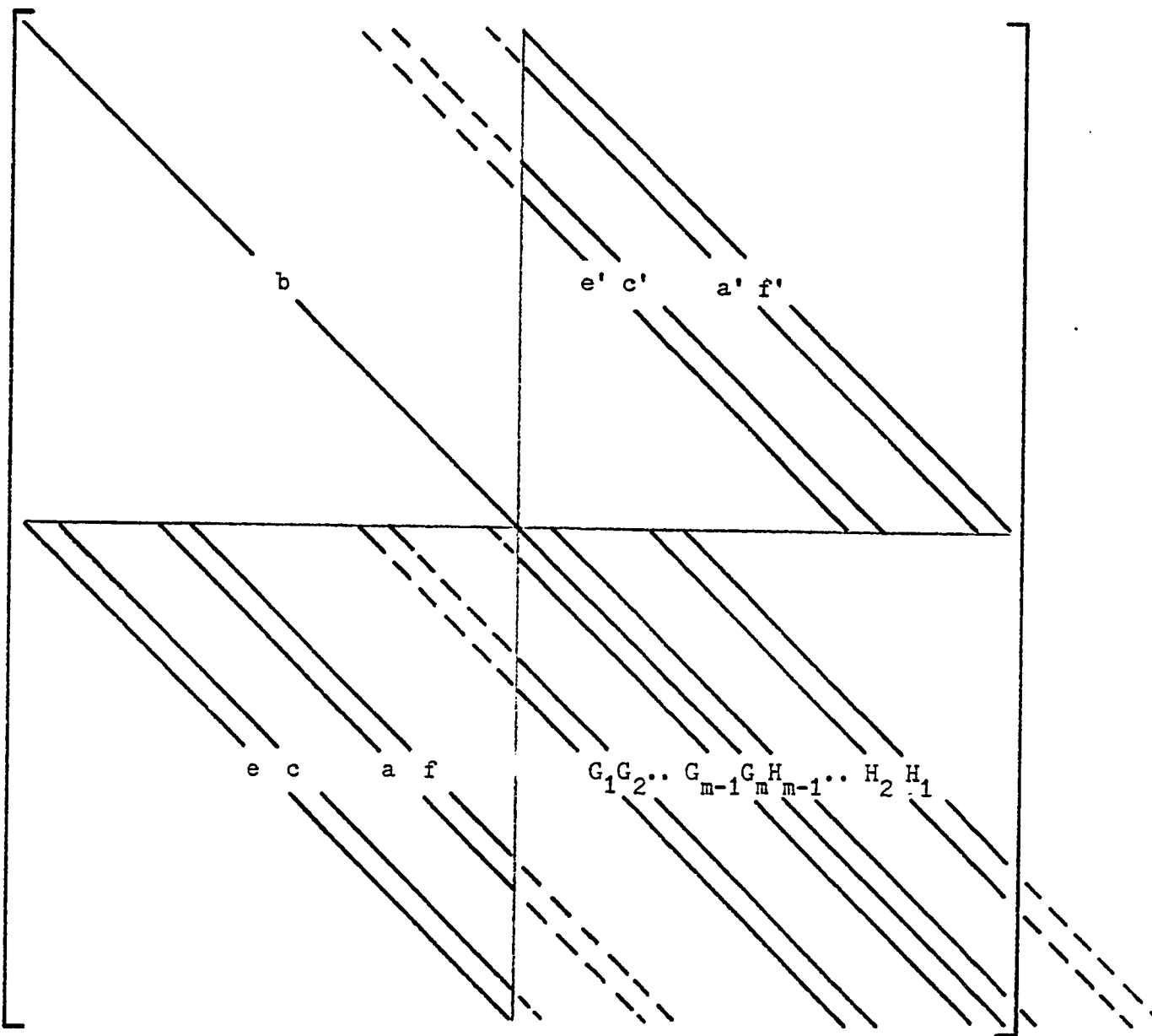


Figure 6.6 - The Composite Matrix Q of RAD

$$G'_{1,j} = -e_{j+N_u} e'_j \quad (6.10)$$

$$G'_{2,j} = -e_{j+N_u} c'_j -c_{j+N_u} e'_{j+1} \quad (6.11)$$

$$G'_{3,j} = -c_{j+N_u} c'_{j+1} \quad (6.12)$$

$$G'_{i,j} = 0 \quad , \quad i = 4, 5, \dots, m-2 \quad (6.13)$$

$$G'_{m-1,j} = -e_{j+N_u} a'_j -a_{j+N_u} e'_{j+m-2} \quad (6.14)$$

$$G'_{m,j} = b_{j+N_u} -e_{j+N_u} f'_j -c_{j+N_u} a'_{j+1} -a_{j+N_u} c'_{j+m-2} -f_{j+N_u} e'_{j+m-1} \quad (6.15)$$

$$H'_{1,j} = -f'_{j+m-1} f_{j+N_u} \quad (6.16)$$

$$H'_{2,j} = -f'_{j+m-2} a_{j+N_u} -a'_{j+m-1} f_{j+N_u} \quad (6.17)$$

$$H'_{3,j} = -a'_{j+m-2} a_{j+N_u} \quad (6.18)$$

$$H'_{i,j} = 0 \quad , \quad i = 4, 5, \dots, m-2 \quad (6.19)$$

$$H'_{m-1,j} = -f'_{j+1} c_{j+N_u} -c'_{j+m-1} f_{j+N_u} \quad (6.20)$$

In the second step, all the computation is within the lower right quarter of matrix Q . In this step the elements are subdivided into three groups as shown in Figure 6.7. These groups are chosen in such a way that the indices can be precalculated and easily programmed.

1 1	1 1 1
0 1 1	1 1 1 1
0 1 :	1 1 1 1 :
...
...
· 1 1	1 1 1 1 · · 1 1
0 1 1	1 1 1 1 · · 1 1 1
0 1 1 1 1 1 1	· · 1 1 1 1 1
0 1 1 1 1 1 1	· · 1 1 1 1 1
0 1 1 1 1 1 2 2 2 2	· · 2 2 2 2 2 2 2
0 1 1 1 1 1 2 2 2 2	· · 2 2 2 2 2 2 2
0 1 1 1 1 1 2 2 2 2	· · 2 2 2 2 2 2 2
0 1 1 1 1 1 2 2 2 2	· · 2 2 2 2 2 2 2
0	· · · · · · · · · · · · · · · ·
· 1 1 1 1 2 2 2 2	· · 2 2 2 2 2 2 2 2 · · 2
0 1 1 1 2 2 2 2	· · 2 2 2 2 2 2 2 2 · · 2 2
0 1 1 2 2 2 2	· · 2 2 2 2 2 2 2 2 · · 2 2 2
0 1 2 2 2 2	· · 2 2 2 2 2 2 2 2 · · 2 2 2 2
0 2 2 2 2	· · 2 2 2 2 2 2 2 2 · · 2 2 2 2
0 2 2 2	· · 2 2 2 2 2 2 2 2 · · 2 2 2 2
· · · · · · · · · · · · · · · ·	· · · · · · · · · · · · · · · ·
· · 2 2 2 2 2 2 2 2	· · 2 2 2 2 2 2 2 2
· 2 2 2 2 2 2 2 2	· · 2 2 2 2 2 2 2
0 2 2 2 2 2 2 2 2	· · 2 2 2 2 2 2 2
0 2 2 2 2 2 2 2	· · 2 2 2 2 2 2
0 2 2 2 2 2 2	· · 2 2 2 2 2

Figure 6.7 - The lower right quarter of matrix \mathcal{Q} of semi-bandwidth m
 (The number indicates the group of the element)

Furthermore, this choice provides a programming procedure for this complex problem without using any if statement which results in a reduction of computer time. The computations within these groups are outlined next.

Group 0

No more computation is needed

Group 1

For $i = 1, 2, 3, \dots, m$ calculate

$$H_{i,1} = H'_{i,1} / G_{m,1} \quad (6.21)$$

Then calculate for $j = 2, 3, \dots, m-3$

$$G_{m,j} = G'_{m,j} - G_{m-1,j} H_{m-1,j-1} \quad (6.22)$$

$$H_{i,j} = \frac{1}{G_{m,j}} (H'_{i,j} - H_{i-1,j-1} G_{m-1,j}) , \quad i=2, 3, \dots, j+2 \quad (6.23)$$

$$H_{m-1,j} = H'_{m-1,j} / G_{m,j} \quad (6.24)$$

Group 2

For $j = m-2, m-1, \dots, N_l - 1$ calculate

$$G_{i,j} = G'_{i,j} - \sum_{k=1}^{i-1} G_{i-k,j} H_{m-k,j-k-m+i} , \quad i=2, 3, \dots, m \quad (6.25)$$

$$H_{1,j} = H'_{1,j} / G_{m,j} \quad (6.26)$$

$$H_{i,j} = \frac{1}{G_{m,j}} (H'_{i,j} - \sum_{k=1}^{i-1} H_{i-k,j-k} G_{m-k,j}) , \quad i=2,3,\dots,m-1 \quad (6.27)$$

Then calculate

$$G_{m,N_l} = G'_{m,N_l} - \sum_{k=1}^{m-1} G_{m-k,N_l} H_{m-k,N_l-k} \quad (6.28)$$

Back Substitution

$$y_j = d_j / b_j , \quad j = 1, 2, \dots, N_u \quad (6.29)$$

$$y_j = \frac{1}{G_{m,j-N_u}} (d_j - e_j y_{j-N_u} - c_j y_{j-N_u+1} - a_j y_{j-N_u+m-2} - f_j y_{j+N_u+m-1} - \sum_{k=1}^{m-1} G_{k,j-N_u} y_{j-m+k}) , \quad j = N_u+1, \dots, N \quad (6.30)$$

$$P_N = y_N \quad (6.31)$$

$$P_j = y_j - \sum_{k=1}^{m-1} H_{k,j-N_u} P_{j+m-k} , \quad j = N-1, N-2, \dots, N_u+1 \quad (6.32)$$

$$P_j = y_j - f_j P_{j+N_u} - a_j P_{j-1+N_u} - c_j P_{j-m+2+N_u} - e_j P_{j-m+1+N_u} , \quad j = N_u, N_u-1, \dots, 1 \quad (6.33)$$

6.3 Implementation of RAD Scheme into the Simulation Package

To implement the restricted alternating diagonal ordering scheme into the simulation package, the following steps are performed:

1. The standard ordering is reordered to RAD scheme. This step is executed once in the entire simulation. This reordering can be accomplished by finding a RAD scheme that will enclose the standard ordering under consideration as shown in Figure 6.8.
2. The coefficient matrix is transformed into RAD scheme.
3. Then the pressure equations are solved. Thereafter, the pressure vector obtained is reordered into standard ordering to go along with the rest of the simulation package.

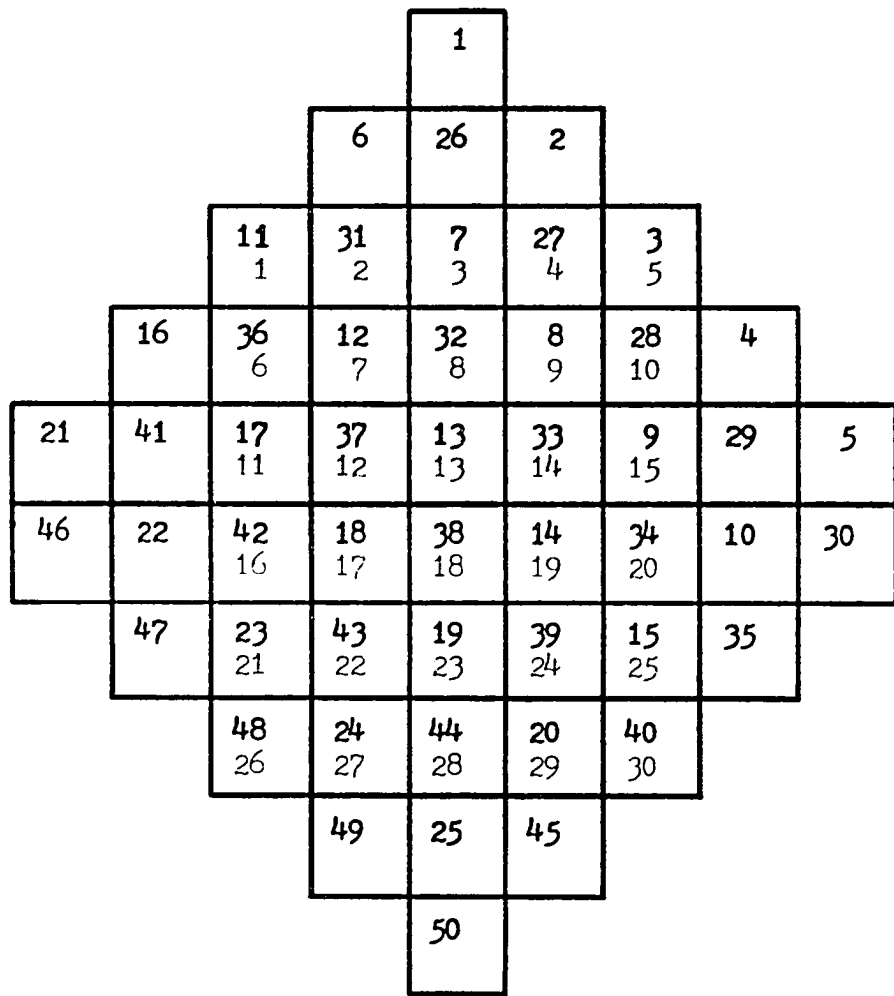


Figure 6.8 - RAD Ordering Enclosing Standard Ordering

CHAPTER VII

SIMULATION PACKAGE

This simulation package is a complex collection of computer subroutines tied together by the simulator mainline. The flow chart for the simulator mainline is given in Figure 7.1. These subroutines are developed either out of necessity or simply for the convenience of the engineer.

In this simulation package, a new feature is introduced to save CPU execution time. A chain of imaginary cells is introduced around the active cells. For sealed reservoirs, this new feature allows the execution of active cells only without checking for boundary cells.

There are nine sections in this simulation package. Every section consists of closely related subroutines. Each of these sections will be discussed in detail.

7.1 Input Section

This section of the simulation package consists of the following subroutines:

1. INPUT
2. READ

and requires the PRINT subroutine.

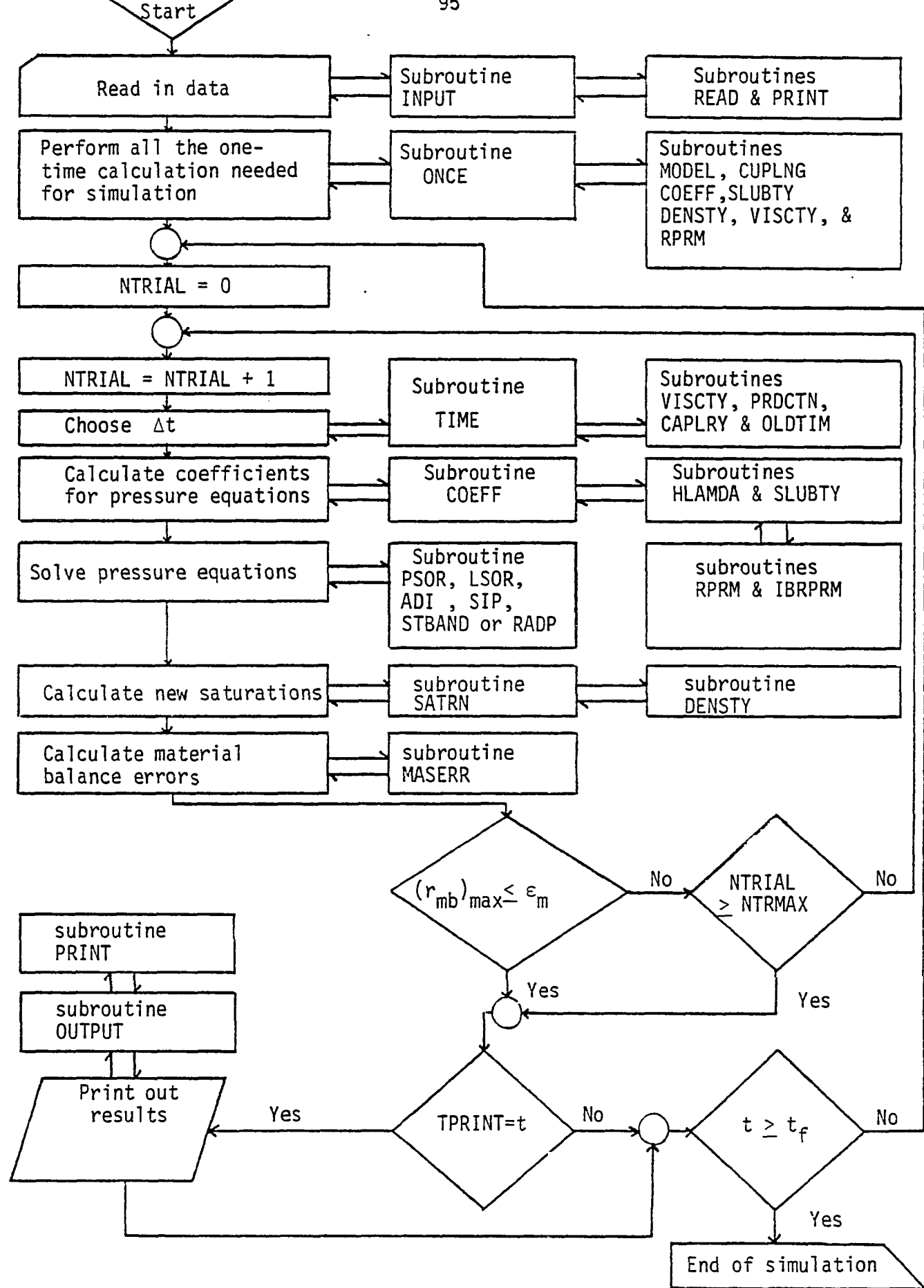


Figure 7.1 - Flow Chart of Simulator Mainline

This section provides a means of reading all input data required in simulation. For input data entered as matrices or vectors, this section will check that the value assigned for each cell is within the range specified for all the matrix or vector values. In addition the entire matrix or vector can be multiplied by a given constant. Also a given constant can be algebraically added to each element of the matrix or vector. If all the elements of the matrix are the same, then the matrix can be entered as a single value. These possible modifications of the elements are very important for history matching. All input data are printed out. Furthermore, the values which lie outside the range specified for the system are printed out along with its cell number and its matrix or vector title so that it can be corrected.

The input data are grouped as follows:

1. Single entries

Number of cells (N_x, N_y)

Compressibilities (C_o, C_w, C_r)

Irreducible saturations (S_{wc}, S_{or}, S_{gc})

Densities at standard conditions ($\rho_o^*, \rho_w^*, \rho_g^*$)

Bubble point pressure (P_{Bp})

Time control parameters ($t_i, t_f, DTMIN, DTMAX, DPLIM, DSLIM$)

Crank-Nicholson parameter (θ)

Print out interval (OUTMOD)

Material balance control parameters ($\varepsilon_m, NTRMAX$)

Pressure control parameters ($\varepsilon, k_{max}, m, \omega$)

2. Production-Injection data

Flowing bottom hole pressure (P_{wf})

Radius of wells (r_w)

Location of wells and their flow rates

According to the values of the flow rates read, the type of well is determined as shown in Figure 7.2. The vector identifier IQ defines the various types of wells. IQ is defined as follows:

$IQ = -2$, if the well is water injection at constant rate

$IQ = -1$, if the well is gas injection at constant rate

$IQ = 0$, if the cell is not a source or sink

$IQ = 1$, if the well produces gas at constant rate

$IQ = 2$, if the well produces oil at constant rate

$IQ = 3$, if the well produces oil at constant pressure

3. Capillary pressure data (P_{cw}, P_{cg})

4. Reservoir geometry

Dimensions ($\Delta x_i, \Delta y_i$)

Thickness (h_i)

Depth (D_i)

5. Rock properties

Porosity (ϕ_i)

Permeability (k_{xi}, k_{yi})

6. Initial conditions

Initial oil pressure (P_{oi})

Initial oil saturation (S_{oi})

Initial water saturation(S_{wi})

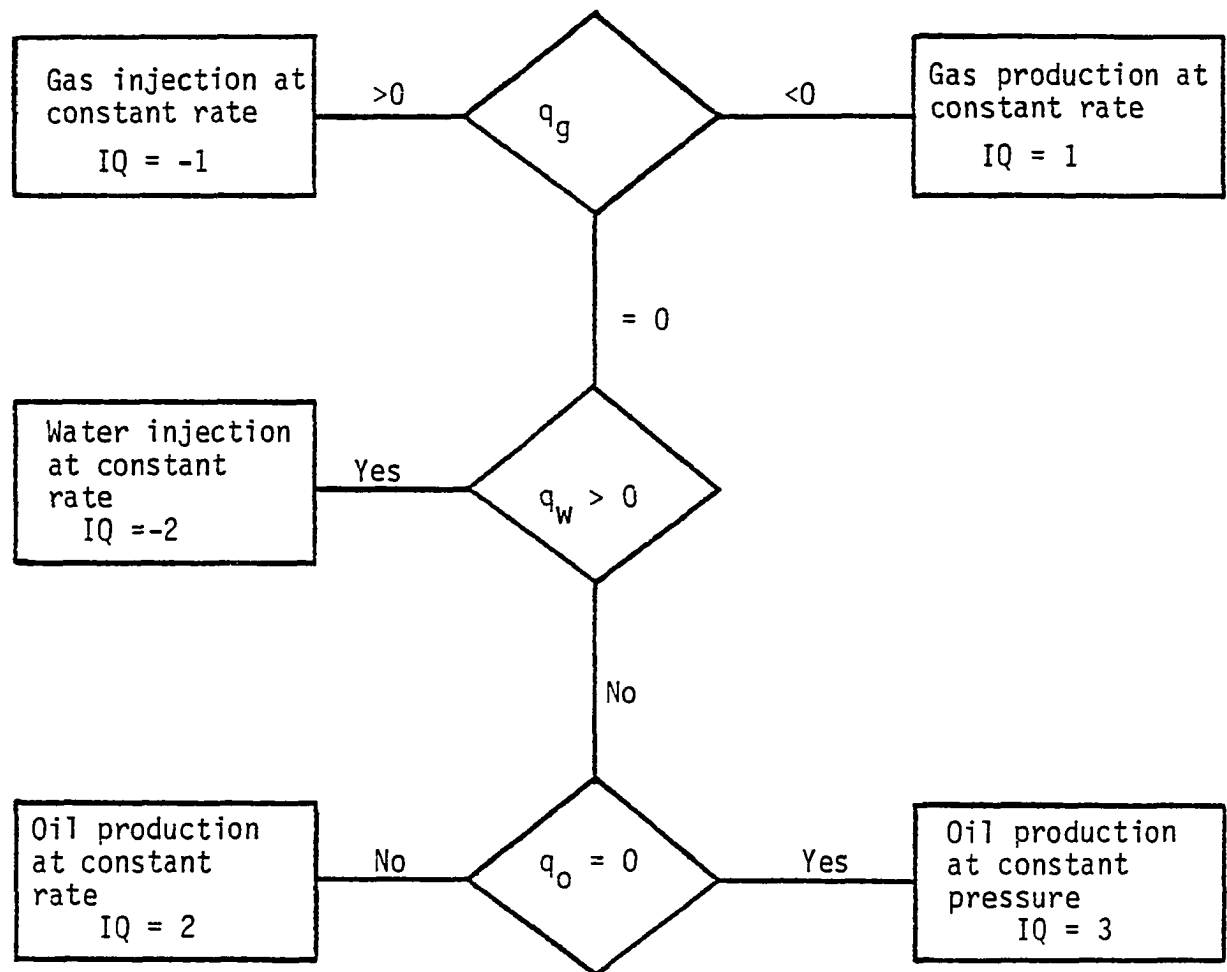


Figure 7.2 - Type of Well Vector Identifier

7.2 One-Time Calculations Section

This section of the simulation package consists of the following subroutines:

1. ONCE
2. MODEL
3. CUPLNG

and requires the following subroutines:

1. SLUBTY
2. DENSTY
3. VISCTY
4. COEFF
5. PRINT

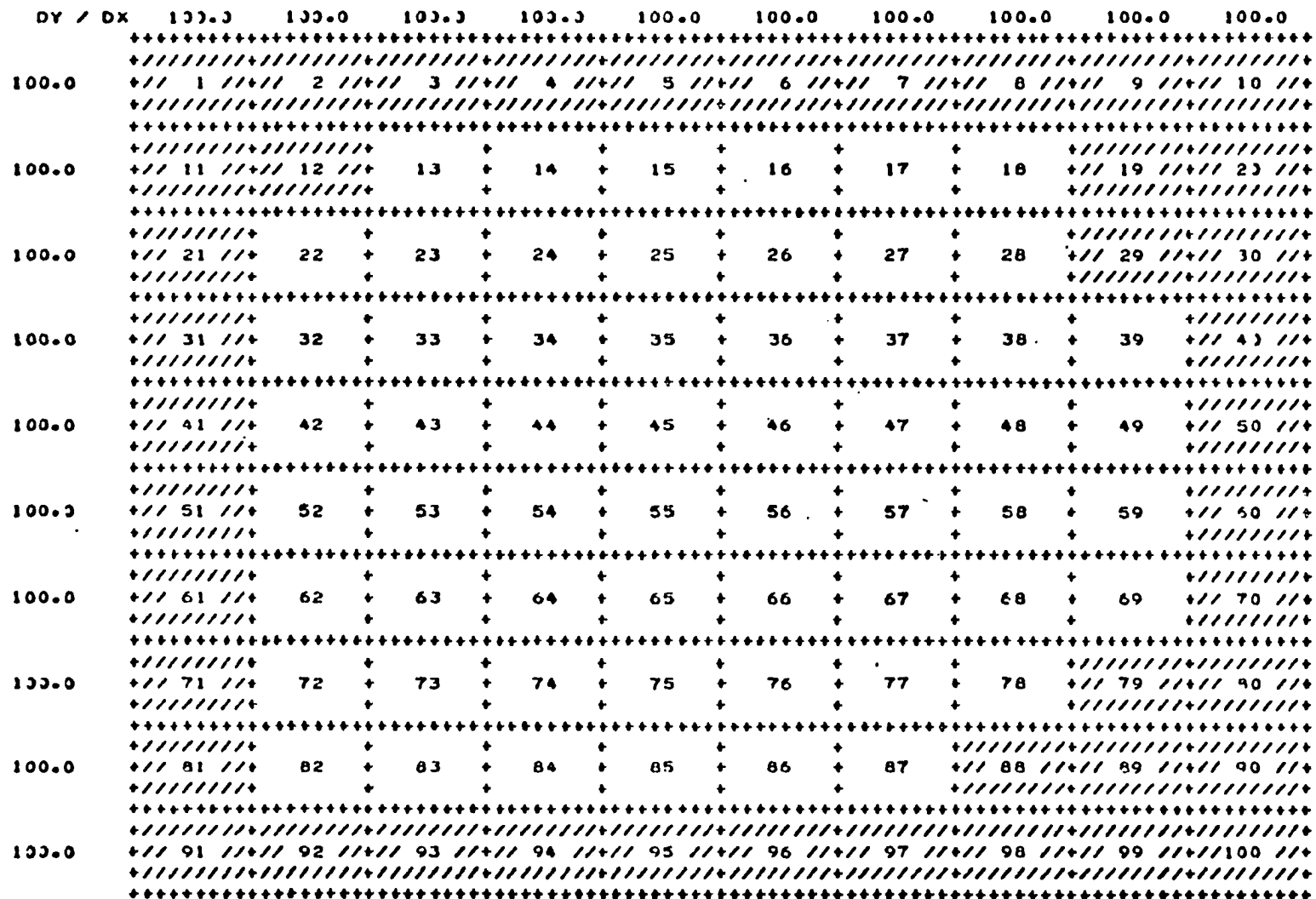
The subroutine ONCE performs the following one-time calculations:

- a - Identification of the active cells
- b - Initial oil, water, and gas in place
- c - Initial bulk volume for each active cell
- d - Weighted dimensions
- e - Calculation of normalizing factor and iteration parameters
for ADI and SIP

The subroutine CUPLNG calculates the couplings among cells using equations (3.39,3.40, and 3.41) for horizontal coupling and similar equations for vertical coupling.

The subroutine MODEL produces a sketch, similar to that presented in Figure 7.3. When a reservoir is discretized for simulation, as was discussed in chapter III, often some of the cells are not active. In addition, the cells in the sketch are numbered as they are identified

FIGURE 7.3 - NUMBERING SCHEME OF RESERVOIR MODEL (IMAGINARY CELLS SHADED) - DISTANCE IN METERS



by the simulator. The x-direction of the cells is shown across the top of the sketch and the y-direction of the cells is shown down the left side. In case the number of cells in the x-direction exceeds 10, then the sketch will be slashed after 10 cells and completed afterwards. This routine serves as a check for the shape of the reservoir simulated. Information required for this routine is the number of cells in the x and y directions, their dimensions, and the thickness of each cell as a check for inactive cells.

7.3 Time Control Section

This section of the simulation package consists of the following subroutines:

1. TIME
2. OLDTIM

and requires the following subroutines:

1. VISCTY
2. PRDCTN
3. CAPLRY

This section updates the time and chooses an appropriate time step (Δt) for time level $n+1$. The choice of Δt is based on the desire to use the maximum Δt possible provided that there is no single cell overdepleted and the truncation and round-off errors are within acceptable tolerance. The following criteria are applied in determining Δt :

1. Select a time step such that the producing cell is not overdepleted⁶. This can be accomplished by selecting a time step such that there is less than 15% change in the fluid saturation in the cell containing the well.

$$\Delta t_{\max} = \min (f_i) \quad \forall i \ni I_0 > 0 \quad (7.1)$$

where

$$f_i = 0.15(VS_o\rho_o/q_o\rho_o^*)_i \quad \text{for oil producing wells} \quad (7.2)$$

$$f_i = 0.15(VS_g\rho_g/q_g\rho_g^*)_i \quad \text{for gas producing wells} \quad (7.3)$$

thus, the maximum time increment is less than the time required to produce 15% of a pore volume of the smallest cell containing a well.

2. Todd, et al¹⁶ suggested the following method to control the truncation error. They suggested to limit the saturation and pressure changes per time step. This can be accomplished if Δt does not exceed Δt_{\max} defined by

$$\Delta t_{\max}^{n+1} = \Delta t^n \frac{DPLIM}{DPMAX} \quad (7.4)$$

$$\Delta t_{\max}^{n+1} = \Delta t^n \frac{DSLIM}{DSMAX} \quad (7.5)$$

where

DPLIM = maximum pressure change desired

DSLIM = maximum saturation change desired

for the three phase model

$$DPMAX = \max \left| p_i^{n+1} - p_i^n \right| \quad \forall i \ni h \neq 0 \quad (7.6)$$

$$DSMAX = \max_{j=0,w,g} \left| (s_j^{n+1} - s_j^n)_i \right| \quad \forall i \ni h \neq 0 \quad (7.7)$$

3. To make the input of the engineer more substantial, the range of Δt is specified

$$DTMIN \leq \Delta t \leq DTMAX \quad (7.8)$$

4. To avoid the round-off error, the chosen Δt is truncated to two decimals.

The subroutine OLDTIM calculates the production, capillary pressure, and gravity terms using equations (3.20) through (3.22) based on the last time step.

7.4 Coefficient Matrix Calculation Section

This section of the simulation package consists of the following subroutines:

1. COEFF
2. HLAMDA
3. IBRPRM

and requires the following subroutines:

1. RPRM
2. SLUBTY

The subroutine COEFF calculates the coefficient matrix using equations (3.7) through (3.12).

The HLAMDA and IBRPRM subroutines calculate the interblock flow coefficient ($h\lambda$) for all active cells and for the three phases. The equations and procedures outlined in section 3.3 are incorporated in these subroutines.

The boundary conditions is incorporated into the coefficient matrix through HLAMDA subroutine.

7.5 Pressure Solution Section

This section can be any of the subroutines that performs iterative or direct methods discussed in chapters IV, V, and VI to solve the pressure equations, namely PSOR, LSOR, ADI, SIP of chapter IV, STBAND of chapter V, and RADP of chapter VI.

7.6 Saturation Calculation Section

This section of the simulation package consists of one subroutine called SATRN and it requires the DENSTY subroutine.

This section calculates the new oil, water, and gas saturations using the equations developed in section 3.2.

The calculated saturations are subjected to the logical constraints.

$$S_{wc} \leq S_w \leq 1 \quad (7.9)$$

$$S_{or} \leq S_o \leq 1 - S_w \quad (7.10)$$

The porosity is updated in this section as follows:

$$\phi_i^{n+1} = \phi_i^n \{1 + C_r(p_i^{n+1} - p_i^n)\} \quad (7.11)$$

7.7 Material Balance Section

This section of the simulation package consists of one subroutine called MASERR and it does not require any other subroutine.

This section calculates the oil, water, gas, and total mass balance relative errors.

$$r_j = \frac{1}{MIP_j} (M_j - MIP_j) , j = o,w,g \quad (7.12)$$

$$r_t = \frac{1}{TM} (M_o + M_w + M_g - TM) \quad (7.13)$$

where

$$M_j = \sum_{i=1}^N \{V\rho_j S_j - \rho_j^* (q_{jc} + q_j \Delta t)\}_i , j = o,w,g \quad (7.14)$$

$$TM = MIP_o + MIP_w + MIP_g \quad (7.15)$$

In order for a model to maintain stability, it should conserve mass at all time⁶. In this study, $(r_{mb})_{max}$ is used as a convergence criterion on mass.

$$(r_{mb})_{max} = \max | r_j | , j = o,w,g,t \quad (7.16)$$

This material balance error must be within the predefined tolerance ϵ_m as follows:

$$(r_{mb})_{max} \leq \epsilon_m \quad (7.17)$$

This check is done in the mainline of the simulator as shown in Figure 7.1.

When the mass balance converges or the number of trials exceeds the maximum allowed, then the cumulative production is updated as follows:

$$q_{oc}^{n+1} = q_{oc}^n + q_0^{n+1}(t^{n+1} - t^n) \quad (7.18)$$

$$q_{gc}^{n+1} = q_{gc}^n + q_g^{n+1}(t^{n+1} - t^n) \quad (7.19)$$

$$q_{wc}^{n+1} = q_{wc}^n + q_w^{n+1}(t^{n+1} - t^n) \quad (7.20)$$

Also the maximum and minimum Δt used since the last print out time is updated.

7.8 Output Section

This section of the simulation package consists of the following subroutines:

1. OUTPUT
2. PRINT

and requires no other subroutine.

This section prints out the results accumulated since the last print out time.

The subroutine PRINT prints out a given matrix along with its title. The x-direction of the cells is numbered across the top of the matrix and the y-direction of the cells is numbered down the left side. In case the number of cells in the x-direction exceeds 10, the matrix will be slashed after 10 cells and completed afterwards.

7.9 Auxiliary Section

This section of the simulation package consists of the following subroutines:

1. RPRM
2. DENSTY
3. VISCTY
4. SLUBTY
5. CAPLRY
6. PRDCTN

and requires no other subroutine.

This section calculates the fluid properties and the production-injection flow rates. The data for this section can be entered as tables or empirical relationships developed from the reduction of field data.

The subroutine RPRM calculates the relative permeabilities.

The subroutine DENSTY calculates the oil, water, and gas densities.

The subroutine VISCTY calculates the oil, water, and gas viscosities.

The subroutine CAPLRY calculates the capillary pressure P_{cw} and P_{cg} .

The subroutine SLUBTY calculates the gas-oil ratios and gas-water ratios.

The subroutine PRDCTN determines the flow rate at source or sink cells. The two popular types of flow are considered.

1. Constant flow rate
2. Flow rate at constant pressure at the wellbore.

This simulation package is designed to utilize the explicit production procedure which requires that the oil, gas and water flow rates be evaluated at last time level. The flow rates are evaluated according to the well type designated by IQ vector defined in section 7.1.

1. Water injection well ($IQ = -2$)

$$q_0 = 0 \quad (7.21)$$

$$q_g = 0 \quad (7.22)$$

$$q_w = + \text{const.} \quad (7.23)$$

2. Gas injection well ($IQ = -1$)

$$q_0 = 0 \quad (7.24)$$

$$q_g = + \text{const.} \quad (7.25)$$

$$q_w = 0 \quad (7.26)$$

3. Gas producing well at constant rate ($IQ = 1$)

$$q_0 = 0 \quad (7.27)$$

$$q_g = - \text{const.} \quad (7.28)$$

$$q_w = \frac{k_{rw}\rho_w}{\mu_w\rho_w^*} \frac{\mu_g\rho_g^*}{k_{rg}\rho_g} q_g \quad (7.29)$$

4. Oil producing well at constant rate ($IQ = 2$)

$$q_0 = - \text{const.} \quad (7.30)$$

$$q_w = \frac{k_{rw}\rho_w}{\mu_w\rho_w^*} \frac{\mu_o\rho_o^*}{k_{ro}\rho_o} q_0 \quad (7.31)$$

$$q_g = \frac{k_{rg}\rho_g}{\mu_g\rho_g^*} \frac{\mu_o\rho_o^*}{k_{ro}\rho_o} q_0 + \frac{1}{\rho_g^*} (\rho_o^* q_o R_{so} + \rho_w^* q_w R_{sw}) \quad (7.32)$$

5. Oil producing well at constant pressure at the wellbore
 (IQ = 3)

$$q_o = \frac{-0.0864 \sqrt{k_x k_y} k_{ro} h \rho_o (P - P_{wf})}{\mu_o \rho_o^* \left\{ \ln \left(\frac{1}{r_w} \sqrt{\frac{\Delta x \Delta y}{\pi}} \right) - \frac{3}{4} \right\}} \quad (7.33)$$

$$q_w = \frac{k_{rw} \rho_w}{\mu_w \rho_w^*} \frac{\mu_o \rho_o^*}{k_{ro} \rho_o} q_o \quad (7.34)$$

$$q_g = \frac{k_{rg} \rho_g}{\mu_g \rho_g^*} \frac{\mu_o \rho_o^*}{k_{ro} \rho_o} q_o + \frac{1}{\rho_g^*} (\rho_o^* q_o R_{so} + \rho_w^* q_w R_{sw}) \quad (7.35)$$

CHAPTER VIII

COMPARATIVE EVALUATION

The simulator outlined in chapter VII was developed and used to simulate Little Axe Unit cf S.E. Denver Pool of Cleveland County in Oklahoma with two sets of permeabilities:

- a) Constant permeability for homogeneous case
- b) Variable permeability for heterogeneous case

The geometry and properties of this reservoir are given in Appendix D.

The pressure equations are solved with six different numerical procedures, namely PSOR, LSOR, ADI, SIP of chapter IV, STBAND of chapter V, and the new method (RADP) of chapter VI. The computer listing of these numerical procedures is given in Appendix E. A sample of computer simulation output is given in Appendix F.

The comparative evaluation of these numerical procedures includes difficulties of iterative methods, storage requirements, CPU time, mass balance errors, and average reservoir pressure.

8.1 Difficulties of Iterative Methods

Iterative methods have a number of difficulties not present in direct methods. Some of these difficulties are:

1 - Nonreliability: It is well known that the iterative methods do not work for every system of equations. Sometimes direct methods do not converge and sometimes they converge, but not to the right answer.

The last three months of the simulation for homogeneous case, the strongly implicit procedure did not converge within the pre-defined tolerance with the maximum number of iterations allowed. However, we obtained all needed results with higher pressure errors.

2 - Iteration parameters: The estimation of iteration parameters is a serious problem that experience and experimental runs are needed to get a suitable parameter.

3 - Convergence criterion: The relative error of successive approximations are used as convergence criterion. Such a criterion gives no indication of how well the computed solution actually satisfies the original equation. Consequently, the above criterion can be misleading.

8.2 - Storage Requirements

The computer storage requirements of the numerical procedures are given in Table 8.1.

Numerical Procedure	Computer Storage (Bytes)	Computer Storage for one cell (Bytes)	Computer Storage Relative to PSOR
PSOR	13632	39.50	1.00
LSOR	18714	54.24	1.37
ADI	34132	98.93	2.50
SIP	34404	99.72	2.52
STBAND	55778	161.68	4.09
RADP	50894	147.52	3.73

Table 8.1 - Computer Storage Requirements

The direct methods require larger computer storage than iterative methods. However, in direct methods, RADP requires 91% of the computer storage required for STBAND.

8.3 - CPU Time Comparison

The CPU time consumed in simulating the reservoir model as a function of real time is given in Tables 8.2 and 8.3. These two tables are plotted on Figure 8.1 and 8.2 for visual comparison.

From Figures 8.1 and 8.2, it is obvious that iterative methods are faster than direct methods.

In direct methods, the new method (RADP) is substantially faster than the band matrix algorithm applied to standard ordering (STBAND). In a 600 days simulation and 345 cell system, RADP requires 65.5% of the computer time required for STBAND to perform the same simulation.

Among the iterative methods used, the PSOR is faster than LSOR, ADI, and SIP. The ADI is slightly better for homogeneous case while SIP is considerably better for heterogeneous run.

It is noticeable that the CPU time curve is linear for direct methods and concaved upward for iterative methods. Therefore, the CPU time for direct methods is predictable in contrary to iterative methods. This feature is due to the nature of direct methods in which the solution to the system of equations is obtained upon the completion of a finite number of arithmetic operations.

8.4 - Mass Balance Errors

Four types of mass balance relative errors for homogeneous and heterogeneous cases are presented in Tables 8.4 through 8.11. The differences among all types of errors for all six methods are too small to draw any general conclusions.

REAL TIME DAYS	NUMERICAL PROCEDURE					
	PSOR	LSOR	ADI	SIP	STBAND	RADP
30	0.97	1.57	2.23	2.50	5.13	3.38
60	1.91	3.17	4.71	5.00	10.17	6.78
90	2.87	4.68	7.18	7.51	15.26	10.14
120	3.81	6.27	9.60	10.01	20.56	13.53
150	4.71	7.91	11.93	12.51	25.89	16.92
180	5.62	9.54	14.27	15.02	31.27	20.30
210	6.52	11.21	16.68	17.52	36.64	23.78
240	7.44	12.94	19.18	20.00	41.87	27.20
270	8.41	14.75	21.73	22.53	47.09	30.58
300	9.43	16.58	24.29	25.03	52.28	33.99
330	10.48	18.51	26.85	27.52	57.45	37.39
360	11.54	20.50	29.39	30.02	62.62	40.82
390	12.65	22.54	31.95	32.49	67.78	44.29
420	13.82	24.66	34.60	34.99	72.94	47.76
450	15.11	26.79	37.37	37.48	78.11	51.20
480	16.46	28.91	40.11	39.98	83.29	54.62
510	17.82	31.07	43.00	43.52	88.59	58.07
540	19.22	33.28	45.81	46.50	93.78	61.57
570	20.80	35.66	49.60	50.42	98.97	65.04
600	22.82	38.25	53.51	56.00	104.14	68.52

TABLE 8.2 - CPU TIME FOR HOMOGENEOUS CASE IN SECONDS

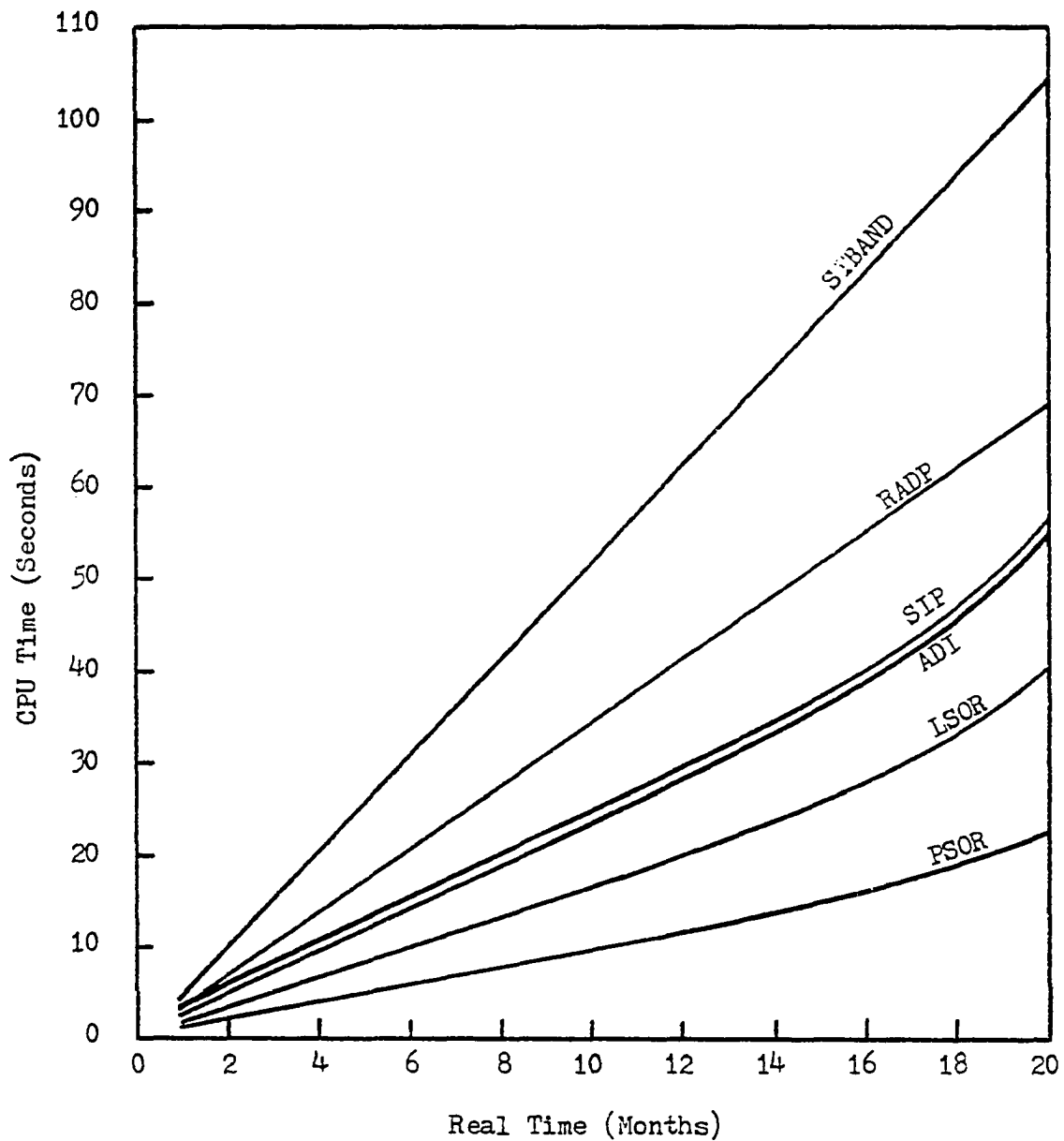


Figure 8.1 - CPU Time vs. Real Time (Homogeneous Case - 345 Cells)

REAL TIME DAYS	NUMERICAL PROCEDURE					
	PSOR	LSOR	ADI	SIP	STBAND	RADP
30	0.94	1.58	2.52	2.11	5.44	3.39
60	1.90	3.17	5.10	4.22	10.80	6.79
90	2.85	4.78	7.76	6.34	16.17	10.23
120	3.79	6.33	10.33	8.32	21.55	13.65
150	4.71	7.85	12.76	10.54	26.92	17.05
180	5.60	9.42	15.25	12.59	32.25	20.44
210	6.55	11.01	17.74	14.72	37.57	23.89
240	7.49	12.65	20.17	16.72	42.83	27.38
270	8.42	14.38	22.72	19.01	48.09	30.88
300	9.41	16.17	25.14	21.00	53.52	34.28
330	10.43	18.06	27.70	23.22	58.82	37.69
360	11.45	20.04	30.27	25.29	64.00	41.13
390	12.63	22.08	33.00	27.42	69.12	44.54
420	13.83	24.09	35.65	29.50	74.22	47.96
450	15.04	26.12	38.27	31.70	79.58	51.37
480	16.39	28.24	40.92	33.75	84.84	54.78
510	17.74	30.38	43.83	35.80	90.05	58.20
540	19.06	32.69	47.37	38.02	95.18	61.64
570	20.58	35.10	51.29	40.10	100.42	65.10
600	22.19	37.62	57.56	43.01	105.59	68.49

TABLE 8.3 - CPU TIME FOR HETEROGENEOUS CASE IN SECONDS

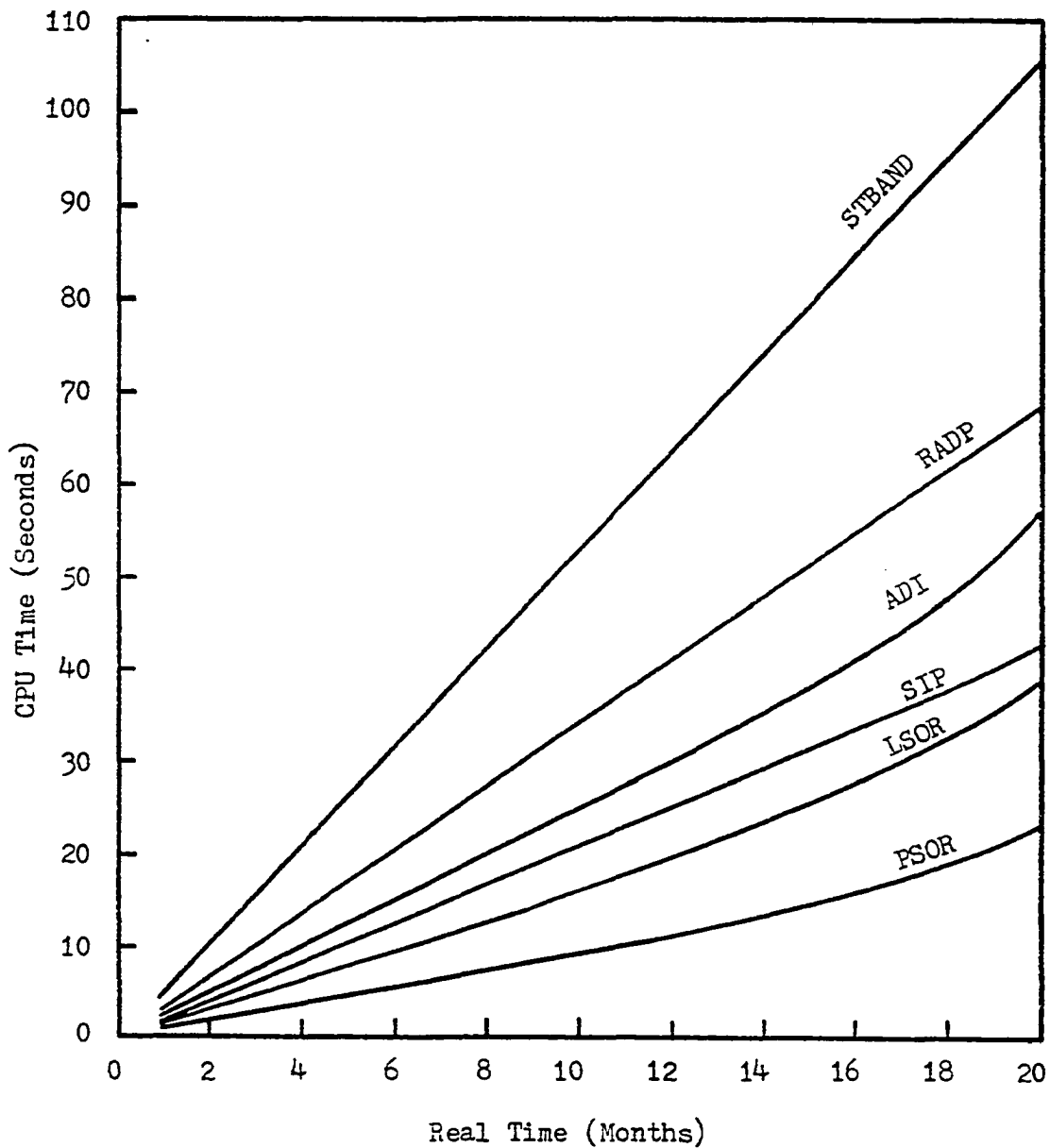


Figure 8.2 - CPU Time vs. Real Time (Heterogeneous Case - 345 Cells)

REAL TIME DAYS	NUMERICAL PROCEDURE					
	PSOR	LSOR	ADI	SIP	STBAND	RADP
30	0.0009	0.0010	0.0010	0.0008	0.0010	0.0010
60	0.0018	0.0018	0.0019	0.0026	0.0019	0.0019
90	0.0026	0.0027	0.0027	0.0033	0.0027	0.0027
120	0.0034	0.0035	0.0035	0.0041	0.0035	0.0035
150	0.0042	0.0042	0.0042	0.0047	0.0042	0.0042
180	0.0049	0.0049	0.0049	0.0045	0.0050	0.0049
210	0.0055	0.0055	0.0056	0.0051	0.0056	0.0056
240	0.0062	0.0062	0.0064	0.0061	0.0063	0.0062
270	0.0068	0.0068	0.0071	0.0068	0.0069	0.0068
300	0.0075	0.0075	0.0082	0.0074	0.0076	0.0075
330	0.0081	0.0081	0.0090	0.0073	0.0082	0.0081
360	0.0090	0.0090	0.0102	0.0084	0.0091	0.0090
390	0.0098	0.0098	0.0113	0.0086	0.0099	0.0098
420	0.0111	0.0111	0.0129	0.0092	0.0112	0.0111
450	0.0122	0.0122	0.0142	0.0099	0.0123	0.0122
480	0.0144	0.0143	0.0163	0.0105	0.0145	0.0144
510	0.0164	0.0163	0.0178	0.0109	0.0164	0.0164
540	0.0191	0.0182	0.0201	0.0111	0.0185	0.0177
570	0.0216	0.0201	0.0230	0.0115	0.0216	0.0213
600	0.0027	-0.0056	0.0267	0.0116	0.0083	0.0054

TABLE 8.4 - TOTAL MASS BALANCE RELATIVE ERROR FOR HOMOGENEOUS CASE

REAL TIME DAYS	NUMERICAL PROCEDURE					
	PSOR	LSOR	ADI	SIP	STBAND	RADP
30	0.0010	0.0010	0.0010	0.0009	0.0010	0.0010
60	0.0019	0.0019	0.0019	0.0020	0.0019	0.0019
90	0.0027	0.0027	0.0027	0.0026	0.0028	0.0027
120	0.0035	0.0035	0.0035	0.0034	0.0036	0.0036
150	0.0043	0.0043	0.0043	0.0031	0.0043	0.0043
180	0.0050	0.0050	0.0051	0.0049	0.0051	0.0050
210	0.0057	0.0057	0.0058	0.0055	0.0058	0.0058
240	0.0065	0.0064	0.0067	0.0064	0.0066	0.0065
270	0.0072	0.0071	0.0075	0.0070	0.0072	0.0072
300	0.0080	0.0079	0.0087	0.0077	0.0081	0.0080
330	0.0086	0.0086	0.0097	0.0078	0.0087	0.0087
360	0.0096	0.0095	0.0112	0.0082	0.0097	0.0096
390	0.0103	0.0103	0.0124	0.0090	0.0104	0.0103
420	0.0114	0.0114	0.0144	0.0094	0.0116	0.0115
450	0.0126	0.0126	0.0158	0.0099	0.0128	0.0127
480	0.0146	0.0145	0.0178	0.0100	0.0147	0.0147
510	0.0163	0.0163	0.0199	0.0102	0.0167	0.0167
540	0.0188	0.0186	0.0231	0.0102	0.0191	0.0191
570	0.0216	0.0213	0.0274	0.0110	0.0219	0.0219
600	0.0184	0.0170	0.0293	0.0113	0.0178	0.0174

TABLE 8.5 - TOTAL MASS BALANCE RELATIVE ERROR FOR HETEROGENEOUS CASE

REAL TIME DAYS	NUMERICAL PROCEDURE					
	PSOR	LSOR	ADI	SIP	STBAND	RADP
30	0.0015	0.0015	0.0015	0.0013	0.0015	0.0015
60	0.0030	0.0031	0.0031	0.0043	0.0031	0.0031
90	0.0045	0.0045	0.0045	0.0056	0.0046	0.0045
120	0.0058	0.0059	0.0059	0.0069	0.0060	0.0059
150	0.0071	0.0072	0.0072	0.0079	0.0073	0.0072
180	0.0083	0.0084	0.0083	0.0075	0.0085	0.0084
210	0.0094	0.0094	0.0094	0.0084	0.0096	0.0095
240	0.0105	0.0104	0.0101	0.0100	0.0106	0.0105
270	0.0113	0.0113	0.0107	0.0113	0.0115	0.0114
300	0.0121	0.0120	0.0107	0.0124	0.0122	0.0121
330	0.0126	0.0125	0.0109	0.0131	0.0128	0.0126
360	0.0128	0.0127	0.0100	0.0139	0.0130	0.0129
390	0.0126	0.0125	0.0095	0.0142	0.0128	0.0126
420	0.0121	0.0120	0.0076	0.0152	0.0123	0.0121
450	0.0107	0.0105	0.0061	0.0164	0.0108	0.0107
480	0.0094	0.0094	0.0031	0.0173	0.0094	0.0093
510	0.0053	0.0055	0.0012	0.0180	0.0055	0.0054
540	0.0017	0.0011	-0.0022	0.0187	0.0015	-0.0004
570	-0.0041	-0.0045	-0.0068	0.0197	-0.0035	-0.0037
600	-0.0477	-0.0615	-0.0127	0.0206	-0.0353	-0.0412

TABLE 8.6 - OIL MASS BALANCE RELATIVE ERROR FOR HOMOGENEOUS CASE

REAL TIME DAYS	NUMERICAL PROCEDURE					
	PSOR	LSOR	ADI	SIP	STBAND	RADP
30	0.0015	0.0016	0.0016	0.0015	0.0016	0.0016
60	0.0031	0.0031	0.0032	0.0032	0.0032	0.0032
90	0.0046	0.0046	0.0046	0.0043	0.0047	0.0047
120	0.0060	0.0060	0.0060	0.0057	0.0061	0.0061
150	0.0073	0.0073	0.0073	0.0052	0.0074	0.0074
180	0.0085	0.0085	0.0085	0.0081	0.0086	0.0086
210	0.0097	0.0096	0.0095	0.0092	0.0098	0.0097
240	0.0105	0.0104	0.0100	0.0108	0.0106	0.0105
270	0.0113	0.0112	0.0106	0.0117	0.0114	0.0113
300	0.0118	0.0116	0.0102	0.0125	0.0119	0.0118
330	0.0122	0.0120	0.0102	0.0126	0.0124	0.0122
360	0.0124	0.0121	0.0087	0.0132	0.0125	0.0124
390	0.0124	0.0120	0.0078	0.0145	0.0125	0.0123
420	0.0120	0.0116	0.0051	0.0152	0.0120	0.0118
450	0.0107	0.0103	0.0037	0.0160	0.0107	0.0104
480	0.0095	0.0092	0.0006	0.0158	0.0094	0.0092
510	0.0058	0.0052	-0.0026	0.0158	0.0052	0.0049
540	0.0061	0.0061	-0.0081	0.0159	0.0056	0.0054
570	-0.0006	0.0001	-0.0159	0.0177	-0.0012	-0.0016
600	-0.0145	-0.0155	-0.0172	0.0174	-0.0166	-0.0175

TABLE 8.7 - OIL MASS BALANCE RELATIVE ERROR FOR HETEROGENEOUS CASE

REAL TIME DAYS	NUMERICAL PROCEDURE					
	PSOR	LSOR	ADI	SIP	STBAND	RADP
30	0.0002	0.0002	0.0002	0.0002	0.0002	0.0002
60	0.0002	0.0002	0.0002	0.0004	0.0002	0.0002
90	0.0002	0.0003	0.0002	0.0004	0.0003	0.0003
120	0.0003	0.0003	0.0003	0.0003	0.0003	0.0003
150	0.0003	0.0003	0.0003	0.0004	0.0003	0.0003
180	0.0003	0.0004	0.0005	0.0006	0.0004	0.0004
210	0.0004	0.0004	0.0007	0.0006	0.0004	0.0004
240	0.0006	0.0007	0.0016	0.0009	0.0006	0.0006
270	0.0008	0.0009	0.0024	0.0009	0.0009	0.0009
300	0.0015	0.0016	0.0048	0.0009	0.0015	0.0015
330	0.0022	0.0023	0.0065	0.0010	0.0022	0.0022
360	0.0040	0.0041	0.0105	0.0011	0.0040	0.0040
390	0.0061	0.0062	0.0136	0.0012	0.0061	0.0061
420	0.0100	0.0102	0.0198	0.0013	0.0100	0.0100
450	0.0142	0.0145	0.0250	0.0014	0.0143	0.0143
480	0.0220	0.0218	0.0336	0.0017	0.0220	0.0220
510	0.0314	0.0309	0.0397	0.0017	0.0310	0.0311
540	0.0441	0.0426	0.0497	0.0012	0.0423	0.0427
570	0.0571	0.0540	0.0625	0.0008	0.0563	0.0562
600	0.0644	0.0603	0.0792	-0.0002	0.0630	0.0634

TABLE 8.8 - WATER MASS BALANCE RELATIVE ERROR FOR HOMOGENEOUS CASE

REAL TIME DAYS	NUMERICAL PROCEDURE					
	PSOR	LSOR	ADI	SIP	STBAND	RADP
30	0.0002	0.0002	0.0002	0.0002	0.0002	0.0002
60	0.0002	0.0002	0.0002	0.0003	0.0002	0.0002
90	0.0002	0.0002	0.0002	0.0003	0.0002	0.0002
120	0.0003	0.0003	0.0003	0.0004	0.0003	0.0003
150	0.0003	0.0003	0.0003	0.0005	0.0003	0.0003
180	0.0004	0.0004	0.0006	0.0006	0.0004	0.0004
210	0.0006	0.0006	0.0010	0.0008	0.0006	0.0006
240	0.0012	0.0013	0.0024	0.0008	0.0013	0.0013
270	0.0017	0.0013	0.0035	0.0008	0.0017	0.0017
300	0.0030	0.0030	0.0066	0.0013	0.0030	0.0030
330	0.0039	0.0041	0.0090	0.0016	0.0040	0.0040
360	0.0059	0.0062	0.0145	0.0017	0.0060	0.0060
390	0.0076	0.0079	0.0185	0.0018	0.0077	0.0077
420	0.0109	0.0113	0.0267	0.0019	0.0111	0.0112
450	0.0151	0.0156	0.0316	0.0020	0.0156	0.0157
480	0.0219	0.0221	0.0404	0.0024	0.0224	0.0226
510	0.0303	0.0310	0.0495	0.0029	0.0318	0.0322
540	0.0374	0.0369	0.0642	0.0027	0.0385	0.0390
570	0.0517	0.0504	0.0846	0.0023	0.0532	0.0540
600	0.0630	0.0607	0.0913	0.0032	0.0639	0.0645

TABLE 8.9 - WATER MASS BALANCE RELATIVE ERROR FOR HETEROGENEOUS CASE

REAL TIME DAYS	NUMERICAL PROCEDURE					
	PSOR	LSOR	ADI	SIP	STBAND	RADP
30	0.0015	0.0015	0.0015	0.0013	0.0015	0.0015
60	0.0030	0.0031	0.0031	0.0043	0.0031	0.0031
90	0.0045	0.0045	0.0045	0.0056	0.0046	0.0045
120	0.0058	0.0059	0.0059	0.0069	0.0060	0.0059
150	0.0071	0.0072	0.0072	0.0079	0.0073	0.0072
180	0.0083	0.0084	0.0083	0.0070	0.0085	0.0084
210	0.0094	0.0094	0.0094	0.0084	0.0096	0.0095
240	0.0105	0.0105	0.0101	0.0100	0.0106	0.0105
270	0.0113	0.0113	0.0107	0.0113	0.0115	0.0114
300	0.0120	0.0120	0.0107	0.0124	0.0122	0.0121
330	0.0126	0.0125	0.0109	0.0131	0.0128	0.0126
360	0.0125	0.0123	0.0100	0.0139	0.0127	0.0125
390	0.0125	0.0125	0.0095	0.0142	0.0128	0.0126
420	0.0105	0.0103	0.0075	0.0152	0.0109	0.0106
450	0.0103	0.0102	0.0061	0.0164	0.0106	0.0104
480	0.0042	0.0041	0.0028	0.0173	0.0047	0.0043
510	0.0030	0.0032	0.0009	0.0180	0.0038	0.0033
540	-0.0100	-0.0090	-0.0035	0.0187	-0.0066	-0.0069
570	-0.0137	-0.0122	-0.0089	0.0197	-0.0124	-0.0145
600	-0.0247	-0.0231	-0.0173	0.0206	-0.0219	-0.0249

TABLE 8.10 - GAS MASS BALANCE RELATIVE ERROR FOR HOMOGENEOUS CASE

REAL TIME DAYS	NUMERICAL PROCEDURE					
	PSOR	LSOR	ADI	SIP	STBAND	RADP
30	0.0015	0.0016	0.0016	0.0015	0.0016	0.0016
60	0.0031	0.0031	0.0032	0.0032	0.0032	0.0032
90	0.0046	0.0046	0.0046	0.0043	0.0047	0.0047
120	0.0060	0.0060	0.0060	0.0057	0.0061	0.0061
150	0.0074	0.0073	0.0073	0.0052	0.0074	0.0074
180	0.0085	0.0085	0.0085	0.0081	0.0086	0.0086
210	0.0097	0.0096	0.0095	0.0092	0.0098	0.0097
240	0.0105	0.0104	0.0100	0.0103	0.0106	0.0105
270	0.0113	0.0112	0.0106	0.0117	0.0114	0.0113
300	0.0118	0.0116	0.0102	0.0125	0.0119	0.0118
330	0.0122	0.0120	0.0102	0.0125	0.0124	0.0122
360	0.0124	0.0121	0.0087	0.0132	0.0125	0.0123
390	0.0124	0.0120	0.0078	0.0145	0.0125	0.0123
420	0.0113	0.0108	0.0051	0.0152	0.0115	0.0112
450	0.0106	0.0102	0.0037	0.0160	0.0106	0.0104
480	0.0061	0.0055	0.0005	0.0155	0.0062	0.0058
510	0.0051	0.0044	-0.0028	0.0156	0.0047	0.0043
540	-0.0040	-0.0047	-0.0089	0.0159	-0.0041	-0.0048
570	-0.0062	-0.0069	-0.0177	0.0177	-0.0066	-0.0075
600	-0.0220	-0.0218	-0.0223	0.0174	-0.0222	-0.0239

TABLE 8.11 - GAS MASS BALANCE RELATIVE ERROR FOR HETEROGENEOUS CASE

8.5 - Average Reservoir Pressure

The average reservoir pressure is given in Tables 8.12 and 8.13. For a given time, the differences of pressures are relatively small to draw any conclusions.

REAL TIME DAYS	NUMERICAL PROCEDURE					
	PSOR	LSOR	ADI	SIP	STBAND	RADP
30	15617	15624	15625	15577	15628	15626
60	15585	15594	15596	15807	15602	15597
90	15587	15593	15595	15762	15605	15598
120	15554	15561	15564	15739	15576	15567
150	15548	15554	15558	15678	15571	15560
180	15521	15526	15530	15420	15546	15534
210	15509	15514	15521	15374	15537	15522
240	15487	15488	15494	15441	15515	15498
270	15474	15475	15483	15481	15504	15485
300	15451	15450	15459	15465	15482	15462
330	15441	15439	15450	15416	15473	15452
360	15419	15414	15429	15413	15452	15429
390	15414	15409	15420	15336	15449	15424
420	15389	15382	15401	15353	15424	15398
450	15397	15389	15391	15419	15433	15406
480	15373	15362	15377	15448	15409	15380
510	15409	15397	15369	15456	15443	15415
540	15287	15271	15361	15424	15424	15394
570	15263	15203	15358	15447	15216	15093
600	14549	14302	15360	15437	14919	14755

TABLE 8.12 - AVERAGE RESERVOIR PRESSURE FOR HOMOGENEOUS CASE

REAL TIME DAYS	NUMERICAL PROCEDURE					
	PSOR	LSOR	ADI	SIP	STBAND	RADP
30	15624	15627	15628	15613	15631	15629
60	15595	15600	15604	15633	15609	15605
90	15604	15602	15607	15554	15616	15610
120	15573	15573	15579	15547	15591	15583
150	15577	15569	15578	15306	15591	15581
180	15552	15543	15553	15508	15570	15558
210	15550	15536	15549	15488	15566	15553
240	15528	15512	15525	15527	15547	15532
270	15522	15502	15521	15508	15542	15525
300	15502	15480	15500	15511	15525	15506
330	15498	15472	15497	15378	15521	15500
360	15477	15449	15477	15356	15502	15480
390	15477	15445	15476	15405	15502	15478
420	15454	15421	15458	15383	15483	15457
450	15464	15428	15459	15394	15492	15465
480	15441	15401	15442	15279	15469	15440
510	15482	15435	15445	15203	15505	15475
540	15468	15406	15434	15120	15480	15448
570	15526	15479	15443	15232	15537	15501
600	15378	15334	15445	15156	15311	15251

TABLE 8.13 - AVERAGE RESERVOIR PRESSURE FOR HETEROGENEOUS CASE

CHAPTER IX

CONCLUSIONS

Based on the numerical simulation results observed in this study, it is possible to draw the following conclusions:

1. Direct methods are more reliable than iterative ones.
Some iterative methods fail to converge at certain times and under certain conditions. The error will propagate from this point on.
2. The search for optimum iteration parameters in iterative methods is a serious problem especially for SIP.
3. The ADI and SIP methods are sensitive to the type of reservoir models while direct methods are not. This observation is implied by the CPU time requirements.
The ADI is slightly better for homogeneous case while SIP is considerably better for heterogeneous run.
4. Iterative methods require less computer storage than direct methods no matter how efficient the direct method is.
5. The iterative methods are faster than direct methods for the 345 cell model simulated in this study.
6. Among the iterative methods used, the PSOR is faster than LSOR, ADI, and SIP.

7. RADP requires about 65.5% of the CPU time consumed by STBAND. RADP requires about 91% of the computer storage required for STBAND. These improvements are due to the fact that RADP generates less new non-zero elements in the direct solution process. Therefore, RADP is more competitive to the iterative methods than STBAND direct method.

NOMENCLATURE

A	coefficient matrix
A	cross-sectional area to flow
A_i, B_i, C_i, F_i, E_i	SIP coefficient vectors
a_i, b_i, c_i, e_i, f_i	coefficients of the general pressure equation
ADI	Alternating Diagonal Implicit
B_1	PVT term
B_2	production term
B_3	capillary pressure term
B_4	gravity term
B_5	second degree derivative term
Q	composite matrix ($=L\backslash U$)
C	compressibility
D	subsea level, positive downward
DPLIM	maximum pressure change desired
DPMAX	maximum pressure change calculated
DSLIM	maximum saturation change desired
DSMAX	maximum saturation change calculated
DTMAX	maximum time step allowed
DTMIN	minimum time step allowed
d	day
d	right-hand side vector of pressure equations

d_i	an element of \underline{d}
f	an arbitrary function
ft	foot
G_{ij}, H_{ij}	vectors in RADP
g	acceleration due to gravity
g_i, h_i	the new coefficients introduced for SIP
h	formation thickness
I	the largest of N_x and N_y
J	the smallest of N_x and N_y
K	Kelvin absolute temperature
k	absolute permeability
kg	kilogram
kPa	kilo-Pascal
k_{max}	maximum number of iterations on pressure
k_r	relative permeability
L	lower triangular matrix
LSOR	Line Successive Overrelaxation
L_d	length of the diagonal along which numbering is applied
l	an element of L
lb_m	pound mass
M	mass
MIP	mass in place
m	meter
m	semi-bandwidth
m	number of iteration parameters in the system
N	number of active cells

N_d	number of diagonals in the system
N_l	number of rows in the lower half of matrix \mathbf{A}
N_u	number of rows in the upper half of matrix \mathbf{A}
N_x	number of cells in the x-direction
N_y	number of cells in the y-direction
NTRMAX	maximum number of trials on material balance
OUTMOD	print out interval
\underline{P}	pressure vector
Pa	Pascal
Psi	pound per square inch
P_{BP}	bubble point pressure
P_{cg}	capillary pressure to gas
P_{cw}	capillary pressure to water
P_i	an element of \underline{P}
P_{pc}	pseudo critical pressure
P_{ref}	reference pressure
P_{wf}	flowing bottom hole pressure of the well
PSOR	Point Successive Overrelaxation
P^*	pressure at standard condition
q	flow rate, positive rates denote injection, negative rates denote production
R	Rankine absolute temperature
RAD	Restricted Alternating Diagonal
RADP	RAD Procedure
R_{so}	solubility of gas into oil
R_{sw}	solubility of gas into water
r	constant multiplier

r_i, r_j	relative error
r_w	well radius
r_{\max}	maximum absolute relative error
$(r_{mb})_{\max}$	mass balance maximum absolute relative error
S	saturation
S	storage
S_{gc}	equilibrium gas saturation
S_{or}	irreducible oil saturation
St.	Standard
S_{wc}	connate water saturation
SCF	Standard Cubic Feet
SIP	Strongly Implicit Procedure
SOR	Successive Overrelaxation
STB	Stock tank barrel
STBAND	band matrix algorithm applied on standard ordering
s	second
T	temperature
T	transmissibility
T_{pc}	pseudo critical temperature
TM	total mass
TPRINT	print out time
T^*	temperature at standard conditions
t	time
U	upper triangular matrix
u	an element of U
V_i	pore volume of cell i

W	work
z	gas compressibility factor
z^*	gas compressibility factor at standard conditions

Greek Letters

α	iteration parameter for SIP
β	iteration parameter for ADI
γ_i	normalizing factor for β
Δt	time increment
$\Delta x, \Delta y$	distance increments
ϵ	pressure tolerance
ϵ_m	mass balance tolerance
η	N_x
θ	Crank-Nicholson parameter
λ	mobility
μ	viscosity
μm	micro-meter
ρ	density
ρ^*	density at standard conditions
ϕ	potential
ϕ	porosity
ω	iteration parameter for SOR

Subscripts and Superscripts

f	final
g	gas phase
i	cell number
i	initial
j	phase identifier (oil,water,or gas)

jc cumulative of phase j
k iteration counter
m mass
n time level
o oil phase
r rock
t total
w water phase
x x-direction
y y-direction

REFERENCES

1. Al-Marhoun, M.A., "Two-Dimensional Two-Phase Petroleum Reservoir Simulator (Development and System Study)," M.S. Thesis (1976), University of Petroleum and Minerals, Dhahran, Saudi Arabia.
2. Birkhoff, G.; Varga, R.S.; and Young, D., "Alternating Direction Implicit Methods," Advances in Computers (1962) 3, 189-273.
3. Brietenbach, E.A.; Thurnau, D.H.; and Van Poollen, H.K., "Solution of the Immiscible Fluid Flow Simulation Equation," Soc. Pet. Eng. J. (June 1969) 155-169.
4. Craft, B.C.; and Hawkins, M.F., "Applied Petroleum Reservoir Engineering" Prentice-Hall, Inc., Englewood Cliffs, N.J. (1959).
5. Craig, F.F., "Compositional Flow in Porous Media: A Reservoir Simulator," Ph.D. Dissertation (1976), University of Oklahoma, Norman, Oklahoma, U.S.A.
6. Crichton, H.B., "Modern Reservoir Engineering - A Simulation Approach," Prentice-Hall, Inc., N.J. (1977).
7. Crout, P.D., "A Short Method for Evaluating Determinants and Solving Systems of Linear Equations with Real or Complex Coefficients," Trans. AIEE (1941), 60, 1235.
8. Gopal, V.N., "Gas Z-Factor Equations Developed for Computer," Oil & Gas J. (August 8, 1977) 58-60.
9. McDonald, A.E.; and Trimble, R.H., "Efficient Use of Mass Storage During Elimination for Sparse Sets of Simulation Equations," Soc. Pet. Eng. J. (Aug. 1977) 300-316.

10. Merchant, A.R.; Arnold, M.D.; and Harvey, A.H., "A Technique for Improving Material Balance Accuracy in Reservoir Simulation Models," SPE No. 4548.
11. Peaceman, D.W. and Rachford, H.H., "The Numerical Solution of Parabolic and Elliptic Differential Equations," J. Soc. Indust. Appl. Math. (1955), 3, 28-41.
12. Price, H.S. and Coats, K.H., "Direct Methods in Reservoir Simulation," Transactions of SPE of AIME (1974, vol. 257, pp 295-308).
13. Stone, H.L., "Estimation of Three-Phase Relative Permeability and Residual Oil Data," JPT, Oct. - Dec., 1973, p. 53.
14. Stone, H.L., "Iterative Solution of Implicit Approximation of Multidimensional Partial Differential Equations," SIAM Numer. Anal. (1968), 5, 530.
15. Suarez, A. and Farouq Ali, S.M., "A Comparative Evaluation of Different Versions of the Strongly Implicit Procedure (SIP)," Fourth SPE Symposium on Numerical Simulation of Reservoir Performance, Los Angeles, California, Feb. 19-20, 1976, SPE No. 5732.
16. Todd, M.R.; O'Dell, P.M.; and Hirasaki, R.J., "Methods of Increased Accuracy in Numerical Reservoir Simulators," Trans. AIME (1972), 253.
17. Varga, R.S., "Matrix Iterative Analysis," Englewood Cliffs, N.J.: Prentice Hall, 1962.
18. Von Rosenberg, D.U., "Methods for the Numerical Solution of Partial Differential Equations," New York: American Elsevier Publishing Co., Inc., 1969.

19. Watts, J.W., "An Iterative Matrix Solution Method Suitable for Anisotropic Problems," SPE Reprint No. 11 (1973), p. 119.
20. Weinstein, H.G.; Stone, H.L.; and Kwan, T.V., "Simultaneous Solution of Multiphase Reservoir Flow Equations," SPE Reprint No. 11 (1973), p.124.
21. Woo, P.T.; Roberts, S.J.; and Gustavson, F.G., "Application of Sparse Matrix Techniques in Reservoir Simulation," SPE No. 4544.

APPENDICES

APPENDIX A

UNITS AND CONVERSION FACTORS

Symbol	Definition	SI Units	Practical Units	English Units	Conversion factor *
A	Area	m^2	m^2	ft^2	0.09290
C	Compressibility	Pa^{-1}	kPa^{-1}	Psi^{-1}	0.14504
D	Depth	m	m	ft	0.30480
g	Gravity	m/s^2	m/s^2	ft/s^2	0.30480
h	Thickness	m	m	ft	0.30480
k	Permeability	m^2	μm^2	darcy	0.98690
P	Pressure	Pa	kPa	Psi	6.89476
$q_{o,w}$	Liquid Flow Rate	$\text{St.m}^3/\text{s}$	$\text{St.m}^3/\text{d}$	STB/d	0.15899
q_g	Gas Flow Rate	$\text{St.m}^3/\text{s}$	$\text{St.m}^3/\text{d}$	SCF/d	0.02832
R_{sj}	Solubility	kg/kg	kg/kg	SCF/STB	$0.17811 \rho_g^* / \rho_j^*$
R_{sj}	Solubility	kg/kg	kg/kg	SCF/SCF	ρ_g^* / ρ_j^*
T	Temperature	K	K	R	5/9
t	Time	s	d	d	1
μ	Viscosity	Pa-s	mPa-s	cp	1
ρ	Density	kg/m^3	kg/m^3	lb_m/ft^3	16.0185

*To obtain the practical unit, multiply the English unit by the corresponding conversion factor.

APPENDIX B

FLOW CHART CONVENTION

The following boxes, each of characteristic shape, are used for constructing the flow charts in this study.



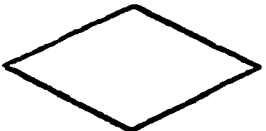
Commencement



Computation



Do loop



If statement



Input (read)



Output (print or punch)



Conclusion

APPENDIX C

CONSTANT VALUES USED IN THIS STUDY

DPLIM = 1000 kPa

DSLIM = 0.15

DTMAX = 10 d

DTMIN = 10 d (0.01 d for SIP)

g = 9.81 m/s²

k_{max} = 55

m = 10

NTRMAX = 20

N_x = 15

N_y = 23

OUTMOD = 30 d

P* = 100 kPa

P_{wf} = 4500 kPa

r_w = 0.1 m

T* = 273.16 K

t_f = 600 d

t_i = 0 d

z* = 1.0

Δx = 100 m

$\Delta y = 100 \text{ m}$
 $\varepsilon = 0.0005$
 $\varepsilon_m = 0.10$
 $\theta = 0.5$
 $\rho_g^* = 0.9 \text{ kg/m}^3$
 $\rho_0^* = 825 \text{ kg/m}^3$
 $\rho_w^* = 1160 \text{ kg/m}^3$
 $\omega = 1.6$

APPENDIX D

Geometry and Properties of the Reservoir Model

- E.1 Constant Properties of the Reservoir Model
- E.2 Relative Permeabilities
- E.3 Viscosities
- E.4 Solubilities
- E.5 Densities
- E.6 Capillary Pressure Data
- E.7 Reservoir Figures

E.1 Constant Properties of the Reservoir Model

$C_o = 2.90 \times 10^{-6} \text{ kPa}^{-1}$
 $C_w = 0.43 \times 10^{-6} \text{ kPa}^{-1}$
 $C_r = 0.58 \times 10^{-6} \text{ kPa}^{-1}$
 $k_x = 0.05 \mu\text{m}^2 \text{ (homogeneous case)}$
 $k_y = 0.05 \mu\text{m}^2 \text{ (homogeneous case)}$
 $P_{BP} = 14000 \text{ kPa}$
 $P_{oi} = 15500 \text{ kPa at } 1450 \text{ m below sea level}$
 $P_{pc} = 5270 \text{ kPa}$
 $S_{gc} = 0.05$
 $S_{or} = 0.3$
 $S_{wc} = 0.3$
 $T = 325 \text{ K}$
 $T_{pc} = 218 \text{ K}$
 $\phi = 0.161 \text{ at } 15500 \text{ kPa}$

E.2 Relative Permeabilities

$$k_{r_w} = (S_w - S_{wc})^2 / (1-S_{wc})^2 \quad (\text{E.1})$$

$$k_{r_o} = (S_o - S_{or})^2 / (1-S_{or} - S_{wc})^2 \quad (\text{E.2})$$

$$k_{r_g} = (S_g - S_{gc})^3 / (1 - S_{gc} - S_{wc} - S_{or})^3 \quad (\text{E.3})$$

$$k_{rg} \geq 0 \quad (\text{E.4})$$

E.3 Viscosities

$$\mu_w = 0.395 \quad (\text{E.5})$$

$$\mu_g = 0.0096 + 6.43967 \times 10^{-7} * P \quad (\text{E.6})$$

$$\mu_o = 0.459 - 6.6 \times 10^{-6} * P \quad , \quad P < P_{BP} \quad (\text{E.7})$$

$$\mu_o = 0.459 - 6.6 \times 10^{-6} * P_{BP} \quad , \quad P \geq P_{BP} \quad (\text{E.8})$$

E.4 Solubilities

$$R_{SO} = 0.09457 + 5.5 \times 10^{-6} * P \quad , \quad P < P_{BP} \quad (\text{E.9})$$

$$R_{SO} = 0.17157 \quad , \quad P \geq P_{BP} \quad (\text{E.10})$$

$$R_{SW} = 0 \quad (\text{E.11})$$

E.5 Densities

$$\rho_o = \rho_o^* (1 - R_{SO}) e^{C_o(P-100)} + R_{SO} \rho_g - 85 \quad (\text{E.12})$$

$$\rho_w = \rho_w^* e^{C_r(P-100)} \quad (\text{E.13})$$

$$\rho_g = \frac{\rho_g^* T^* z^* P}{P^* T z} \quad (\text{E.14})$$

The compressibility factor (z) is calculated from the following equations⁸:

$$z = P_r(0.1391T_r - 0.2988) + 0.0007T_r + 0.9969 \quad , \quad P_r \leq 1.2 \quad (\text{E.15})$$

$$z = P_r(0.0984T_r - 0.2053) + 0.0621T_r + 0.8580 \quad , \quad 1.2 < P_r \leq 2.8 \quad (\text{E.16})$$

$$z = P_r(-0.0284T_r + 0.0625) + 0.4714T_r - 0.0011 \quad , \quad P_r > 2.8 \quad (\text{E.17})$$

$$P_r = \frac{P}{P_{pc}} \quad (\text{E.18})$$

$$T_r = \frac{T}{T_{pc}} \quad (\text{E.19})$$

E.6 Capillary pressure data¹⁰

S_w	P_{cw}	S_o	P_{cg}
0.1	28.344	0.1	31.144
0.2	0.655	0.2	0.462
0.3	0.496	0.3	0.290
0.4	0.421	0.4	0.138
0.5	0.352	0.5	-0.007
0.6	0.283	0.6	-0.152
0.7	0.214	0.7	-0.296
0.8	0.145	0.8	-0.441
0.86	0.076	0.89	-0.586

E.7 Reservoir Figures

Figure

- E.1 Discretized Reservoir System
- E.2 Reservoir Thickness
- E.3 Digitized Reservoir Thickness
- E.4 Top of the Reservoir Depth
- E.5 Digitized Middle of the Reservoir Depth
- E.6 Digitized Reservoir Initial Pressure
- E.7 Reservoir Heterogeneous Permeability
- E.8 Digitized Reservoir Heterogeneous Permeability
- E.9 Configuration of Wells
- E.10 Production - Injection Flow Rates

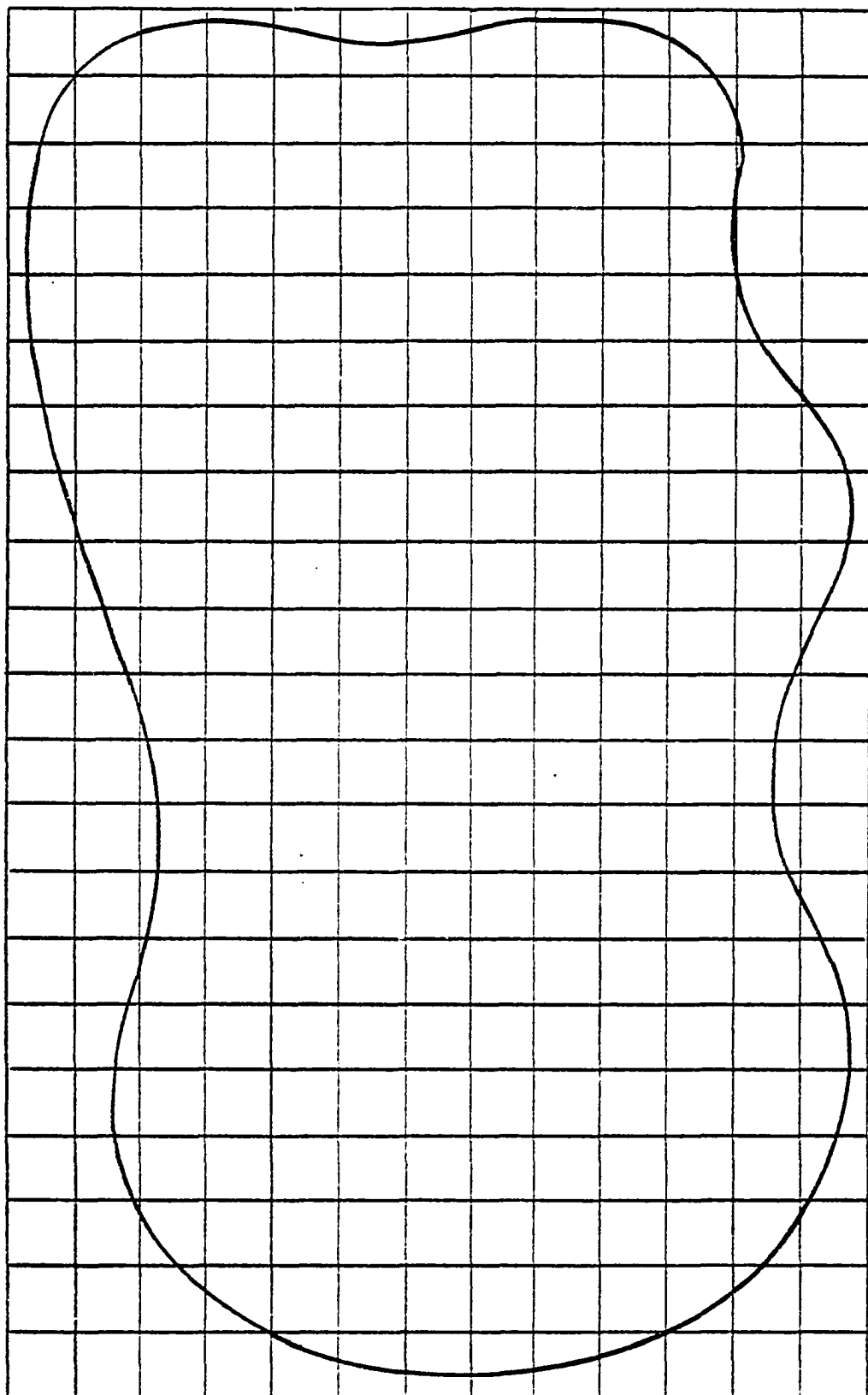


Figure E.1 - Discretized Reservoir System

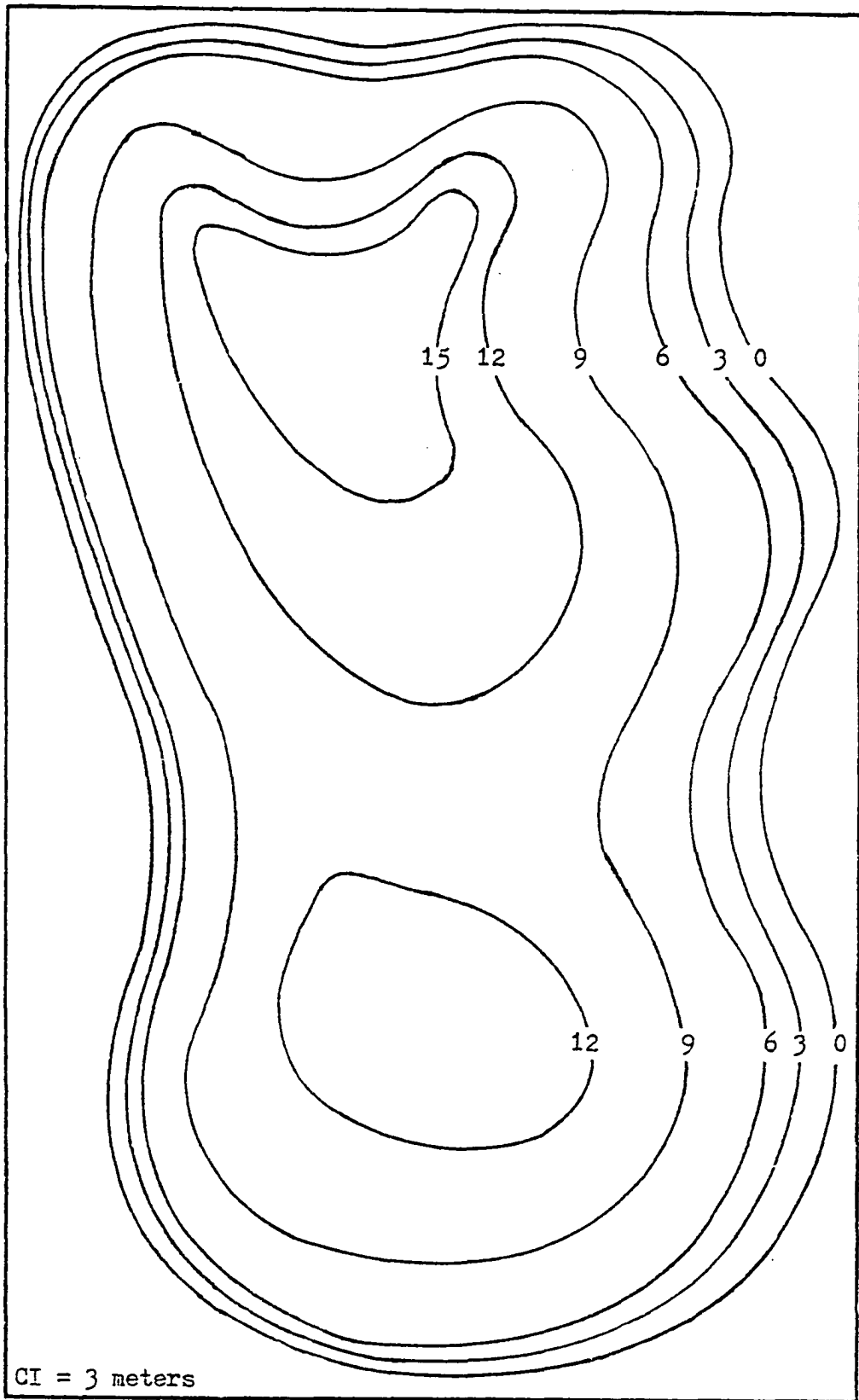


Figure E.2 - Reservoir Thickness(meters)

0	1	5	5	3	2	3	5	5	5	0	0	0
1	7	8	8	8	8	8	9	9	8	6	0	0
3	9	11	12	9	9	14	14	11	9	6	0	0
3	9	12	15	15	15	16	14	11	8	6	0	0
3	9	12	16	17	17	16	12	9	8	6	0	0
3	9	12	15	17	17	15	12	11	8	6	2	0
2	8	11	14	15	16	16	14	12	11	8	5	1
0	7	10	12	14	15	14	14	13	11	9	7	2
0	3	9	12	13	14	14	13	13	11	9	7	1
0	1	8	11	12	13	13	13	12	10	8	5	0
0	0	6	9	10	11	12	12	10	9	7	3	0
0	0	6	9	10	11	11	11	10	9	6	2	0
0	0	3	9	10	11	11	11	10	9	6	3	0
0	0	3	9	12	13	12	12	11	9	7	3	0
0	0	6	9	12	14	14	14	12	11	8	6	1
0	0	8	10	13	14	14	14	13	11	9	6	1
0	1	9	11	12	13	14	14	12	11	9	6	1
0	0	8	10	11	11	12	11	11	10	8	4	0
0	0	3	7	9	10	10	10	9	9	7	3	0
0	0	0	3	7	8	8	8	7	6	3	0	0
0	0	0	0	0	2	2	2	2	0	0	0	0

Figure E.3 - Digitized Reservoir Thickness (meters)

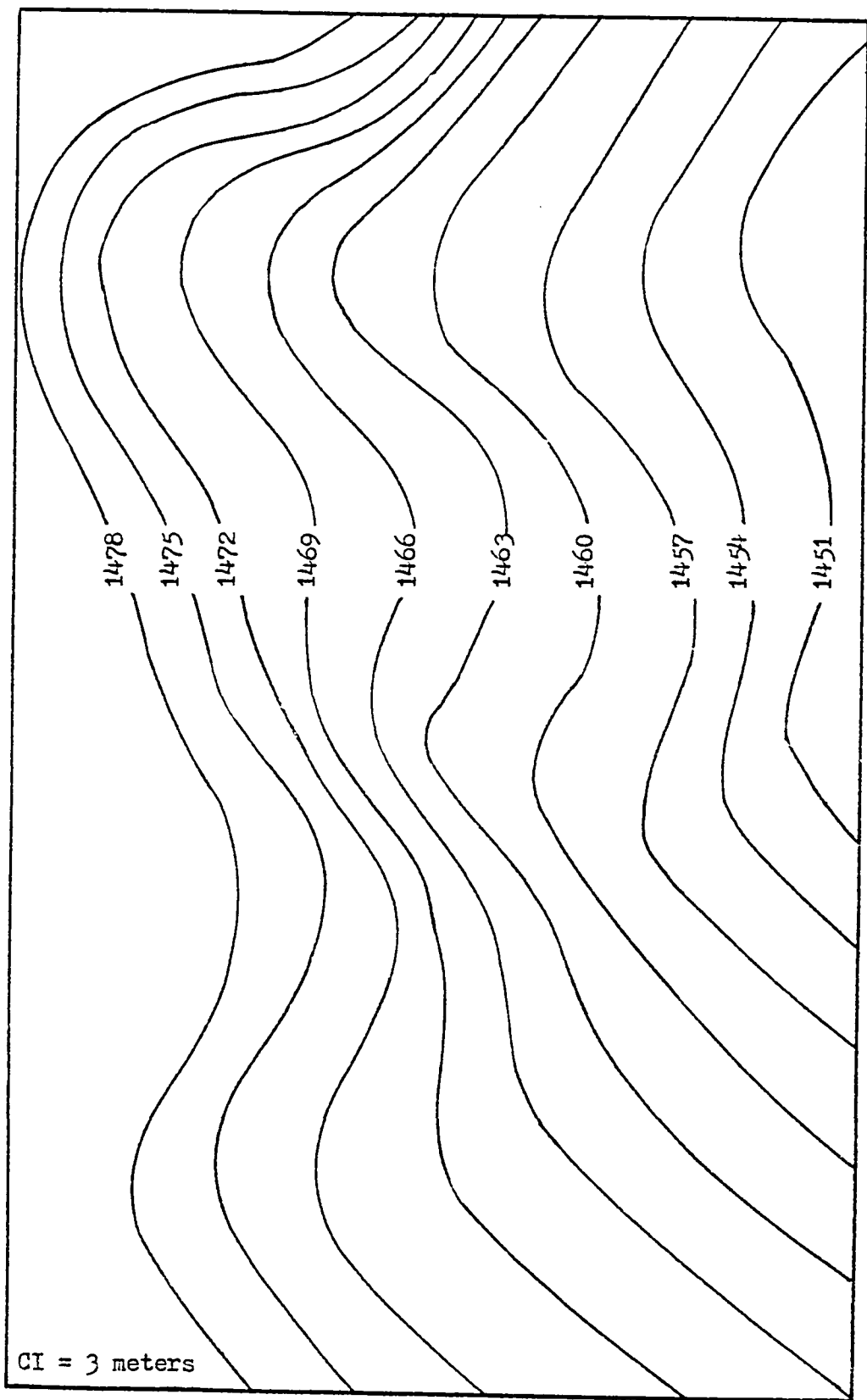


Figure E.4 - Top of the Reservoir Depth (meters below sea level)

0	1481	1481	1481	1479	1475	1471	1466	1463	1461	0	0	0
1481	1481	1479	1478	1476	1473	1468	1466	1464	1461	1457	0	0
1478	1477	1476	1474	1471	1469	1468	1466	1463	1460	1456	0	0
1478	1477	1475	1475	1472	1470	1468	1465	1462	1459	1456	0	0
1478	1477	1476	1476	1474	1471	1468	1464	1461	1459	1456	0	0
1479	1479	1477	1477	1475	1474	1471	1466	1463	1460	1457	1453	0
1480	1479	1478	1478	1476	1474	1473	1470	1466	1463	1459	1458	1452
0	1482	1480	1477	1476	1475	1472	1470	1469	1463	1461	1458	1452
0	1480	1480	1478	1476	1474	1472	1470	1469	1465	1462	1458	1452
0	1481	1481	1479	1475	1473	1472	1469	1467	1464	1461	1457	0
0	0	1481	1480	1476	1472	1469	1468	1465	1463	1460	1456	0
0	0	1482	1482	1479	1474	1470	1467	1464	1463	1459	1454	0
0	0	1483	1483	1481	1478	1472	1469	1465	1463	1459	1456	0
0	0	1483	1483	1482	1481	1476	1472	1468	1464	1461	1458	0
0	0	1482	1482	1481	1480	1476	1473	1470	1468	1463	1461	1458
0	0	1482	1481	1481	1479	1476	1473	1471	1468	1466	1463	1459
0	1482	1482	1481	1480	1478	1476	1474	1471	1470	1467	1464	1461
0	0	1481	1481	1479	1477	1476	1474	1473	1470	1468	1464	0
0	0	1479	1479	1478	1476	1475	1474	1473	1472	1469	1466	0
0	0	0	1479	1479	1477	1475	1474	1473	1471	1469	0	0
0	0	0	0	0	1476	1474	1472	1471	0	0	0	0

Figure E.5 - Digitized Middle of the Reservoir Depth(meters)

0	15700	15700	15700	15687	15661	15635	15603	15584	15571	0	0	0
15700	15700	15687	15680	15667	15648	15616	15603	15590	15571	15545	0	0
15680	15674	15667	15654	15635	15622	15616	15603	15584	15564	15539	0	0
15680	15674	15661	15661	15642	15629	15616	15597	15577	15558	15539	0	0
15680	15674	15667	15654	15635	15616	15590	15571	15558	15539	0	0	0
15687	15687	15674	15674	15661	15654	15635	15603	15584	15564	15545	15519	0
15693	15687	15680	15680	15667	15654	15648	15629	15603	15584	15558	15551	15513
0	15706	15693	15674	15667	15661	15642	15629	15622	15597	15571	15551	15513
0	15693	15693	15680	15667	15654	15642	15629	15622	15597	15577	15551	15513
0	15700	15700	15687	15661	15648	15642	15622	15609	15590	15571	15545	0
0	0	15700	15693	15667	15642	15622	15616	15597	15584	15564	15513	0
0	0	15706	15706	15687	15654	15629	15609	15590	15584	15558	15526	0
0	0	15712	15712	15700	15680	15642	15622	15597	15584	15558	15539	0
0	0	15712	15712	15706	15700	15667	15642	15616	15590	15571	15551	0
0	0	15706	15706	15700	15693	15667	15648	15629	15616	15584	15571	15551
0	0	15706	15700	15700	15687	15667	15648	15635	15616	15603	15584	15558
0	15706	15706	15700	15693	15680	15667	15654	15635	15629	15609	15590	15571
0	0	15700	15700	15687	15674	15667	15654	15648	15629	15616	15590	0
0	0	15687	15687	15680	15667	15661	15654	15648	15642	15622	15603	0
0	0	0	15687	15687	15674	15661	15654	15648	15635	15622	0	0
0	0	0	0	0	15667	15654	15642	15635	0	0	0	0

Figure E.6 - Digitized Reservoir Initial Pressure(kilo-Pascal)

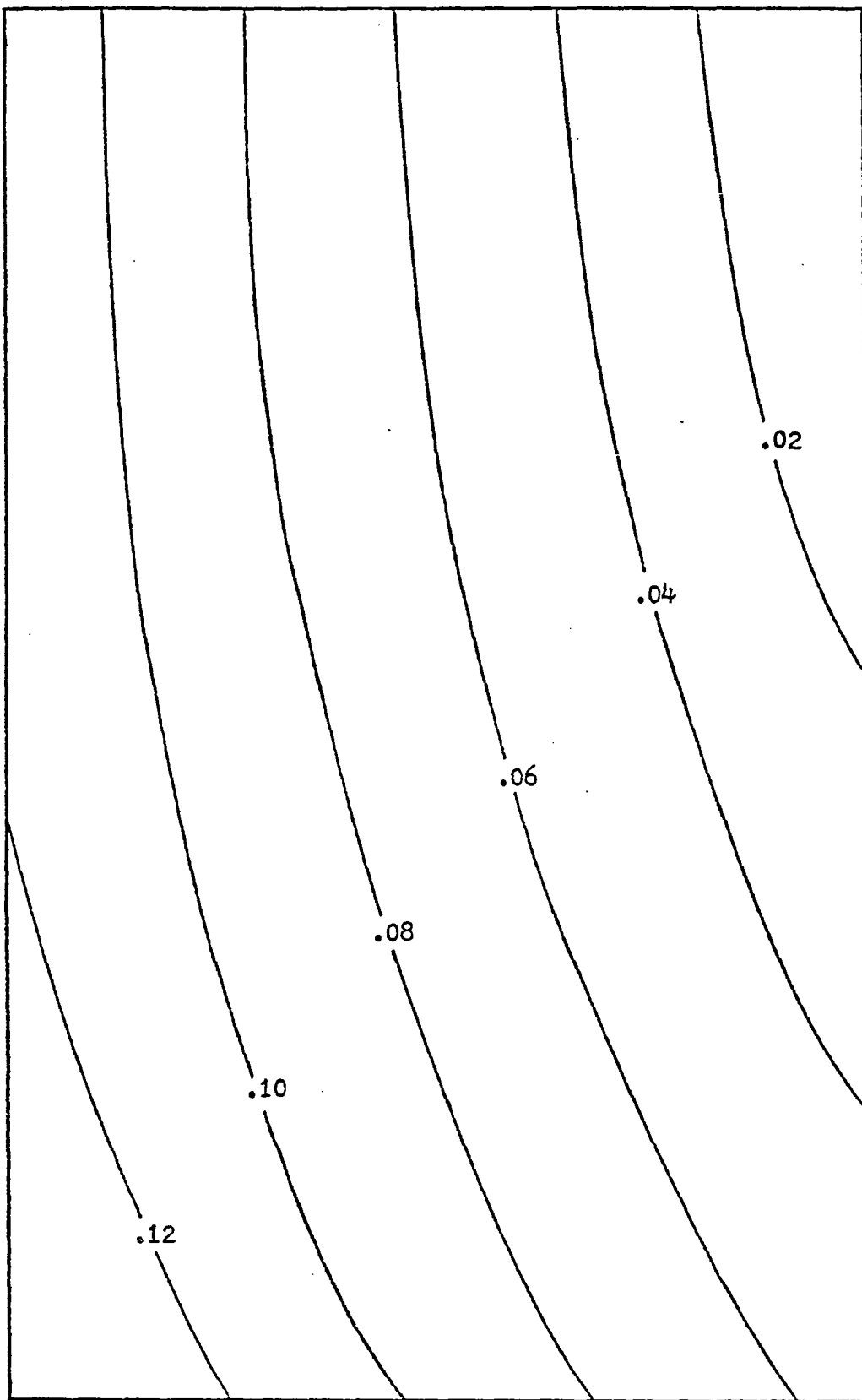


Figure E.7 - Reservoir Heterogeneous Permeability(micro-meter^2)

0	.10	.09	.08	.07	.06	.06	.05	.04	.03	0	0	0
.10	.10	.09	.08	.07	.06	.06	.05	.04	.03	.02	0	0
.10	.10	.09	.08	.07	.06	.06	.05	.04	.03	.02	0	0
.10	.10	.09	.08	.07	.06	.06	.05	.04	.03	.02	0	0
.10	.10	.09	.08	.08	.07	.06	.05	.04	.03	.02	0	0
.10	.10	.09	.08	.08	.07	.06	.05	.04	.04	.03	.02	0
.10	.10	.10	.09	.08	.07	.06	.05	.04	.04	.03	.02	.02
0	.10	.10	.09	.08	.07	.06	.06	.05	.04	.03	.02	.02
0	.10	.10	.09	.08	.07	.06	.06	.05	.04	.04	.03	.02
0	.10	.10	.09	.08	.07	.06	.06	.05	.04	.04	.03	0
0	0	.10	.09	.08	.08	.07	.06	.06	.05	.04	.03	0
0	0	.10	.10	.09	.08	.07	.06	.06	.05	.04	.04	0
0	0	.10	.10	.09	.08	.07	.06	.06	.05	.04	.04	0
0	0	.10	.10	.09	.08	.08	.07	.06	.05	.04	.04	0
0	0	.11	.10	.09	.08	.08	.07	.06	.06	.05	.04	.04
0	0	.11	.10	.10	.09	.08	.07	.06	.06	.05	.04	.04
0	.12	.11	.10	.10	.09	.08	.07	.06	.06	.05	.04	.04
0	0	.11	.11	.10	.09	.08	.08	.07	.06	.06	.05	0
0	0	.11	.11	.10	.10	.09	.08	.07	.06	.06	.05	0
0	0	0	.11	.10	.10	.09	.08	.08	.07	.06	0	0
0	0	0	0	0	.10	.10	.09	.08	0	0	0	0

Figure E.8 - Digitized Reservoir Heterogeneous Permeability(micro-meter²)

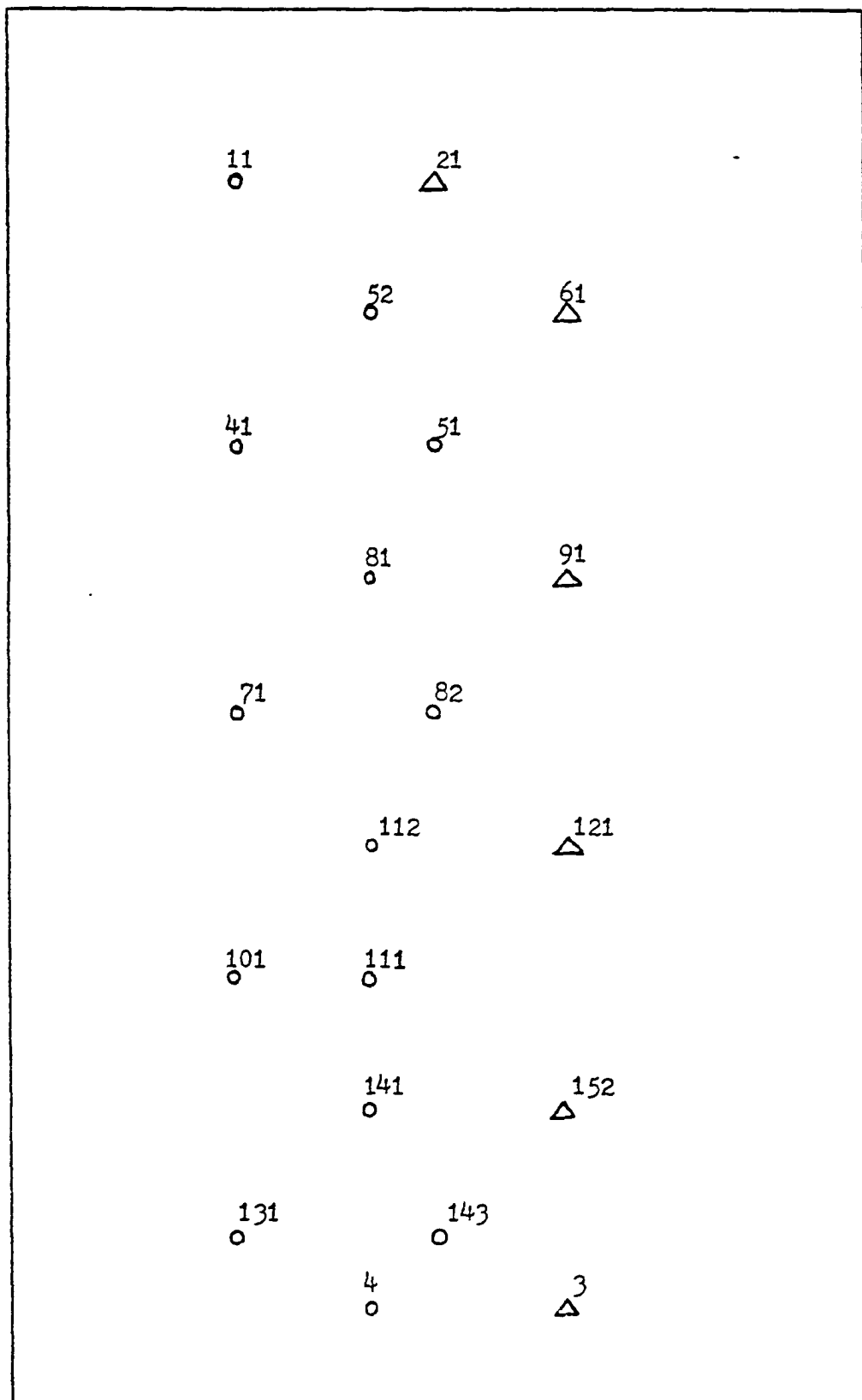


Figure E.9 - Configuration of Wells

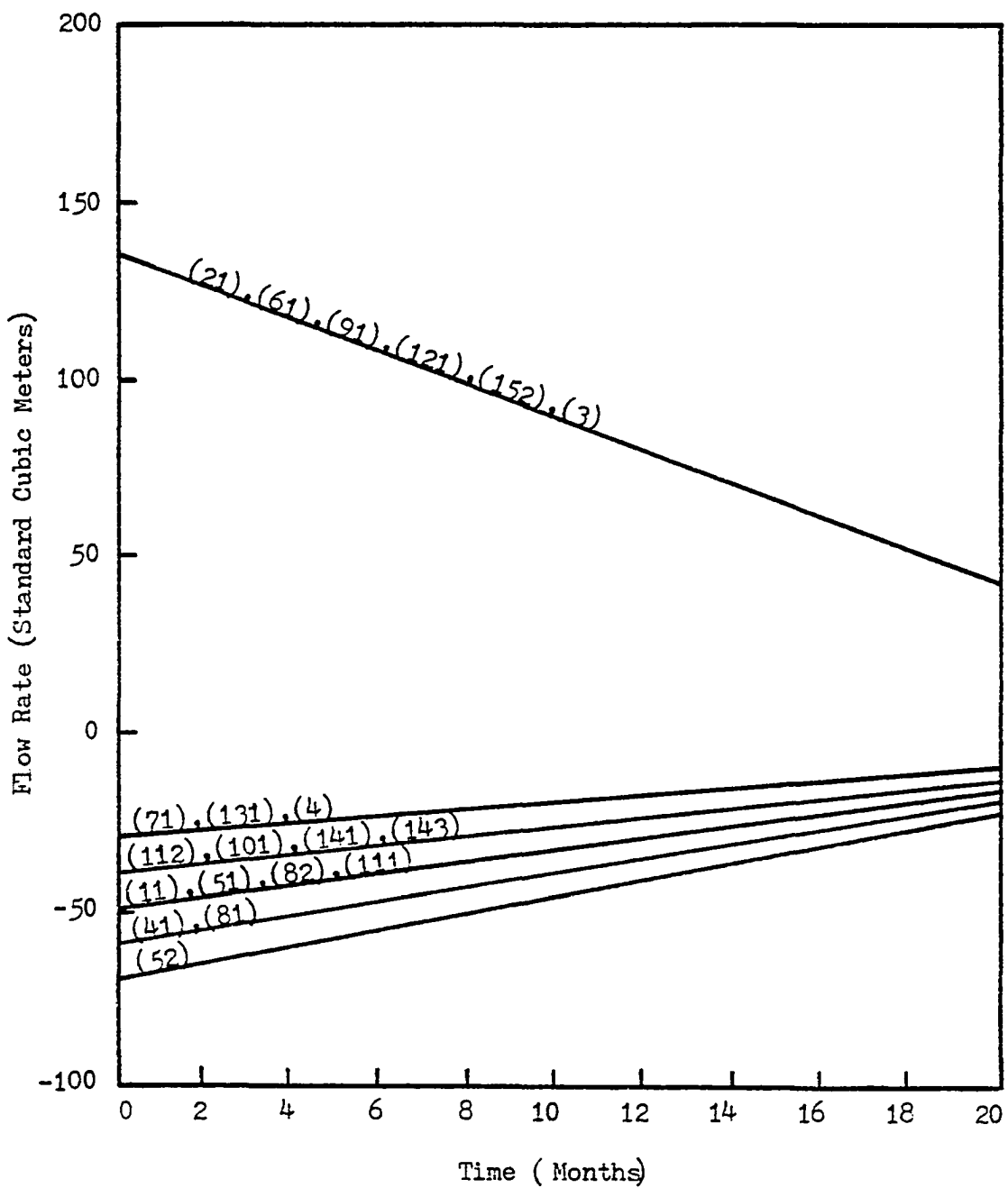


Figure E.10 - Production-Injection Flow Rates
(Well numbers are between parenthesis)

APPENDIX E
COMPUTER LISTING OF THE NUMERICAL PROCEDURES

FORTRAN IV G LEVEL 21

MATH

DATE - 70006

C-----
 C SUBJECT: TWO-DIMENSIONAL THREE-PHASE PETROLEUM RESERVOIR SIMULATORMAP 10
 C A COMPUTER STUDY TO SUPPLEMENT A PH.D. DISSERTATION. MAR 20
 C LOCATION: UNIVERSITY OF OKLAHOMA, NORMAN, OKLAHOMA, U.S.A. MAR 30
 C DEPARTMENT: PETROLEUM & GEOLOGICAL ENGINEERING MAR 40
 C COMPUTER: IBM 360 MAR 50
 C AUTHOR: MUHAMMAD ALI AL-MARHOUN MAR 60
 C ADVISOR: H. B. CRICHLow MAR 70
 C DATE: SPRING 1978 MAR 80
 C-----MAP 90
 C-----MAP 100
 0001 BLOCK DATA MAP 110
 C-----MAP 120
 C PURPOSE OF SUBROUTINE MAP 130
 C INITIALIZATION MAP 140
 C-----MAP 150
 0002 COMMON/C01/ E(345),A(345),B(345),C(345),F(345),P(345),D(345) MAR 160
 0003 COMMON/C07/ . IO(345),OO(345),QW(345),OG(345),NW,INDW(100),PWF,RW MAR 170
 0004 COMMON/C09/ PRMX(345),PRMY(345) MAR 180
 0005 COMMON/C10/ HKX(345),HKY(345) MAR 190
 0006 COMMON/C11/ QOC(345),QWC(345),QGC(345),RT,ROC,RWC,RGC,NWN(103) MAR 200
 0007 COMMON/C12/ POR(345),VOL(345),CO,CW,CR,TVOL MAR 210
 0008 COMMON/C13/ RPRMD(345),RPRMW(345),RPRMG(345) MAR 220
 0009 COMMON/C14/ SO(345),SW(345),SG(345),SWC,SOR,SGC,PPP MAR 230
 0010 COMMON/C15/ VISO(345),VISW(345),VISG(345) MAR 240
 0011 COMMON/C16/ HLAMTY(345),HLAMTX(345),HLAMOX(345),HLAMOY(345), MAR 250
 H HLAMWX(345),HLAMWY(345),HLAMGX(345),HLAMGY(345) MAR 260
 0012 COMMON/C19/ DENO(345),DENW(345),DENG(345),DENOSC,DENWSC,DENGSC MAR 270
 D ,DPH(345) MAR 280
 0013 COMMON/C20/ PCW(345),PCG(345),FCWS(10),SWS(10),PCGS(10),SOS(10) MAR 290
 0014 COMMON/C21/ PSAVE(345),SOSAVE(345),SWSAVE(345),SGSAVE(345) MAR 300
 O ,DT(345),BD(345),BW(345) MAR 310
 0015 COMMON/C22/ THETA,DT,AMAXDT,AMINDT MAR 320
 0016 COMMON/C24/ QDCS(345),QWCS(345),QGCS(345) MAR 330
 0017 COMMON/C27/ ISA(345),IAS(345),ML,NE,NB1,AA(16,175),CC(16,175) MAR 340
 0018 COMMON/C28/ IPS(390),M1,M2,ISS,AR(410),CB(410),EE(410),FF(410) MAR 350
 0019 COMMON/C29/ G(17,195),HH(16,195),Y(410) MAR 360
 0020 DATA AP,CB,EE,FF,Y,G,HH,AA,CC/14085*0.0/ MAR 370
 0021 DATA E,A,B,C,F,D,OO,QW,OG,HKX,HKY,VOL,QDCS,QWCS,QGCS, MAR 380
 1 HLAMTY,HLAMTX,HLAMOX,HLAMOY,HLAMWX,HLAMWY,HLANGX,HLANGY MAR 390
 2 ,PSAVE,DENO,DENW,DENG,PCW,PCG,SOSAVE,SWSAVE,SGSAVE, MAR 400
 3 QOC,QWC,QGC,RPRMO,RPRMW,RPRMG,VISO,VISW,VISG,SG,IO MAR 410
 4 /14490*0.0,345*0/ MAR 420
 0022 DATA DPH,POR,PRMX,PRMY,P,SO,SW/2415*0.0/ MAR 430
 0023 DATA AMAXDT,AMINDT,DT/3.0,1.0E 10,1.0/ MAR 440
 0024 END MAR 450

```

C-----MAIN-----DATE = 78116-----20/4/7/21-----PAGE 0001
C-----SIMULATOR MAINLINE-----MAR 460
C-----COMMON/C01/ E(345),A(345),U(345),C(345),F(345),P(345),D(345)-----MAR 470
C-----COMMON/C02/ NX,NY,NXY,N,IND(345),NXH1,NYH1-----MAR 480
C-----COMMON/C03/ EPS,K,KMAX,RMAX,M,W,ICNVRG,BETA(90),GAMA(345),NNR(30)-----MAR 490
C-----COMMON/C04/ TIM,TFINAL,DTRMIN,DTRMAX,DPLIM,DSLIM,OUTMOD,TPRINT-----MAR 500
C-----COMMON/C05/ EPSM,RMBMAX,NTRIAL,NTRMAX,AMIP0,AMIPW,AMIPG,TMCPU,TMMAR-----MAR 510
C-----COMMON/C06/ DX(20),DY(25),DXM(20),DYM(25)-----MAR 520
C-----COMMON/C07/ I0(345),Q0(345),QW(345),QG(345),NW,INDM(100),PMF,RW-----MAR 530
C-----COMMON/C08/ PRMX(345),PRMY(345)-----MAR 540
C-----COMMON/C09/ H(345)-----MAR 550
C-----COMMON/C10/ HKX(345),HKY(345)-----MAR 560
C-----COMMON/C11/ QDC(345),OWC(345),OGC(345),RT,ROCC,RWC,RGC,RWN(100)-----MAR 570
C-----COMMON/C12/ PUR(345),VUL(345),CO,CW,CR,TVOL-----MAR 580
C-----COMMON/C13/ RPRMO(345),RPRMW(345),RPRNG(345)-----MAR 590
C-----COMMON/C14/ SOL(345),SW,SG(345),SGC,SOR,SGC,PBP-----MAR 600
C-----COMMON/C15/ VISU(345),VISW(345),VISG(345)-----MAR 610
C-----COMMON/C16/ HLAMTY(345),HLAMTX(345),HLANDX(345),HLAMOY(345),-----MAR 620
H-----HLAMWX(345),HLAMWY(345),HLANGX(345),HLANGY(345)-----MAR 630
C-----COMMON/C17/ DXSUM,DYSUM,DXD(X(20),DYD(Y(25)-----MAR 640
C-----COMMON/C18/ DENO(345),DENW(345),DENG(345),DENOSC,DENWSC,DENGSC-----MAR 650
C-----COMMON/C19/ *DPI(345)-----MAR 660
C-----COMMON/C20/ PCW(345),PCG(345),PCWS(10),SUS(10),PCGS(10),SOS(10)-----MAR 670
C-----COMMON/C21/ PSAVE(345),SOSAVE(345),SWSAVE(345)-----MAR 680
C-----COMMON/C22/ *DT(345),DO(345),BW(345)-----MAR 690
C-----COMMON/C23/ THETA,DT,AMAXDT,AMINOT-----MAR 700
C-----COMMON/C24/ NUD,NUDX(175),NLD,NLDX(175),NU,NUOP1,NLDP1,MM-----MAR 710
C-----COMMON/C25/ DUCS(345),QWCS(345),QGCCS(345)-----MAR 720
C-----COMMON/C27/ RSD(345),RSW(345)-----MAR 730
C-----COMMON/C28/ ISA(345),IAS(345),ML,NE,NBI,AA(16,175),CC(16,175)-----MAR 740
C-----COMMON/C29/ IRS(390),MI,M2,ISS,AR(410),CD(410),EE(410),FF(410)-----MAR 750
C-----COMMON/C30/ G(17,195),HH(16,195),Y(410)-----MAR 760
C-----COMMON/C31/ ALPHA(10)-----MAR 770
C-----CALL, INPUT-----MAR 780
C-----ONCE-----MAR 790
C-----ATTENTION : CALL RS FOR RADP ONLY-----MAR 800
C-----CALL RS-----MAR 810
C-----RS-----MAR 820
C-----RS-----MAR 830
C-----RS-----MAR 840
C-----RS-----MAR 850
C-----RS-----MAR 860
C-----RS-----MAR 870
C-----RS-----MAR 880
C-----RS-----MAR 890
C-----RS-----MAR 900
C-----RS-----MAR 910
C-----RS-----MAR 920
C-----RS-----MAR 930
C-----RS-----MAR 940
C-----RS-----MAR 950
C-----RS-----MAR 960
C-----RS-----MAR 970

```

```

C   CALL ONE OF THE FOLLOWING SIX DIFFERENT METHODS      MAR  980
C-----          MAR  990
0043  CALL      PSOR                               MAR 1000
0044  CALL      LSOR                               MAR 1010
0045  CALL      ADIP                               MAR 1020
0046  CALL      SIP                                MAR 1030
0047  CALL      STBAND(IND(1),IND(N))              MAR 1040
0048  CALL      RADP                               MAR 1060
0049  CALL      CPUTIM(TINC)                      MAR 1070
0050      TIMCPU = TIMCPU + TINC                  MAR 1080
0051  CALL      SATRN                             MAR 1090
0052  CALL      MASERR                            MAR 1100
0053  PRINT 200, NTRIAL,DT,TIN,RT,RGC,RWC,RGC,K,RMAX,ICNVRG MAR 1110
0054  IF(RMDMAX .LE. EPSM ) GO TO 30             MAR 1120
0055  IF( NTRIAL .LT. NTRMAX) GO TO 20           MAR 1130
0056  30 IF((TPRINT-TIM) .GT. 0.0001*DTHIN ) GO TO 40 MAR 1140
0057  CALL      OUTPUT                            MAR 1150
0058  40 IF((TFINAL-TIM) .GT. 0.0001*DTHIN ) GO TO 10 MAR 1160
0059  STOP                               MAR 1170
0060  100 FORMAT(10X,'NLEVEL =',I5      )          MAR 1180
0061  200 FORMAT( 28X,I10,2F10.2,4F10.4,I10, F10.4, I10) MAR 1190
0062  300 FORMAT(1H1) , :                         MAR 1200
0063  END                               MAR 1210

```

FORTRAN IV G LEVEL 21

MAIN

DATE = 78086

20/46/33

PAGE 0001

```

C----- MAR 1220
0001      SUBROUTINE PSOR          MAR 1230
C----- MAR 1240
C PURPOSE OF SUBROUTINE          MAR 1250
C TO PERFORM POINT SUCCESSIVE OVERRELAXATION METHOD MAR 1260
C TO SOLVE THE PRESSURE EQUATIONS MAR 1270
C----- MAR 1280
0002      COMMON/C01/ E(345),A(345),B(345),C(345),F(345),P(345),D(345) MAR 1290
0003      COMMON/C02/ NX,NY,NXY,N,IND(345),NXM1,NYM1          MAR 1300
0034      COMMON/C03/ EPS,K,KMAX,RMAX,M,W,ICNVRG,BETA(90),GAMA(345),NNR(30) MAR 1310
0005      K      = 0          MAR 1320
0006      ICNVRG = 0          MAR 1330
0007      10     K      = K + 1          MAR 1340
0008      RMAX   = 0.0          MAR 1350
C----- MAR 1360
C COMPUTATION OF OVER-RELAXED PRESSURES          MAR 1370
C----- MAR 1380
0039      DO 20     J = 1, N          MAR 1390
0010      I      = IND(J)          MAR 1400
0011      PS    = P(I)          MAR 1410
0012      P(I)  = (D(I)- E(I)*P(I-NX )- A(I)*P(I-1 )          MAR 1420
*           - C(I)*P(I+1 )- F(I)*P(I+NX ))/B(I)          MAR 1430
0013      P(I)  = PS + W * (P(I) - PS)          MAR 1440
0014      R    = ABS((P(I)-PS)/P(I))          MAR 1450
0015      IF( R .GT. RMAX) RMAX = R          MAR 1460
0016      20 CONTINUE          MAR 1470
C----- MAR 1480
C CHECK FOR CONVERGENCE          MAR 1490
C----- MAR 1500
0017      IF( RMAX .LE. EPS) GO TO 30          MAR 1510
0018      IF(K .GE. KMAX ) GO TO 40          MAR 1520
0019      GO TO 10          MAR 1530
0020      30 ICNVRG = 1          MAR 1540
0021      40 RETURN          MAR 1550
0022      END          MAR 1560

```

```

0001      SUBROUTINE  LSOR                               MAR 1570
C-----MAR 1580
C      PURPOSE OF SUBROUTINE                           MAR 1590
C      TO PERFORM LINE SUCCESSIVE OVERRELAXATION METHOD MAR 1600
C      TO SOLVE THE PRESSURE EQUATIONS                MAR 1610
C-----MAR 1620
0002      COMMON/C01/  E(345),A(345),B(345),C(345),F(345),P(345),D(345) MAR 1630
0003      COMMON/C02/  NX,NY,NXY,N,IND(345),NXM1,NYM1          MAR 1640
0004      COMMON/C03/  EPS,K,KMAX,RMAX,M,W,ICNVRG,BETA(90),GAMA(345),NNR(30) MAR 1650
0005      DIMENSION   PSAVE(345),DX(345)                  MAR 1660
0006      DATA        DX/345*0.0/                      MAR 1670
0007      ICNVRG    = 0                                  MAR 1680
0008      K         = 0                                  MAR 1690
0009      10      K         = K + 1                      MAR 1700
0010      RMAX     = 0.3                                MAR 1710
C-----MAR 1720
C      COMPUTATION OF OVER-RELAXED PRESSURES           MAR 1730
C-----MAR 1740
0011      JE       = 0                                  MAR 1750
0012      DO 30    KK = 2, NYM1                      MAR 1760
0013      JS       = JE + 1                          MAR 1770
0014      JE       = JE + NNR(KK)                   MAR 1780
0015      DO 20    J = JS , JE                      MAR 1790
0016      I         = IND(J)                      MAR 1800
0017      PSAVE(I) = P(I)                      MAR 1810
0018      20 DX(I)      = D(I)-E(I)*P(I-NX )-F(I)*P(I+NX ) MAR 1820
0019      CALL      THOMSH(JS,JE,DX)                 MAR 1830
0020      DO 30    J = JS , JE                      MAR 1840
0021      I         = IND(J)                      MAR 1850
0022      P(I)      = PSAVER(I)+W*(P(I)-PSAVE(I)) MAR 1860
0023      R         = ABS((P(I)-PSAVE(I))/P(I))      MAR 1870
0024      IF( R .GT. RMAX)  RMAX = R              MAR 1880
0025      30 CONTINUE                         MAR 1890
C-----MAR 1900
C      CHECK FOR CONVERGENCE                     MAR 1910
C-----MAR 1920
0026      IF( RMAX .LE. EPS) GO TO 40            MAR 1930
0027      IF(K .GE. KMAX ) GO TO 50            MAR 1940
0028      GO TO 10                           MAR 1950
0029      40      ICNVRG    = 1                  MAR 1960
0030      50      RETURN                         MAR 1970
0031      END                                MAR 1980

```

FORTRAN IV G LEVEL 21

THOMSH

DATE = 78086

23/46/33

PAGE 0301

0001	SUBROUTINE THOMSH (JS , JE,R)	MAR 1990
C-----		MAR 2000
C PURPOSE OF SUBROUTINE		MAR 2010
C TO PERFORM THE THOMAS ALGORITHM ON A CLOSED BAND MATRIX		MAR 2020
C-----		MAR 2030
0002	COMMON/C01/ E(345),A(345),B(345),C(345),F(345),P(345),D(345)	MAR 2040
0003	COMMON/C02/ NX,NY,NXY,N,IND(345),NXM1,NYH1	MAR 2050
0004	DIMENSION R(NXY),BETA(345)	MAR 2060
0005	DATA BETA/345*1.0/	MAR 2070
0006	JEP1 = JE+JS	MAR 2080
0007	I = IND(JS)	MAR 2090
0008	BETA(I) = B(I)	MAR 2100
0009	R(I) = R(I)/B(I)	MAR 2110
0010	JSPI = JS + 1	MAR 2120
0011	DO 20 J = JSPI,JE	MAR 2130
0012	I = IND(J)	MAR 2140
0013	IM1 = I-1	MAR 2150
0014	BETA(I) = B(I)-A(I)*C(IM1)/BETA(IM1)	MAR 2160
0015	20 R(I) = (R(I)-A(I)*R(IM1))/BETA(I)	MAR 2170
0016	I = IND(JE)	MAR 2180
0017	P(I) = R(I)	MAR 2190
0018	DO 30 J = JSPI,JE	MAR 2200
0019	I = IND(JEP1 - J)	MAR 2210
0020	30 P(I) = R(I) - C(I)*P(I+1)/BETA(I)	MAR 2220
0021	RETURN	MAR 2230
0022	END	MAR 2240

```

0001      SUBROUTINE ADIP
C-----  

C   PURPOSE OF SUBROUTINE                               MAR 2250  

C   TO PERFORM THE ALTERNATING DIRECTION IMPLICIT PROCEDURE MAR 2260  

C   TO SOLVE THE PRESSURE EQUATIONS                  MAR 2270  

C-----  

0002      COMMON/C01/  E(345),A(345),B(345),C(345),F(345),P(345),D(345)  MAR 2310  

0003      COMMON/C02/  NX,NY,NXY,N,IND(345),NXM1,NYM1                 MAR 2320  

0004      COMMON/C03/  EPS,K,KMAX,RMAX,M,W,ICNVRG,BETA(90),GAMA(345),NNR(30) MAR 2330  

0005      COMMON/C06/  DX(20),DY(25),DXM(20),DYM(25)                   MAR 2340  

0006      COMMON/C15/  HLAMTY(345),HLAMTX(345),HLAMOX(345),HLAMCY(345),  
H      HLAMWX(345),HLAMWY(345),HLAMGX(345),HLANGY(345)          MAR 2350  

0007      DIMENSION  BB(345),DD(345),PSAVE(345)                      MAR 2360  

0008      DATA       DD/345*0.0/                                     MAR 2370  

0009      DO 10      I = 1,NXY                                    MAR 2380  

0010      BB(I)      = 0.0                                      MAR 2390  

0011      10      DD(I)      = 0.0                                MAR 2400  

0012      K          = 0                                      MAR 2410  

0013      KB         = 0                                      MAR 2420  

0014      ICNVRG    = 0                                      MAR 2430  

0015      30      K          = K + 1                            MAR 2440  

0016      KB         = KB + 1                            MAR 2450  

0017      RMAX       = 0.0                                  MAR 2460  

0018      DO 35      J = 1, N                             MAR 2470  

0019      I          = IND(J)                            MAR 2480  

0020      35      PSAVE(I)    = P(I)                            MAR 2490  

C-----  

C   SELECTION OF ACCELERATION PARAMETER             MAR 2500  

C-----  

0021      IF(KB .EQ. (M+1)) KB = 1                         MAR 2510  

0022      BET        = BETA(KB)                           MAR 2520  

C-----  

C   X-DIRECTION SWEEP                                MAR 2530  

C-----  

0023      DO 40      J = 1,N                            MAR 2540  

0024      I          = IND(J)                            MAR 2550  

0025      BB(I)      = B(I) + E(I) + F(I) - GAMA(I)*BET    MAR 2560  

0026      40      DD(I)      = D(I)-E(I)*P(I-NX)+(E(I)+F(I)-GAMA(I)*BET)*P(I) MAR 2570  

C          -F(I)*P(I+NX)                            MAR 2580  

0027      CALL       TRIHOR(A,BB,C,DD,P)                MAR 2590  

C-----  

C   Y-DIRECTION SWEEP                                MAR 2600  

C-----  

0028      DO 50      J = 1,N                            MAR 2610  

0029      I          = IND(J)                            MAR 2620  

0030      BB(I)      = B(I)+A(I) + C(I) - GAMA(I)*BET    MAR 2630  

0031      50      DD(I)      = D(I)-A(I)*P(I-1)+(A(I)+C(I)-GAMA(I)*BET)*P(I) MAR 2640  

C          -C(I)*P(I+1)                            MAR 2650  

0032      CALL       TRIVER(E,BB,F,DD,P)                MAR 2660  

C-----  

C   CALCULATION OF RMAX                                MAR 2670  

C-----  


```

FORTRAN IV G LEVEL 21

ADIP

DATE = 78086

20/46/33

PAGE 0002

0033	DO 60	J=1,N	MAR 2770
0034	I	= IND(J)	MAR 2780
0035	DIFF	= P(I) - PSAVE(I)	MAR 2790
0036	R	= ABS(DIFF /P(I))	MAR 2800
0037	IF(R .GT. RMAX) RMAX = R		MAR 2810
0038	60 CONTINUE		MAR 2820
C----- MAR 2830			
C CHECK FOR CONVERGENCE			MAR 2840
C----- MAR 2850			
0039	IF(RMAX .LE. EPS) GO TO 70		MAR 2860
0040	IF(K .GE. KMAX) GO TO 80		MAR 2870
0041	GO TO 30		MAR 2880
0042	70 ICNVRG = 1		MAR 2890
0043	80 RRETURN		MAR 2900
0044	END		MAR 2910

FORTRAN IV G LEVEL 21

TRIHOR

DATE = 78086

20/46/33

PAGE 0001

```

0001      SUBROUTINE  TRIHOR(A,B,C,R,P)          MAR 2920
C-----MAR 2930
C      PURPOSE OF SUBROUTINE          MAR 2940
C      TO PERFORM THE THOMAS ALGORITHM ON A CLOSED BAND MATRIX  MAR 2950
C-----MAR 2960
0002      COMMON/C02/  NX,NY,NXY,N,IND(345),NXM1,NYM1          MAR 2970
0003      DIMENSION  A(NXY),B(NXY),C(NXY),R(NXY),P(NXY),BETA(345)  MAR 2980
0004      DATA       BETA/345*1.0/          MAR 2990
0005      NPI       = N + 1          MAR 3000
0006      I          = IND( 1)          MAR 3010
0007      BETA(I)   = B(I)          MAR 3020
0008      R(I)      = R(I)/B(I)          MAR 3030
0009      DO       20 J = 2, N          MAR 3040
0010      I          = IND(J)          MAR 3050
0011      IM1       = I-1          MAR 3060
0012      BETA(I)   = B(I)-A(I)*C(IM1)/BETA(IM1)          MAR 3070
0013      20      R(I)   = (R(I)-A(I)*R(IM1))/BETA(I)          MAR 3080
0014      I          = IND(N)          MAR 3090
0015      P(I)      = R(I)          MAR 3100
0016      DO       30 J = 2, N          MAR 3110
0017      I          = IND(NPI - J)          MAR 3120
0018      30      P(I)   = R(I) - C(I)*P(I+1)/BETA(I)          MAR 3130
0019      RETURN          MAR 3140
0020      END          MAR 3150

```

FORTRAN IV G LEVEL 21

TRIVER

DATE = 78086

20/46/33

PAGE 0001

```

0001      SUBROUTINE TRIVER(E,B,F,R,P)          MAR 3160
C-----MAR 3170
C   PURPOSE OF SUBROUTINE                      MAR 3180
C   TO PERFORM THE THOMAS ALGORITHM ON A WIDE BAND MATRIX MAR 3190
C-----MAR 3200
0002      COMMON/C02/ NX,NY,NXY,N,IND(345),NXM1,NYM1          MAR 3210
0003      DIMENSION E(NXY),B(NXY),F(NXY),R(NXY),P(NXY),BETA(345)  MAR 3220
0004      DATA BETA/345*1.0/          MAR 3230
0005      NP1      = N + 1          MAR 3240
0006      DO 20      J = 1,N          MAR 3250
0007      I        = IND(J)          MAR 3260
0008      IMNX     = I-NX          MAR 3270
0009      BETA(I)  = B(I)-E(I)*F(IMNX )/BETA(IMNX)          MAR 3280
0010      20      R(I)    =(R(I)-E(I)*R(IMNX ))/ BETA(I)          MAR 3290
0011      DO 40      J = 1,N          MAR 3300
0012      I        = IND(NP1 - J)          MAR 3310
0013      40      P(I)    =R(I)-F(I)*P(I+NX )/BETA(I)          MAR 3320
0014      RETURN          MAR 3330
0015      FND          MAR 3340

```

FORTRAN IV G LEVEL 21

SIP

DATE = 78116

20/47/21

PAGE 0001

```

0001      SUBROUTINE SIP                               MAR 3350
C-----                                           MAR 3360
C      PURPOSE OF SUBROUTINE                         MAR 3370
C      TO PERFORM STRONGLY IMPLICIT PROCEDURE       MAR 3380
C      TO SOLVE THE PRESSURE EQUATIONS              MAR 3390
C-----                                           MAR 3400
0002      COMMON/C01/ E(345),A(345),B(345),C(345),F(345),P(345),D(345)  MAR 3410
0003      COMMON/C02/ NX,NY,NXY,N,IND(345),NXM1,NYM1          MAR 3420
0004      COMMON/C03/ EPS,K,KMAX,RMAX,M,W,ICNVRG,BETA(90),GAMA(345),NNR(30) MAR 3430
0005      COMMON/C21/ PSAVE(345),SOSAVE(345),SWSAVE(345),SGSAVE(345)    MAR 3450
0006      COMMON/C30/ .DT(345),BD(345),BW(345)                 MAR 3460
0007      COMMON/C30/ ALPHA(10)                                MAR 3465
0008      DIMENSION EE(345),AA(345),CC(345),FF(345),Y(345),DPSAVE(345) MAR 3470
0009      DATA EE,AA,CC,FF,Y/1725*0.0/                      MAR 3490
0009      DO 5      J = 1,N                                MAR 3760
0010      I = IND(J)                                     MAR 3770
0011      5      D(I) = D(I)-E(I)*PSAVE(I-NX)-A(I)*PSAVE(I-1)-B(I)*PSAVE(I) MAR 3780
0011      1      -C(I)*PSAVE(I+1)-F(I)*PSAVE(I+NX)           MAR 3790
0012      ICNVRG = 0                                    MAR 3800
0013      K = 0                                         MAR 3810
0014      KZETA = 0                                    MAR 3820
0015      30     K = K + 2                                MAR 3830
0016      RMAX = 0.0                                    MAR 3840
C-----                                           MAR 3850
C      CALCULATION OF CURRENT ITERATION PARAMETER ALFA   MAR 3860
C-----                                           MAR 3870
0017      IF( MOD(KZETA ,M) .EQ. 0 } KZETA = 0          MAR 3880
0018      KZETA = KZETA + 1                            MAR 3890
0019      ALFA = ALPHA(KZETA)                          MAR 3900
C-----                                           MAR 3910
C      ODD-NUMBERED ITERATION                         MAR 3920
C-----                                           MAR 3930
0020      DO 40     J = 1, N                                MAR 3940
0021      I = IND(J)                                     MAR 3950
0022      IMNX = I-NX                                   MAR 3960
0023      DPSAVE(I) = P(I)                             MAR 3970
0024      IM1 = I-1                                     MAR 3980
0025      ALFAG = ALFA*CC(IMNX)*E(I)/(CC(IMNX)*ALFA + 1.0) MAR 3990
0026      ALFAH = ALFA*FF(IM1)*A(I)/(FF(IM1)*ALFA + 1.0)  MAR 4000
0027      EE(I) = E(I)-ALFAG                           MAR 4010
0028      AA(I) = A(I)-ALFAH                           MAR 4020
0029      BB = B(I)+ALFAG+ALFAH-EE(I)*FF(IMNX)-AA(I)*CC(IM1) ; MAR 4030
0030      CC(I) = (C(I)-ALFAG)/BB                     MAR 4040
0031      FF(I) = (F(I)-ALFAH)/BB                     MAR 4050
0032      40     Y(I) = (D(I)-EE(I)*Y(IMNX)-AA(I)*Y(IM1))/BB MAR 4060
0033      NP1 = N + 1                                  MAR 4070
0034      DO 50     J = 1,N                                MAR 4080
0035      I = IND(NP1-J)                               MAR 4090
0036      50     P(I) = Y(I)-CC(I)*P(I+1)-FF(I)*P(I+NX)  MAR 4100
C-----                                           MAR 4110
C      EVEN-NUMBERED ITERATION                        MAR 4120
C-----                                           MAR 4130

```

FORTRAN IV G LEVEL 21

SIP

DATE = 78116

20/47/21

PAGE 0002

```

0037      DO 60      J = 1, N                               MAR 4140
0038          I      = IND(NP1-J)                           MAR 4150
0039          IPNX   = I + NX                            MAR 4160
0040          IP1    = I + 1                            MAR 4170
0041          ALFAG  = ALFA*EE(IP1)*C(I)/(EE(IP1)*ALFA + 1.0)  MAR 4180
0042          ALFAH  = ALFA*AA(IPNX)*F(I)/(AA(IPNX)*ALFA + 1.0)  MAR 4190
0043          FF(I)  = F(I)-ALFAH                         MAR 4200
0044          CC(I)  = C(I)-ALFAG                         MAR 4210
0045          BB     = B(I)+ALFAG+ALFAH-CC(I)*AA(IP1)-FF(I)*EE(IPNX)  MAR 4220
0046          AA(I)  = (A(I)-ALFAH)/BB                      MAR 4230
0047          EE(I)  = (E(I)-ALFAG)/BB                      MAR 4240
0048      60      Y(I)  = (D(I)-CC(I)*Y(IP1)-FF(I)*Y(IPNX))/BB  MAR 4250
0049      DO 70      J=1,N                           MAR 4260
0050          I      = IND(J)                           MAR 4270
0051      70      P(I)  = Y(I)-EE(I)*P(I-NX)-AA(I)*P(I-1)  MAR 4280
C-----                                     MAR 4290
C      CALCULATION OF RMAX                  MAR 4300
C-----                                     MAR 4310
0052      DO 80      J=1,N                           MAR 4320
0053          I      = IND(J)                           MAR 4330
0054          DIFF   = P(I) -DPSAVE(I)                     MAR 4340
0055          R      = ABS(DIFF/(P(I)+PSAVE(I)))        MAR 4350
0056          IF( R .GT.  RMAX)  RMAX = R               MAR 4360
0057      80  CONTINUE                                MAR 4370
C-----                                     MAR 4380
C      CHECK FOR CONVERGENCE                 MAR 4390
C-----                                     MAR 4400
0058          IF( RMAX .LE. EPS) GO TO 90             MAR 4410
0059          IF(K .GE. KMAX ) GO TO 100             MAR 4420
0060          GO TO 30                                MAR 4430
0061      90      ICNVRG  = 1                          MAR 4440
0062      100  DO 110      J = 1,N                   MAR 4450
0063          I      = IND(J)                           MAR 4460
0064      110      P(I)  = P(I) + PSAVE(I)           MAR 4470
0065          RETURN                                MAR 4480
0066          END                                    MAR 4490

```

FORTRAN IV G LEVEL 21

STRAND

DATE = 7B086

20/46/33

PAGE 0001

```

0001      SUBROUTINE STBAND(IS,IE)          MAR 4500
C-----MAR 4510
C   PURPOSE OF SUBROUTINE               MAR 4520
C   TO PERFORM THE STBAND PROCEDURE    MAR 4530
C   TO SOLVE THE PRESSURE EQUATIONS.  MAR 4540
C-----MAR 4550
0002      COMMON/C01/ E(345),A(345),B(345),C(345),F(345),P(345),D(345)  MAR 4560
0003      COMMON/C02/ NX,NY,NXY,N,IND(345),NXM1,NYM1                  MAR 4570
0004      DIMENSION GAMA(345),ALFA(15),G(15,345),H(15,345)           MAR 4580
0005      DATA     GAMA/345*3.0/                                MAR 4590
0006      DO 10      J = 1,NXY                         MAR 4600
0007          G(NX,J) = E(J)                           MAR 4610
0008          G(1,J) = A(J)                           MAR 4620
0009          H(1,J) = C(J)                           MAR 4630
0010          H(NX,J) = F(J)                           MAR 4640
0011          P(J) = 0.0                               MAR 4650
0012      DO 10      I = 2,NXM1                      MAR 4660
0013          G(I,J) = J.0                           MAR 4670
0014          10      H(I,J) = 0.0                     MAR 4680
0015      DO 70      J = IS,IE                      MAR 4690
0016          IF(ABS(B(J)) .LE. 1.0E-10 ) GO TO 70  MAR 4700
0017          ALFA(NX) = G(NX,J)                     MAR 4710
0018      DO 20      II = 1,NXM1                    MAR 4720
0019          I = NX - II                          MAR 4730
0020          ALFA(I) = G(I,J)                      MAR 4740
0021          IP1 = I+I                           MAR 4750
0022      DO 20      K = IP1,NX                   MAR 4760
0023          20      ALFA(I) = ALFA(I)-ALFA(K)*H(K-I,J-K)  MAR 4770
0024          BETA = B(J)                           MAR 4780
0025      DO 30      K = 1,NX                      MAR 4790
0026          30      BETA = BETA-ALFA(K)*H(K,J-K)  MAR 4800
0027      DO 50      I = 1,NXM1                    MAR 4810
0028          JPI = J+I                           MAR 4820
0029          IP1 = I+I                           MAR 4830
0030      DO 40      K = IP1,NX                   MAR 4840
0031          40      H(I,J) = H(I,J)-ALFA(K-I)*H(K,JPI-K)  MAR 4850
0032          50      H(I,J) = H(I,J)/BETA        MAR 4860
0033          H(NX,J) = H(NX,J)/BETA            MAR 4870
0034      DO 60      I = 1,NX                      MAR 4880
0035          GAMA(J) = D(J)                      MAR 4890
0036      DO 60      K = 1,NX                      MAR 4900
0037          60      GAMA(J) = GAMA(J)-ALFA(K)*GAMA(J-K)  MAR 4910
0038          GAMA(J) = GAMA(J)/BETA            MAR 4920
0039      70 CONTINUE                            MAR 4930
0040      DO 80      JJ = IS,IE                  MAR 4940
0041          J = IE+IS-JJ                      MAR 4950
0042          P(J) = GAMA(J)                      MAR 4960
0043      DO 80      K = 1,NX                      MAR 4970
0044          80      P(J) = P(J)-H(K,J)*P(J+K)  MAR 4980
0045          RETURN                           MAR 4990
0046          END                               MAR 5000

```

0001	SUBROUTINE	RADP	MAR 7250
C-----			MAR 7260
C PURPOSE OF SUBROUTINE			MAR 7270
C TO PERFORM THE RAD PROCEDURE			MAR 7280
C TO SOLVE THE PRESSURE EQUATIONS.			MAR 7290
C-----			MAR 7300
0002	COMMON/C01/	E(345),A(345),B(345),C(345),F(345),P(345),D(345)	MAR 7310
0003	COMMON/C23/	NUD,NUDX(175),NLD,NLDX(175),NU,NUDP1,NUDP1,M	MAR 7320
0004	COMMON/C28/	IRS(390),M1,M2,ISS,AA(410),CC(410),EE(410),FF(410)	MAR 7330
0005	COMMON/C29/	G(17,195), H(16,195),Y(410)	MAR 7340
C-----			MAR 7350
C TRANSFER COEFFICIENT MATRIX FROM STANDARD ORDERING TO RAD			MAR 7360
C UPPER RIGHT QUARTER OF THE COMPOSITE MATRIX			MAR 7370
C-----			MAR 7380
0006	DO 10	K = 1,NUD	MAR 7390
0007		J = NUDX(K)	MAR 7400
0008		I = IRS(J)	MAR 7410
0009		AA(J) = A(I)/B(I)	MAR 7420
0010		CC(J) = C(I)/B(I)	MAR 7430
0011		EE(J) = E(I)/B(I)	MAR 7440
0012		FF(J) = F(I)/B(I)	MAR 7450
0013	10	Y(J) = D(I)/B(I)	MAR 7460
0014	DO 20	K = 1,NLD	MAR 7470
0015		J = NLDX(K)	MAR 7480
0016		I = IRS(J)	MAR 7490
0017		AA(J) = A(I)	MAR 7500
0018		G(M,J-NU) = B(I)	MAR 7510
0019		CC(J) = C(I)	MAR 7520
0020		EE(J) = E(I)	MAR 7530
0021		FF(J) = F(I)	MAR 7540
0022	20	Y(J) = D(I)	MAR 7550
C-----			MAR 7560
C CONTRIBUTION OF AA,CC,EE,FF VECTORS			MAR 7570
C-----			MAR 7580
0023	DO 30	JJ = 1, NLD	MAR 7590
0024		K = NLDX(JJ)	MAR 7600
0025		J = K - NU	MAR 7610
0026		J1 = J + 1	MAR 7620
0027		K1 = J + M1	MAR 7630
0028		K2 = J + M2	MAR 7640
0029		G(1,J) = -EE(K)*EE(J)	MAR 7650
0030		G(2,J) = -EE(K)*CC(J)-CC(K)*EE(J1)	MAR 7660
0031		G(3,J) = -CC(K)*CC(J1)	MAR 7670
0032		G(M1,J) = -EE(K)*AA(J)-AA(K)*EE(K2)	MAR 7680
0033		G(M ,J) = G(M,J)-EE(K)*FF(J)-CC(K)*AA(J1)	MAR 7690
	1	-AA(K)*CC(K2)-FF(K)*EE(K1)	MAR 7700
0034		H(1,J) = -FF(K)*FF(K)	MAR 7710
0035		H(2,J) = -FF(K2)*AA(K)-AA(K)*FF(K)	MAR 7720
0036		H(3,J) = -AA(K2)*AA(K)	MAR 7730
0037		H(M1,J) = -FF(J1)*CC(K)-CC(K)*FF(K)	MAR 7740
0038	DO 30	I = 4, M2	MAR 7750
0039		G(I ,J) = 0.0	MAR 7760

FORTRAN IV G LEVEL 21

RADP

DATE = 78086

20/46/33

PAGE 0002

```

0040      30   H(I,J) = 0.0                               MAR 7770
C-----                                     MAR 7780
C-----                                     MAR 7790
C-----                                     MAR 7800
0041      DO 40   I = 1,3                               MAR 7810
0042      40   H(I,ISS) = H(I,ISS)/G(M,ISS)             MAR 7820
0043      H(M1,ISS) = H(M1,ISS)/G(M,ISS)               MAR 7830
0044      DO 60   JJ = 2,3                               MAR 7840
0045      J      = NLDX(JJ) - NU                      MAR 7850
0046      JO     = J - 1                                MAR 7860
0047      J2     = JJ + 2                                MAR 7870
0048      G(M,J) = G(M,J)-G(M1,J)*H(M1,J)            MAR 7880
0049      H(I,J) = H(I,J)/G(M,J)                      MAR 7890
0050      DO 50   I = 2, J2                            MAR 7900
0051      50   H(I,J) = (H(I,J)-H(I-1,JO)*G(M1,J))/G(M,J)  MAR 7910
0052      60   H(M1,J) = H(M1,J)/G(M,J)                MAR 7920
C-----                                     MAR 7930
C----- GROUP NO. 2                               MAR 7940
C-----                                     MAR 7950
0053      DO 90   JJ = 4,NLD                           MAR 7960
0054      J      = NLDX(JJ)-NU                      MAR 7970
0055      JM    = J - M                                MAR 7980
0056      DO 70   I = 2,M                            MAR 7990
0057      JMI   = JM + I                                MAR 8000
0058      KE    = I - 1                                MAR 8010
0059      DO 70   K = 1,KE                            MAR 8020
0060      70   G(I,J) = G(I,J)-G(I-K,J)*H(M-K,JMI-K)  MAR 8030
0061      H(I,J) = H(I,J)/G(M,J)                      MAR 8040
0062      DO 90   I = 2, M1                            MAR 8050
0063      KE    = I - 1                                MAR 8060
0064      DO 80   K = 1, KE                            MAR 8070
0065      80   H(I,J) = H(I,J)-H(I-K,J-K)*G(M-K,J)    MAR 8080
0066      90   H(I,J) = H(I,J)/G(M,J)                MAR 8090
C-----                                     MAR 8100
C----- BACK SUBSTITUTION                         MAR 8110
C-----                                     MAR 8120
0067      DO 110  K = 1,NLD                           MAR 8130
0068      J      = NLDX(K)                            MAR 8140
0069      JNU   = J - NU                                MAR 8150
0070      JM    = J - M                                MAR 8160
0071      Y(J)  = Y(J)-EE(J)*Y(JNU)-CC(J)*Y(JNU+1)  MAR 8170
      1          -AA(J)*Y(JNU+M2)-FF(J)*Y(JNU+M1)    MAR 8180
0072      DO 100  KK = 1, M1                           MAR 8190
0073      100  Y(J) = Y(J)-G(KK,JNU)*Y(JM+KK)        MAR 8200
0074      110  Y(J) = Y(J)/G(M,JNU)                  MAR 8210
0075      DO 120  JJ = 2,NLD                           MAR 8220
0076      J      = NLDX(NLDP1-JJ)                    MAR 8230
0077      JM    = J + M                                MAR 8240
0078      JNU   = J - NU                                MAR 8250
0079      DO 120  K = 1, M1                           MAR 8260
0080      120  Y(J) = Y(J) - H(K,JNU) * Y(JM - K)    MAR 8270
0081      DO 130  K = 1,NUD                           MAR 8280

```

FORTRAN IV G LEVEL 21

RADP

DATE = 78086

20/46/33

PAGE 0003

0082	J	= NUDX(NUDP1-K)	MAR 8290
0083	JNU	= J + NU	MAR 8300
0084	130 Y(J)	= Y(J) - FF(J)* Y(JNU)-AA(J)* Y(JNU-1) - CC(J)* Y(JNU-M2)-EE(J)* Y(JNU-M1)	MAR 8310 MAR 8320
	I		MAR 8330
	C-----		
	C TRANSFORM PRESSURE TO STANDARD ORDERING		MAR 8340
	C-----		MAR 8350
0085	DO 140 K = 1,NUD		MAR 8360
0086	J	= NUDX(K)	MAR 8370
0087	140 P(IRS(J)) = Y(J)		MAR 8380
0088	DO 150 K = 1,NLD		MAR 8390
0089	J	= NLDX(K)	MAR 8400
0090	150 P(IRS(J)) = Y(J)		MAR 8410
0091	RRETURN		MAR 8420
0092	END		MAR 8430

FORTRAN IV G LEVEL 21

RS

DATE = 78086

20/46/33

PAGE 0001

0001	SUBROUTINE RS	MAR 8440
	C-----	MAR 8450
	C PURPOSE OF SUBROUTINE	MAR 8460
	C TC REORDER THE STANDARD ORDERING INTO RAD	MAR 8470
	C-----	MAR 8480
0002	COMMON/CJ2/ NX,NY,NXY,N,IND(345),NXM1,NYM1	MAR 8490
0003	COMMON/C23/ NUD,NUDX(175),NLD,NLDX(175),NU,NUDP1,NLDP1,M	MAR 8500
0004	COMMON/C28/ IRS(390),M1,M2,ISS,AA(410),CC(410),EE(410),FF(410)	MAR 8510
0005	READ 300, NUD,NLD,L0,ND	MAR 8520
0006	NR = LD+ND	MAR 8530
0007	M = LD + 2	MAR 8540
0008	NU = NR /2	MAR 8550
0009	IF(MOD(ND, 2) .NE. 0) NU=NM/2+M	MAR 8560
0010	M1 = M - 1	MAR 8570
0011	M2 = M - 2	MAR 8580
0012	READ 300, (NUDX(J),IRS(NUDX(J)),J=1,NUD)	MAR 8590
0013	READ 300, (NLDX(J),IRS(NLDX(J)),J=1,NLD)	MAR 8600
0014	30 PRINT 200	MAR 8610
0015	DO 40 J = 1,NU	MAR 8620
0016	JNU = J + NU	MAR 8630
0017	40 PRINT 100, J,IRS(J),JNU,IRS(JNU)	MAR 8640
0018	ISS = NLDX(1) - NU	MAR 8650
0019	NLDP1 = NLD + 1	MAR 8660
0020	NUDP1 = NUD + 1	MAR 8670
0021	RETURN	MAR 8680
0022	100 FORMAT(20X,2I10,10X,2I10)	MAR 8690
0023	200 FORMAT(1H1,27X,"RAD", 5X,"GAUSS",16X,"RAD", 5X,"GAUSS",/, 1 28X,"====", 5X,"=====",16X,"====", 5X,"=====")	MAR 8700
0024	300 FORMAT(20I4)	MAR 8710
0025	END	MAR 8720
		MAR 8730

APPENDIX F

A SAMPLE OF COMPUTER SIMULATION OUTPUT

	KILOGRAM	ST. CUBIC METER
OIL IN PLACE	0.1260E 10	0.1528E 07
WATER IN PLACE	0.1125E 10	0.9701E 06
GAS IN PLACE(FREE & DISSOLVED)	0.2162E 09	0.2402E 09
TOTAL FLUIDS IN PLACE	0.2602E 10	0.2427E 09

OUTPUT NO. 1

=====

TIME	30.0000
CPU TIME	10.3230
MAXIMUM TIME STEP	13.0504
MINIMUM TIME STEP	0.0636
MAX. ABS. MASS BALANCE RELATIVE ERROR	0.1126E-02
TOTAL MASS BALANCE RELATIVE ERROR	-3.6304E-03
OIL MASS BALANCE RELATIVE ERROR	-0.1126E-02
WATER MASS BALANCE RELATIVE ERROR	0.8827E-04
GAS MASS BALANCE RELATIVE ERROR	-0.1123E-02
AVERAGE RESERVOIR PRESSURE	14814.

WELLS REPORT

=====

NEGATIVE QUANTITY INDICATES PRODUCTION
 POSITIVE QUANTITY INDICATES INJECTION
 ALL UNITS ARE IN STANDARD CUBIC METERS

178

SER. NO.	WELL NO.	X- AXIS	Y- AXIS	DAILY	OIL CUMULATIVE	GAS DAILY	GAS CUMULATIVE	WATER DAILY	WATER CUMULATIVE	GAS-OIL RATIO
1	11	5	4	-51.87	-1556.20	-8158.23	-0.24E 06	-0.00	-0.00	157.27
2	52	7	6	-73.41	-2202.17	-11544.68	-0.35E 06	-0.00	-0.00	157.27
3	41	5	8	-63.68	-1820.46	-9543.69	-0.29E 06	-0.00	-0.00	157.27
4	51	8	8	-51.87	-1556.20	-8158.23	-0.24E 06	-0.00	-0.00	157.27
5	81	7	10	-60.68	-1820.46	-9543.60	-0.29E 06	-0.30	-0.30	157.27
6	71	5	12	-33.28	-998.32	-5233.58	-0.16E 06	-0.00	-0.00	157.27
7	82	8	12	-51.87	-1556.20	-8158.23	-0.24E 06	-0.00	-0.00	157.27
8	112	7	14	-46.98	-1409.39	-7349.59	-0.22E 06	-0.30	-0.00	157.27
9	101	5	16	-39.15	-1174.49	-6157.16	-0.18E 06	-0.00	-0.00	157.27
10	111	7	16	-51.87	-1556.20	-8158.23	-0.24E 06	-0.00	-0.30	157.27
11	141	7	18	-46.98	-1409.39	-7388.59	-0.22E 06	-0.00	-0.30	157.27
12	131	5	20	-30.34	-910.23	-4771.79	-0.14E 06	-0.00	-0.00	157.27
13	143	8	20	-43.06	-1291.94	-6772.88	-0.20E 06	-0.30	-0.30	157.27
14	4	7	21	-29.36	-880.87	-4617.66	-0.14E 06	-0.00	-0.00	157.27
15	21	8	4	0.0	0.0	0.0	0.0	86.62	2599.70	
16	61	10	6	0.0	0.0	0.0	0.0	86.87	2606.22	
17	91	10	10	0.0	0.0	0.0	0.0	110.00	3300.00	
18	121	10	14	0.0	0.0	0.0	0.0	110.00	3300.00	
19	152	10	18	0.0	0.0	0.0	0.0	110.00	3300.00	
20	3	10	21	0.0	0.0	0.0	0.0	103.73	3112.03	

-0.20E 05

-0.32E 07

0.18E 05

OIL PRESSURE AT THE MIDDLE OF THE CELL

J	1	2	3	4	5	6	7	8	9	10	
1	0.	0.	0.	0.	0.	0.	0.	0.	0.	0.	
2	0.	0.	14510.	14528.	14560.	14661.	14835.	15017.	15128.	15190.	
3	0.	14490.	14495.	14515.	14534.	14669.	14842.	15058.	15126.	15181.	
4	0.	14502.	14506.	14492.	14420.	14645.	14848.	15204.	15132.	15189.	
5	0.	14489.	14495.	14538.	14511.	14615.	14725.	14920.	15059.	15210.	
6	0.	14477.	14481.	14489.	14498.	14543.	14538.	14799.	15015.	15513.	
7	0.	14452.	14445.	14451.	14442.	14518.	14583.	14723.	14925.	15117.	
8	0.	14428.	14422.	14394.	14316.	14462.	14555.	14593.	14846.	15043.	
9	0.	0.	14386.	14389.	14397.	14462.	14525.	14674.	14873.	15065.	
10	0.	0.	14393.	14385.	14431.	14432.	14411.	14665.	14900.	15375.	
11	0.	0.	14395.	14386.	14369.	14452.	14521.	14658.	14879.	15094.	
12	0.	0.	0.	14349.	14282.	14427.	14529.	14574.	14850.	15372.	
13	0.	0.	0.	14366.	14366.	14425.	14527.	14693.	14920.	15157.	
14	0.	0.	0.	14368.	14381.	14401.	14404.	14710.	14968.	15631.	
15	0.	0.	0.	14354.	14361.	14413.	14484.	14717.	14946.	15187.	
16	0.	0.	0.	14330.	14254.	14419.	14427.	14722.	14948.	15144.	
17	0.	0.	0.	14372.	14389.	14439.	14534.	14759.	14985.	15235.	
18	0.	0.	14361.	14361.	14390.	14447.	14482.	14766.	15027.	15587.	
19	0.	0.	0.	14386.	14370.	14470.	14585.	14774.	15038.	15306.	
20	0.	0.	0.	14354.	14284.	14454.	14574.	14681.	15349.	15361.	
21	0.	0.	0.	0.	14391.	14449.	14496.	14791.	15136.	16230.	
22	0.	0.	0.	0.	0.	0.	14615.	14855.	15182.	15645.	
23	0.	0.	0.	0.	0.	0.	0.	0.	0.	0.	

J	11	12	13	14	15
1	0.	0.	0.	0.	0.
2	15223.	0.	0.	0.	0.
3	15226.	15266.	0.	0.	0.
4	15236.	15277.	0.	0.	0.
5	15250.	15280.	0.	0.	0.
6	15282.	15279.	0.	0.	0.
7	15195.	15245.	15283.	0.	0.
8	15152.	15222.	15242.	15294.	0.
9	15158.	15219.	15253.	15331.	0.
10	15222.	15230.	15261.	15309.	0.
11	15182.	15234.	15274.	0.	0.
12	15185.	15249.	15326.	0.	0.
13	15228.	15287.	15337.	0.	0.
14	15327.	15333.	15358.	0.	0.
15	15279.	15334.	15371.	0.	0.
16	15256.	15343.	15376.	15409.	0.
17	15338.	15363.	15394.	15429.	0.
18	15398.	15407.	15426.	15443.	0.
19	15401.	15439.	15469.	0.	0.
20	15445.	15482.	15491.	0.	0.
21	15612.	15552.	0.	0.	0.
22	0.	0.	0.	0.	0.
23	0.	0.	0.	0.	0.

		1	2	3	4	5	6	7	8	9	10	
23	0.0											
22	0.0											
21	0.0											
20	0.0											
19	0.0											
18	0.0											
17	0.0											
16	0.0											
15	0.0											
14	0.0											
13	0.0											
12	0.0											
11	0.0											
10	0.0											
9	0.0											
8	0.0											
7	0.0											
6	0.0											
5	0.0											
4	0.0											
3	0.0											
2	0.0											
1	0.0											

WATER SATURATION

		I	1	J	2	3	4	5	6	7	8	9	10
		I	1	I	2	3	4	5	6	7	8	9	10
		I	1	I	2	3	4	5	6	7	8	9	10
1	0.0	0.0	0.0	0.0	0.0	0.0	0.0	0.0	0.0	0.0	0.0	0.0	0.0
2	0.0	0.0	0.0	0.0	0.0	0.0	0.0	0.0	0.0	0.0	0.0	0.0	0.0
3	0.0	0.0	0.0	0.0	0.0	0.0	0.0	0.0	0.0	0.0	0.0	0.0	0.0
4	0.0	0.0	0.0	0.0	0.0	0.0	0.0	0.0	0.0	0.0	0.0	0.0	0.0
5	0.0	0.0	0.0	0.0	0.0	0.0	0.0	0.0	0.0	0.0	0.0	0.0	0.0
6	0.0	0.0	0.0	0.0	0.0	0.0	0.0	0.0	0.0	0.0	0.0	0.0	0.0
7	0.0	0.0	0.0	0.0	0.0	0.0	0.0	0.0	0.0	0.0	0.0	0.0	0.0
8	0.0	0.0	0.0	0.0	0.0	0.0	0.0	0.0	0.0	0.0	0.0	0.0	0.0
9	0.0	0.0	0.0	0.0	0.0	0.0	0.0	0.0	0.0	0.0	0.0	0.0	0.0
10	0.0	0.0	0.0	0.0	0.0	0.0	0.0	0.0	0.0	0.0	0.0	0.0	0.0
11	0.0	0.0	0.0	0.0	0.0	0.0	0.0	0.0	0.0	0.0	0.0	0.0	0.0
12	0.0	0.0	0.0	0.0	0.0	0.0	0.0	0.0	0.0	0.0	0.0	0.0	0.0
13	0.0	0.0	0.0	0.0	0.0	0.0	0.0	0.0	0.0	0.0	0.0	0.0	0.0
14	0.0	0.0	0.0	0.0	0.0	0.0	0.0	0.0	0.0	0.0	0.0	0.0	0.0
15	0.0	0.0	0.0	0.0	0.0	0.0	0.0	0.0	0.0	0.0	0.0	0.0	0.0
16	0.0	0.0	0.0	0.0	0.0	0.0	0.0	0.0	0.0	0.0	0.0	0.0	0.0
17	0.0	0.0	0.0	0.0	0.0	0.0	0.0	0.0	0.0	0.0	0.0	0.0	0.0
18	0.0	0.0	0.0	0.0	0.0	0.0	0.0	0.0	0.0	0.0	0.0	0.0	0.0
19	0.0	0.0	0.0	0.0	0.0	0.0	0.0	0.0	0.0	0.0	0.0	0.0	0.0
20	0.0	0.0	0.0	0.0	0.0	0.0	0.0	0.0	0.0	0.0	0.0	0.0	0.0
21	0.0	0.0	0.0	0.0	0.0	0.0	0.0	0.0	0.0	0.0	0.0	0.0	0.0
22	0.0	0.0	0.0	0.0	0.0	0.0	0.0	0.0	0.0	0.0	0.0	0.0	0.0
23	0.0	0.0	0.0	0.0	0.0	0.0	0.0	0.0	0.0	0.0	0.0	0.0	0.0

GAS SATURATION

23	22	21	20	19	18	17	16	15	14	13	12	11	10	9	8	7	6	5	4	3	2	1	J
0.0	0.0	0.0	0.0	0.0	0.0	0.0	0.0	0.0	0.0	0.0	0.0	0.0	0.0	0.0	0.0	0.0	0.0	0.0	0.0	0.0	0.0	I	
0.0	0.0	0.0	0.0	0.0	0.0	0.0	0.0	0.0	0.0	0.0	0.0	0.0	0.0	0.0	0.0	0.0	0.0	0.0	0.0	0.0	0.0	1	
0.0	0.0	0.0	0.0	0.0	0.0	0.0	0.0	0.0	0.0	0.0	0.0	0.0	0.0	0.0	0.0	0.0	0.0	0.0	0.0	0.0	0.0	2	
0.0	0.0	0.0	0.0	0.0	0.0	0.0	0.0	0.0	0.0	0.0	0.0	0.0	0.0	0.0	0.0	0.0	0.0	0.0	0.0	0.0	0.0	3	
0.0	0.0	0.0	0.0	0.0	0.0	0.0	0.0	0.0	0.0	0.0	0.0	0.0	0.0	0.0	0.0	0.0	0.0	0.0	0.0	0.0	0.0	4	
0.0	0.0	0.0	0.0	0.0	0.0	0.0	0.0	0.0	0.0	0.0	0.0	0.0	0.0	0.0	0.0	0.0	0.0	0.0	0.0	0.0	0.0	5	
0.0	0.0	0.0	0.0	0.0	0.0	0.0	0.0	0.0	0.0	0.0	0.0	0.0	0.0	0.0	0.0	0.0	0.0	0.0	0.0	0.0	0.0	6	
0.0	0.0	0.0	0.0	0.0	0.0	0.0	0.0	0.0	0.0	0.0	0.0	0.0	0.0	0.0	0.0	0.0	0.0	0.0	0.0	0.0	0.0	7	
0.0	0.0	0.0	0.0	0.0	0.0	0.0	0.0	0.0	0.0	0.0	0.0	0.0	0.0	0.0	0.0	0.0	0.0	0.0	0.0	0.0	0.0	8	
0.0	0.0	0.0	0.0	0.0	0.0	0.0	0.0	0.0	0.0	0.0	0.0	0.0	0.0	0.0	0.0	0.0	0.0	0.0	0.0	0.0	0.0	9	
0.0	0.0	0.0	0.0	0.0	0.0	0.0	0.0	0.0	0.0	0.0	0.0	0.0	0.0	0.0	0.0	0.0	0.0	0.0	0.0	0.0	0.0	10	

OUTPUT NO. 2

=====

TIME	60.0000
CPU TIME	13.7285
MAXIMUM TIME STEP	18.4000
MINIMUM TIME STEP	11.6000
MAX. ABS. MASS BALANCE RELATIVE ERROR	0.4186E-02
TOTAL MASS BALANCE RELATIVE ERROR	-0.2003E-02
OIL MASS BALANCE RELATIVE ERROR	-0.3502E-02
WATER MASS BALANCE RELATIVE ERROR	0.9373E-04
GAS MASS BALANCE RELATIVE ERROR	-0.4186E-02
AVERAGE RESERVOIR PRESSURE	13761.

183

WELLS REPORT

=====

NEGATIVE QUANTITY INDICATES PRODUCTION
 POSITIVE QUANTITY INDICATES INJECTION
 ALL UNITS ARE IN STANDARD CUBIC METERS

SER. NO.	WELL NO.	X- AXIS	Y- AXIS	OIL DAILY	OIL CUMULATIVE	GAS DAILY	GAS CUMULATIVE	WATER DAILY	WATER CUMULATIVE	GAS-OIL RATIO
1	11	5	4	-50.77	-3079.32	-7984.80	-0.48E 36	-0.33	-0.33	157.27
2	52	7	6	-71.85	-4357.52	-11299.25	-0.69E 06	-0.00	-0.00	157.27
3	41	5	8	-59.39	-3602.22	-9340.71	-0.57E 06	-0.00	-0.00	157.27
4	51	8	8	-50.77	-3079.32	-7984.80	-0.48E 36	-0.33	-0.33	157.27
5	81	7	10	-59.39	-3602.22	-9340.71	-0.57E 06	-0.00	-0.00	157.27
6	71	5	12	-32.57	-1975.41	-5122.32	-0.31E 06	-0.33	-0.33	157.27
7	82	8	12	-50.77	-3079.32	-7984.80	-0.48E 06	-0.00	-0.00	157.27
8	112	7	14	-45.98	-2788.81	-7231.52	-0.44E 06	-0.00	-0.00	157.27
9	101	5	16	-38.32	-2324.01	-6026.26	-0.37E 36	-0.33	-0.33	157.27
10	111	7	16	-50.77	-3079.32	-7984.80	-0.48E 06	-0.00	-0.00	157.27
11	141	7	18	-45.98	-2788.81	-7231.52	-0.44E 06	-0.00	-0.00	157.27
12	131	5	20	-29.73	-1801.11	-4670.35	-0.28E 06	-0.00	-0.00	157.27
13	143	8	20	-42.15	-2556.41	-6628.89	-0.40E 06	-0.00	-0.00	157.27
14	4	7	21	-28.74	-1743.01	-4519.73	-0.27E 06	-0.33	-0.33	157.27
15	21	8	4	0.0	0.0	0.0	0.0	76.92	4906.17	
16	61	10	6	0.0	0.0	0.0	0.0	75.60	4874.20	
17	91	12	13	0.0	0.0	0.0	0.0	96.59	6197.56	
18	121	10	14	0.0	0.0	0.0	0.0	95.00	6150.13	
19	152	10	18	0.0	0.0	0.0	0.0	95.27	6158.12	
20	3	13	21	0.0	0.0	0.0	0.0	86.29	5700.63	

-0.40E 05

-0.63E 07

0.34E 05

OIL PRESSURE AT THE MIDDLE OF THE CELL

I	J	1	2	3	4	5	6	7	8	9	10
1	0.	0.	0.	13487.	13504.	13532.	13626.	13820.	14002.	14110.	14168.
2	0.	0.	0.	13469.	13472.	13471.	13504.	13631.	13822.	14049.	14111.
3	0.	0.	0.	13481.	13485.	13467.	13381.	13604.	13814.	14375.	14121.
4	0.	0.	0.	13468.	13472.	13483.	13478.	13574.	13672.	13885.	14028.
5	0.	0.	0.	13455.	13458.	13462.	13465.	13501.	13479.	13769.	14198.
6	0.	0.	0.	13431.	13421.	13424.	13408.	13478.	13530.	13662.	13883.
7	0.	0.	0.	13406.	13398.	13365.	13280.	13420.	13505.	13530.	13904.
8	0.	0.	0.	0.	0.	13357.	13350.	13418.	13472.	13611.	13825.
9	0.	0.	0.	0.	0.	13361.	13349.	13359.	13383.	13595.	13835.
10	0.	0.	0.	0.	0.	13347.	13321.	13399.	13459.	13585.	13822.
11	0.	0.	0.	0.	0.	13300.	13225.	13365.	13460.	13488.	13800.
12	0.	0.	0.	0.	0.	13307.	13304.	13354.	13450.	13605.	13846.
13	0.	0.	0.	0.	0.	13299.	13309.	13319.	13307.	13610.	13874.
14	0.	0.	0.	0.	0.	13276.	13281.	13326.	13398.	13612.	13853.
15	0.	0.	0.	0.	0.	13245.	13157.	13329.	13317.	13612.	13851.
16	0.	0.	0.	0.	0.	13286.	13299.	13339.	13423.	13665.	13873.
17	0.	0.	0.	0.	0.	13269.	13268.	13292.	13339.	13356.	13659.
18	0.	0.	0.	0.	0.	13294.	13266.	13357.	13460.	13662.	13912.
19	0.	0.	0.	0.	0.	13255.	13172.	13333.	13442.	13528.	13912.
20	0.	0.	0.	0.	0.	0.	13276.	13320.	13349.	13661.	14032.
21	0.	0.	0.	0.	0.	0.	0.	0.	13471.	13729.	14052.
22	0.	0.	0.	0.	0.	0.	0.	0.	0.	0.	14578.
23	0.	0.	0.	0.	0.	0.	0.	0.	0.	0.	0.

I	J	11	12	13	14	15
1	0.	0.	0.	0.	0.	0.
2	14198.	0.	0.	0.	0.	0.
3	14200.	14239.	0.	0.	0.	0.
4	14211.	14250.	0.	0.	0.	0.
5	14224.	14251.	0.	0.	0.	0.
6	14250.	14248.	0.	0.	0.	0.
7	14154.	14204.	14238.	0.	0.	0.
8	14137.	14177.	14193.	14244.	0.	0.
9	14113.	14171.	14200.	14250.	0.	0.
10	14187.	14181.	14208.	14257.	0.	0.
11	14128.	14177.	14216.	0.	0.	0.
12	14121.	14184.	14262.	0.	0.	0.
13	14157.	14214.	14263.	0.	0.	0.
14	14261.	14254.	14274.	0.	0.	0.
15	14191.	14242.	14276.	0.	0.	0.
16	14157.	14242.	14273.	14304.	0.	0.
17	14204.	14255.	14286.	14321.	0.	0.
18	14306.	14301.	14316.	14332.	0.	0.
19	14292.	14328.	14355.	0.	0.	0.
20	14332.	14368.	14375.	0.	0.	0.
21	14494.	14417.	0.	0.	0.	0.
22	0.	0.	0.	0.	0.	0.
23	0.	0.	0.	0.	0.	0.

11
48

WATER SATURATION

	1	1	1	1	1	2	3	4	5	6	7	8	9	10
1	0.0	0.0	0.0	0.0	0.0	J.3	0.0							
2	0.0	0.0	0.0	0.0	0.0	0.3007	0.3007	0.3007	0.3007	0.3007	0.3007	0.3007	0.3007	0.3005
3	0.0	0.0	0.0	0.0	0.0	0.3007	0.3007	0.3007	0.3007	0.3007	0.3007	0.3007	0.3007	0.3004
4	0.0	0.0	0.0	0.0	0.0	0.3007	0.3007	0.3007	0.3007	0.3007	0.3007	0.3007	0.3007	0.3003
5	0.0	0.0	0.0	0.0	0.0	0.3007	0.3007	0.3007	0.3007	0.3007	0.3007	0.3007	0.3007	0.3002
6	0.0	0.0	0.0	0.0	0.0	0.3007	0.3007	0.3007	0.3007	0.3007	0.3007	0.3007	0.3007	0.3001
7	0.0	0.0	0.0	0.0	0.0	0.3007	0.3007	0.3007	0.3007	0.3007	0.3007	0.3007	0.3007	0.3000
8	0.0	0.0	0.0	0.0	0.0	0.3007	0.3007	0.3007	0.3007	0.3007	0.3007	0.3007	0.3007	0.3000
9	0.0	0.0	0.0	0.0	0.0	0.3007	0.3007	0.3007	0.3007	0.3007	0.3007	0.3007	0.3007	0.3000
10	0.0	0.0	0.0	0.0	0.0	0.3007	0.3007	0.3007	0.3007	0.3007	0.3007	0.3007	0.3007	0.3000
11	0.0	0.0	0.0	0.0	0.0	0.3007	0.3117	0.3117	0.3117	0.3117	0.3117	0.3117	0.3117	0.3116
12	0.0	0.0	0.0	0.0	0.0	0.3007	0.3007	0.3007	0.3007	0.3007	0.3007	0.3007	0.3007	0.3005
13	0.0	0.0	0.0	0.0	0.0	0.3007	0.3007	0.3007	0.3007	0.3007	0.3007	0.3007	0.3007	0.3004
14	0.0	0.0	0.0	0.0	0.0	0.3007	0.3007	0.3007	0.3007	0.3007	0.3007	0.3007	0.3007	0.3003
15	0.0	0.0	0.0	0.0	0.0	0.3007	0.3007	0.3007	0.3007	0.3007	0.3007	0.3007	0.3007	0.3003
16	0.0	0.0	0.0	0.0	0.0	0.3007	0.3007	0.3007	0.3007	0.3007	0.3007	0.3007	0.3007	0.3003
17	0.0	0.0	0.0	0.0	0.0	0.3007	0.3007	0.3007	0.3007	0.3007	0.3007	0.3007	0.3007	0.3003
18	0.0	0.0	0.0	0.0	0.0	0.3005	0.3005	0.3005	0.3005	0.3005	0.3005	0.3005	0.3005	0.3003
19	0.0	0.0	0.0	0.0	0.0	0.3005	0.3005	0.3005	0.3005	0.3005	0.3005	0.3005	0.3005	0.3003
20	0.0	0.0	0.0	0.0	0.0	0.3005	0.3005	0.3005	0.3005	0.3005	0.3005	0.3005	0.3005	0.3003
21	0.0	0.0	0.0	0.0	0.0	0.3005	0.3005	0.3005	0.3005	0.3005	0.3005	0.3005	0.3005	0.3003
22	0.0	0.0	0.0	0.0	0.0	0.3005	0.3005	0.3005	0.3005	0.3005	0.3005	0.3005	0.3005	0.3003
23	0.0	0.0	0.0	0.0	0.0	J.3	0.0							
						12	13	14	15	16	17	18	19	186

